NTNU – Trondheim
Norwegian University of
Science and Technology

Vibrational motion in molecules

Benedicte Ofstad

Chemistry
Submission date: July 2014
Supervisor: Per-Olof Åstrand, IKJ
Co-supervisor: Kenneth Ruud, Universitetet i Tromsø
Magnus Ringholm, Universitetet i Tromsø

Norwegian University of Science and Technology
Department of Chemistry

Preface

I would like to thank my supervisor Prof. Dr. Per-Olof Åstrand for always giving prompt and thorough feedback. I do appreciate the vast amount of useful input I have received, and for being pushed to my limits. I dare say I have never learned more throughout my degree than when writing this thesis.

I would also like to thank my two other supervisors, Dr. Magnus Ringholm and Prof. Dr. Kenneth Ruud, for all their guiding and help.

Thank you, Andreas Løve Selvik, for assisting me with Linux and Git.

Thank you, Fredrik Ofstad, for proofreading the thesis.

Trondheim, July 2014
Benedicte Ofstad

Sammendrag

Nullpunktsvibrasjonelle korrigeringer er utført ved bruk av analytiske geometri- og egenskaps-derivater på DFT nivå. Korrigeringene er oppnådd ved bruk av en variasjon-perturbasjons-tilnærming, og er utført rundt et variasjonsbestemt ekspansjonspunkt, her benevnet som den effektive geometrien. Dette leder til at anharmonisiteten av potensialet blir inkludert i korrigeringen. Korrigeringer opp til den andre perturbasjonsordenen er her evaluert for første gang. Geometrien, de intermolekylære frekvensene, og de intramolekylære frekvensene, er blitt evaluert for $(H_2O)_2$ og HOH-D_2O dimerene ved bruk av det nyimplementerte analytiske kubiske kraftfeltet på DFT-nivå. De implementerte pertubasjonskorreksjonene er beregnet for dipolmomentet og polariserbarheten til H_2O, D_2O, NH_3, og CH_4. Bruken av DFT, de analytiske geometriderivatene og de analystiske egenskaps-derivatene har vært velykket. Den ekstra perubasjonskorreksjonen har vist seg å være signifikant for både dipolmomentet og polariserbarheten.

Abstract

Zero-point vibrational corrections are carried out with analytical geometry and property derivatives at DFT level. This correction is obtained using a variation-perturbation approach, and is carried out around a variationally determined expansion point, denoted the effective geometry, leading to the inclusion of the anharmonicity of the potential. The corrections up to the second perturbation order are evaluated for the first time. The effective geometry, intermolecular frequencies, and intramolecular frequencies of the $(H_2O)_2$ dimer and the HOH-D_2O dimer are calculated using the newly implemented analytical cubic force field at DFT level. The perturbation corrections implemented are evaluated for the dipole moment and polarizability of H_2O, D_2O, NH_3, and CH_4. Employing DFT, analytical geometry derivatives and property derivatives have been successful. The extra perturbation correction has been deemed significant for both the dipole moment and polarizability.

Contents

Chapter 1

Introduction

In addition to providing information about molecular structure and functionality, vibrational spectroscopy has become a valuable tool in assisting the interpretation and prediction of experimental data [22, 20]. In order to produce sufficiently accurate predictions of vibrational frequencies, zero point vibrational corrections must be included. This holds true for spectral information specifically dealing with vibration, but also for magnetic and electric molecular properties.

The aim of this master thesis is to extend upon the vibrational analysis implemented in the DALTON package[2]. In order to set this thesis in context, the relevant implementations in DALTON will briefly be reviewed.

The first contribution to what is now the method for vibrational analysis was developed for the calculating of intermolecular frequencies for bimolecular complexes by Åstrand et al.[5] in 1994. This approach entails performing the harmonic expansion around the point which minimizes the sum of the potential energy and the zero point vibrational energy, instead of the conventional potential energy minima. This method was later expanded upon to evaluate rovibrational averages of molecular properties in diatomic molecules[6, 71, 7, 8]. Higher order perturbations were then included for both diatomic molecules[9] in 1999 and polyatomic molecules in 2000[10]. As of today, this approach in DALTON adopts numerical derivatives for the cubic force field and property derivatives.

Atomic orbial energy based derivative theory was introduced in DALTON[69, 77, 40, 32] in 2008. Using this framework, analytical higher derivatives have been implemented[70] also with the ability of using DFT functionals[39]. This leads us to the objectives of this thesis:

The approach for molecular vibrations will be extended in three ways: Carrying out calculations using DFT, carrying out calculations using analytical property and geometric derivatives, and carrying out an extra correction to the vibrationally averaged property.

These extensions will be implemented as an external software, written in Python.

This software is to extract the required information from DALTON, replicate the vibrational analysis as already implemented and further carry out additional corrections. The external software will be able to carry out corrections at both the equilibrium geometry, and the effective geometry.

First the vibrational analysis will be implemented and the portion of the software that is a replication of DALTON will be validated against the literature. Once this is done, examples of calculations will be performed at DFT level employing the analytical geometry and property derivatives, rendering calculation with no numerical derivatives.

There will be two main types of examples of these extensions: The first system explored in 1994, namely bimolecular complexes, will be revisited and evaluated with the new analytical derivatives and DFT functionals. Secondly, the vibrational averaging of molecular properties and the different orders of corrections implemented will be determined for the polarizability and dipole moment using atomic orbital energy based derivative theory for several molecules. The scope will only include ground vibrational and electronic states. Temperature and mass effects will not be included.

Chapter 2

Theory

2.1 The Born-Oppenheimer Approximation

When modelling molecules, one has to consider both the nuclei and the electrons when evaluating the potential energy. As the molecules become large, this quickly becomes an immense system. An approximation which is nearly always used when facing such a task is the Born-Oppenheimer approximation [16, 15]. This enables the separation of the nuclear from the electronic motion. The approximation is based on the fact that the electronic energy level spacings are much larger than the spacing between the vibrational levels. These energy levels will therefore not mix to any significant extent. A more intuitive way of thinking about it, is that nuclei are much heavier than the electrons. The electrons will rearrange themselves very fast compared to the nucleus, and will therefore always be in equilibrium. This approximation lets us leave our picture of the molecule of electrons and nuclei, all having to be taken into consideration, and lets us focus on only the nuclei. The Born-Oppenheimer approximation also results in the ability to neglect all spin, both electric and nuclear, in addition to all relativistic effects[36].

2.2 Rotation and Translation

Translational motion can safely be separated from vibration, as the energy gap between these two motions is very large. The mixing of these energy levels will therefore not take place. Rotational motion is more in the grey zone. It is, however, found that the rotational motions can also be separated from the internal vibrational motions. For a mathematical proof of this see Ref. [54].

The rotational and translational components will be projected out of the Hessian using the Eckart conditions [31]. The rotation and vibration may still be coupled, but the Eckart condition minimizes this coupling.

The first step in creating the projection matrix is by setting up the following matrix:

$$T = \begin{bmatrix} 1 & 0 & 0 & \cdots \\ 0 & 1 & 0 & \cdots \\ 0 & 0 & 1 & \cdots \\ -y & x & 0 & \cdots \\ 0 & -z & y & \cdots \\ z & 0 & -x & \cdots \end{bmatrix} \tag{2.1}$$

Eq (2.1) is only a fragment of the total matrix; three of these fragments are needed for every atom of the system (the x, y and z component). The full matrix T will have the dimension $6 \times 3N$ where N is the number of atoms. The upper part of the matrix is associated with the translation, the lower with the rotation.

This matrix undergoes orthonormalization, and is multiplied by -1.

$$T = -T^{\text{ortho}} \tag{2.2}$$

The matrix is multiplied with its transpose, and the identity matrix is then subtracted from it to recieve the final projection matrix $T_{\text{rot-trans}}$.

$$T_{\text{rot-trans}} = T \times T^T - I \tag{2.3}$$

The projection is carried out by:

$$V_{\text{vib}}^{(2)} = T_{\text{rot-trans}} \times H \times T_{\text{rot-trans}} \tag{2.4}$$

Here we are projecting out translation and rotation from the second derivative of the potential energy, denoted the Hessian. As the only Hessian used from now on will be the vibrational Hessian, the subscript *vib* will be dropped from here on out.

2.3 Normal coordinate basis

All the derivatives in the equations are in normal coordinates. In order to convert them, the normal coordinate transformation matrix must be created.

The fundamental frequencies and the normal coordinate transformation matrix can be extracted from the mass weighted vibrational Hessian matrix, granted the system is at an energy minimum [30]. Firstly, the vibrational Hessian must be converted to the force constant matrix in mass weighted coordinates.

$$V_m^{(2)} = M^{-\frac{1}{2}} V^{(2)}(f) M^{-\frac{1}{2}} \tag{2.5}$$

The M matrix is a $3N \times 3N$ matrix containing the atomic masses along the diagonal. The next step in attaining the normal frequencies is solving the secular equations for the force constant matrix, and thereby obtaining the eigenvalues and eigenvectors. If using cartesian coordinates, six of the eigenvalues should be zero as they correspond to the translational and vibrational motion of the system, this can be used as a check to validate the system being at a minimum.

The normal coordinates and the fundamental frequencies are found by diagonalizing $V_m^{(2)}$:

$$V_m^{(2)} \nu = \lambda \nu \tag{2.6}$$

The frequencies correspond to the square root of the eigenvalues:

$$\text{frequencies} = \sqrt{|\lambda|} \tag{2.7}$$

While the transformation matrix, which will be denoted N, corresponds to the the eigenvectors:

$$N = \nu \tag{2.8}$$

2.4 Perturbation Theory

We will employ the Hylleraas variational perturbation theory[52]. This method is based on Rayleigh-Schrödinger perturbation theory. The energy, wavefunction and Hamiltonian are functions of the order of perturbation, λ:

$$\begin{aligned}\langle \Psi | H - E | \Psi \rangle = \big\langle \Psi^{(0)} + \lambda \Psi^{(1)} + \lambda^2 \Psi^{(2)} + ... | (H^{(0)} - E^{(0)}) + \lambda (H^{(1)} - E^{(1)}) \\ + \lambda^2 (H^{(2)} - E^{(2)}) + ... | \Psi^{(0)} + \lambda \Psi^{(1)} + \lambda^2 \Psi^{(2)} + ... \big\rangle\end{aligned} \tag{2.9}$$

Orthonormality is assumed within this approach, ie:

$$\big\langle \Psi^{(0)} | \Psi^{(0)} \big\rangle = 1 \qquad \big\langle \Psi | \Psi^{(0)} \big\rangle = 1 \qquad \big\langle \Psi^{(0)} | \Psi^{(i)} \big\rangle = 0, \quad i \neq 0 \tag{2.10}$$

The equation 2.9 is solved for each order of λ, for example, for $\lambda = 1 : E^{(1)} = \big\langle \Psi^{(0)} | H^{(0)} | \Psi^{(0)} \big\rangle$. This far, the approach is identical to Rayleigh-Schrödinger perturbation approach.

For the standard Rayleigh-Schrödinger perturbation approach, the wavefunction is found by expanding Eq.2.9 to an appropriate order of λ, a series of algebraic steps is then performed. This leads to the wavefunction being derived with respect to the energy and the Hamiltonian.

Within the variational perturbation approach, however, the expression for the wavefunction is found by minimizing with respect to the trial function $\Psi^{(m)}$, this is where the *variational* component of the approach comes in.

2.5 The vibrational wavefunction

As we are describing a *vibrational* system, it is natural to use the harmonic oscillator model as a zeroth order approximation. The harmonic oscillator can be used in systems where the potential energy can be described well by Hooke's law, expressed for a diatomic by:

$$V(q^2) = \frac{1}{2} k_{\mathrm{f}} q^2 \tag{2.11}$$

V is the potential energy, k_f is a force constant and q is the mass weighted normal coordinate associated with the vibration. Mass weighted normal coordinates are used as they are found to greatly simplify the procedure of deducing the equations that will be needed.

The Hamiltonian for a molecule with N vibrational modes using the harmonic oscillator potential energy becomes:

$$H^{(0)} = \frac{1}{2} \sum_{i=1}^{N} \left[-\frac{\partial^2}{\partial^2 q_i} + k_{\mathrm{f}} q^2 \right] \tag{2.12}$$

As both mass weighted coordinates and atomic units are used, both $\hbar$ and the mass m disappear from the first term. The superscript in $H^{(0)}$ refers to the perturbation order, which in this case is zero. The constant k_{f} is found to minimize the potential energy, i.e. $k_{\mathrm{f}} = V_{eq}^{(2)}$, the second derivative of the potential energy at equilibrium. As the coordinates used are mass weighted, so is the $V_{eq}^{(2)}$. If no subscript is given, we will assume to be at the equilibrium, dropping the 'eq' subscript, $H^{(0)}$ thus becomes:

$$H^{(0)} = \frac{1}{2} \sum_{i=1}^{N} \left[-\frac{\partial^2}{\partial^2 q_i} + V_{ii}^{(2)} q_i^2 \right] \tag{2.13}$$

The first term accounts for the kinetic energy, the second for the potential energy. The kinetic part of the Hamiltonian is the same for all systems as the kinetic

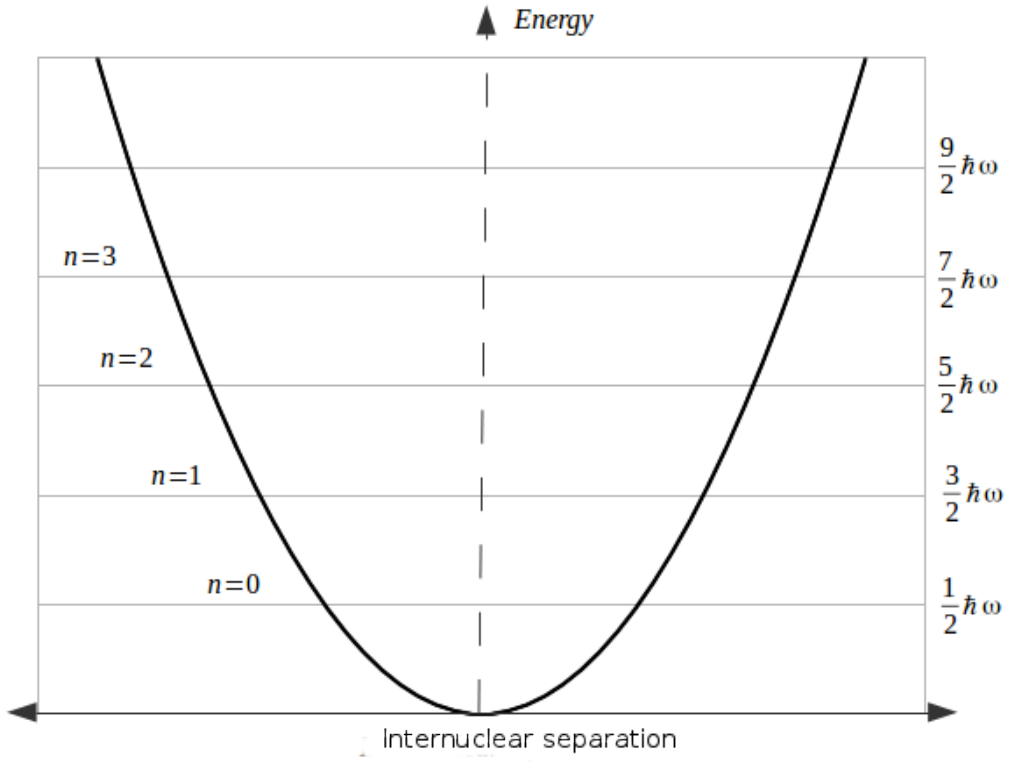

Figure 2.1: Graphical representation of how the energy changes as a function of the internuclear distance for a diatomic molecule for the harmonic oscillator.

energy of an atom is not affected by the number or orientation of the other atoms in the system. The potential energy of a harmonic oscillator, however, will be different for different vibrational systems. The Hamiltonian's ability to describe a system therefore improved by refining the *potential* energy term. One method of obtaining an accurate potential energy is by a Taylor expansion of the potential energy function.

Starting by performing a Taylor expansion on the potential energy:

$$\begin{aligned} V(q_1, q_2, ..., q_N) =& V^{(0)} + \sum_{i=1}^{N} V_i^{(1)} q_i + \frac{1}{2} \sum_{i=1}^{N} V_{ii}^{(2)} q_i^2 \\ &+ \frac{1}{6} \sum_{ijk=1}^{N} V_{ijk}^{(3)} q_i q_j q_k + \frac{1}{24} \sum_{ijkl=1}^{N} V_{ijkl}^{(4)} q_i q_j q_k q_l \\ &+ \frac{1}{120} \sum_{ijklm=1}^{N} V_{ijklm}^{(5)} q_i q_j q_k q_l q_m + \frac{1}{720} \sum_{ijklmn=1}^{N} V_{ijklmn}^{(6)} q_i q_j q_k q_l q_m q_n + [...] \end{aligned} \tag{2.14}$$

A criterion for using Taylor expansions is that the expansion must converge. The variable q is defined as the distance from the equilibrium bond length, $q = r - r_e$. In this case, the term with the largest order will become either positive or negative infinity when r goes towards infinity no matter how many terms the function is expanded to. This function will therefore diverge. As can be seen from Fig.(2.2), the function can still be used within a certain range of the equilibrium, and this range is expanded with an increased number of expansion terms. Care must still be taken if employing a model based on this Taylor expansion for vibrations at high temperatures (high energy).

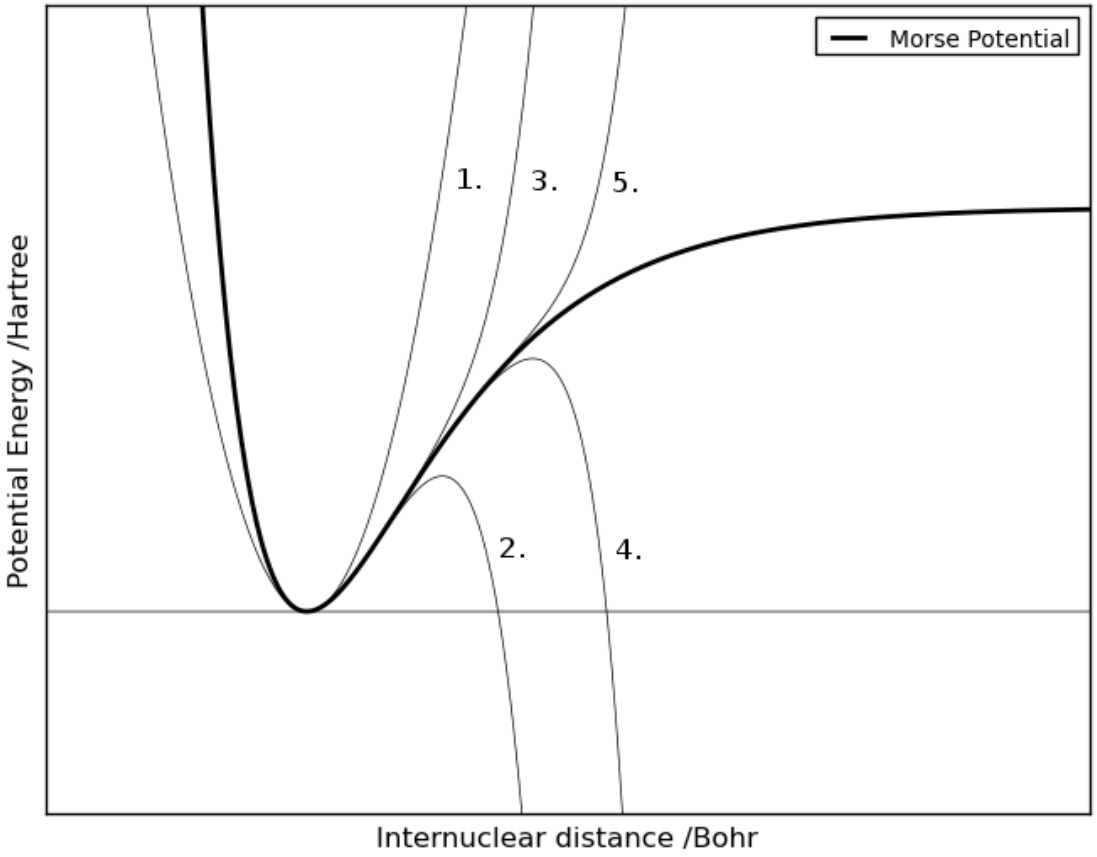

Figure 2.2: A representation of how the Taylor expansion of the potential energy behaves at large intermolecular distances for a diatomic molecule. The functions $V^{(2)}$, $V^{(4)}$, and $V^{(6)}$ go towards positive infinity with the last term being of even rank. The functions $V^{(3)}$, and $V^{(5)}$ have last terms of odd rank and thereby go towards negative infinity. Here we depict that although the Taylor expansion does not converge it is a good approximation within a given range of intermolecular distance.

Increasingly accurate Hamiltonians can be created by including higher orders from the Taylor expansion of the potential energy as perturbations to the Hamiltonian. The first few order of perturbation of the Hamiltonian are written as:

$$H^{(1)} = \frac{1}{6}\sum_{ijk=1}^{N} V^{(3)}_{ijkl} q_i q_j q_k$$

The $V_i^{(1)}$ term is not included as it is zero at the equilibrium geometry.

$$H^{(2)} = \frac{1}{24}\sum_{ijkl=1}^{N} V^{(4)}_{ijkl} q_i q_j q_k q_l$$

$$H^{(3)} = \frac{1}{120}\sum_{ijklm=1}^{N} V^{(5)}_{ijklm} q_i q_j q_k q_l q_m$$

The zeroth order Hamiltonian has eigenvalues, (and thereby energies) on the following form:

$$E_n^{(0)} = \sum_{i=1}^{N}(\frac{1}{2} + n)\omega_i \tag{2.15}$$

The n denotes the quantum number, and $\omega_i = \sqrt{V_{ii}^{(2)}}$, where the mass weighted Hessian is given in Hartrees.

Just as only the zeroth order hamiltonian has known eigenvalues, it also has known wavefunctions:

$$\psi_n^{(0)} = N_n H_n e^{-\frac{1}{2}\omega_i q_i^2} \tag{2.16}$$

The N_n is the normalization constant, and H_n a hermite polynomial. The $e^{-\frac{1}{2}\omega q_i^2}$ is characterized as a gaussian function, and all knowledge of gaussian functions can therefore be extended to the vibrational wavefunction. When inserting the correct values for the normalization constant and the hermite polynomial, the wavefunctions for the different quantum numbers become:

$$\psi_0^{(0)}(q) = \left(\frac{\sqrt{\omega}}{\pi^{\frac{1}{2}}}\right)^{\frac{1}{2}} e^{-\frac{\omega}{2}q^2} \tag{2.17}$$

$$\psi_1^{(0)}(q) = \left(\frac{\sqrt{\omega}}{2\pi^{\frac{1}{2}}}\right)^{\frac{1}{2}} 2q\sqrt{\omega}e^{-\frac{\omega}{2}q^2} \tag{2.18}$$

$$\psi_2^{(0)}(q) = \left(\frac{\sqrt{\omega}}{8\pi^{\frac{1}{2}}}\right)^{\frac{1}{2}} (4q^2 - 2)\sqrt{\omega}e^{-\frac{\omega}{2}q^2} \tag{2.19}$$

$$\psi_3^{(0)}(q) = \left(\frac{\sqrt{\omega}}{48\pi^{\frac{1}{2}}}\right)^{\frac{1}{2}} (8q^2 - 12q)\sqrt{\omega}e^{-\frac{\omega}{2}q^2} \tag{2.20}$$

Both the energy terms and the wavefunction for the higher order perturbations must be found explicitly. The energies will be found through Rayleigh Schrödinger perturbation[73, 49]. For the wavefunctions we will be using a *variational perturbation theory* as developed by Åstrand et al. [10, 9, 72] based on an approach by Kern and Matcha [56].

Any continuous function can be created by a sum of gaussians, as the limit of gaussians used goes towards infinity. As the harmonic oscillator wavefunction is on the form of a gaussian function, the perturbed wavefunction can be made up of a basis of the unperturbed wavefunctions. This ensures that the orthonormality principle of the wavefunction is conserved. The first order wavefunction is thus found by expanding in terms of a complete set of harmonic-oscillators:

$$\begin{aligned}\Psi^{(1)} = \sum_{i=1}^{N}\sum_{r=1}^{\infty} a_{r,i}^{(1)}\phi_{r,i} + \sum_{\substack{i,j=1\\ i\neq j}}^{N}\sum_{r,s=1}^{\infty} b_{rs,ij}^{(1)}\phi_{rs,ij} \\ + \sum_{\substack{i,j,k=1\\ i\neq j\neq k}}^{N}\sum_{rst=1}^{\infty} c_{rst,ijk}^{(1)}\phi_{rst,ijk}\end{aligned} \tag{2.21}$$

Where $a_{r,i}^{(1)}$, $b_{rs,ij}^{(1)}$, $c_{rst,ijk}^{(1)}$ are coefficients. These coefficients need to be chosen so as to minimize the energy of the system. Note that with this, we are employing the *variational principle*. The $\phi_{r,s,...,t,i,j,..t}$ are defined as a product of the wavefunctions: $\psi_{r,i}, \psi_{s,j}, ..., \psi_{t,k}, i \neq j, \neq k$. The i, j, k subscripts denote normal coordinates of the molecule.

The second order wavefunction is expanded in a similar fashion using the same notation:

$$\begin{aligned}\Psi^{(2)} = \sum_{i=1}^{N}\sum_{r=1}^{\infty} a_{r,i}^{(2)}\phi_{r,i} + \sum_{\substack{i,j=1\\ i\neq j}}^{N}\sum_{r,s=1}^{\infty} b_{rs,ij}^{(2)}\phi_{rs,ij} \\ + \sum_{\substack{ijk=1\\ i\neq j\neq k}}^{N}\sum_{rst=1}^{\infty} c_{rst,ijk}^{(2)}\phi_{rst,ijk} \\ + \sum_{\substack{ijkl=1\\ i\neq j\neq k\neq l}}^{N}\sum_{rstu=1}^{\infty} d_{rstu,ijkl}^{(2)}\phi_{rstu,ijkl}\end{aligned} \tag{2.22}$$

The wavefunctions can be expanded to any amount of expansion coefficients. Only the amount of expansion coefficients needed for further calculations are included here.

2.6 Effective geometry

As an alternative to the traditional approach of perturbing the Hamiltonian, featured in equation 2.23, an approach by Åstrand et al. where the $V^{(1)}$ term is included in the $H^{(1)}$ expression can also be used[9]:

$$H^{(1)} = \sum_{i=1}^{N} V_i^{(1)} q_i + \frac{1}{6} \sum_{ijk=1}^{N} V_{ijkl}^{(3)} q_i q_j q_k \tag{2.23}$$

When performing a perturbation expansion for a potential energy surface, one traditionally expands about the equilibrium geometry. The equilibrium geometry is the molecular geometry corresponding to the minimum on the potential energy surface, [61] the condition $V_e^{(1)} = 0$ will therefore apply. The subscript 'e' will denote that we are working at the equilibrium geometry. A second expansion point is additionally considered, this alternative expansion point is referred to as the *effective geometry*, and will be denoted with the subscript 'eff'. A comparison of the geometries and property corrections obtained using either the equilibrium or the effective geometry will be made.

The motivation for using an alternative effective geometry is to describe the anharmonicity of molecular vibration in the zeroth order wave function.

Starting by choosing an *arbitrary* expansion point r_{exp}, a Taylor expansion is carried out for the potential energy about r_{exp}. :

$$V(q) = V^{(0)} + V^{(1)} q + \frac{1}{2} V^{(2)} q^2 + \frac{1}{6} V^{(3)} q^3 + ... \tag{2.24}$$

Where $q = r - r_{\text{exp}}$. The effective geometry is found by performing a harmonic expansion around the point, minimizing the sum of the potential energy and the zero point vibrational energy of the stretching vibration, as proposed by Åstrand et al.[5].

$$E^{(0)} = V^{(0)} + \left\langle \Psi_0^{(0)} | H^{(0)} | \Psi_0^{(0)} \right\rangle$$

$$E^{(0)} = V^{(0)} + \frac{1}{2} \sum_{i=1}^{N} \omega_i \quad \xrightarrow{\text{minimizing}} \quad = V_{\text{eff}}^{(0)} + \frac{1}{2} \sum_{i=1}^{N} \omega_{i,\text{eff}} \tag{2.25}$$

This expansion point leads to fast converging results when calculating energies and structures for molecules [5]. The method was developed further by including higher order perurbations for molecular properties, first for diatomic molecules [9], and later also for polyatomic molecules [10].

If Equation 2.25 is differentiated, ie. minimized, with respect to r_{eff} the following condition is found:

$$V_{\text{eff}}^{(1)} + \frac{V_{\text{eff}}^{(3)}}{4\omega_{\text{eff}}} = 0 \tag{2.26}$$

for diatomic molecules [9] , and

$$V_{\text{eff},j}^{(1)} + \frac{1}{4}\sum_{i=1}^{N} \frac{V_{\text{eff},iij}^{(3)}}{\omega_i} = 0 \tag{2.27}$$

for polyatomic molecules[10]. Only part the semi-diagonal cubic force field is needed. It is sufficient to calculate the diagonals of the j squares making up the cubic force field, opening for the possibility of making the calculation less computationally heavy.

It has been shown that this condition leads to much simpler expressions for averaging of properties, in particular the leading anharmonic correction to the vibrational ground state vanishes [9, 10]. It was also shown that the effective geometry corresponds to the vibrationally averaged molecular geometry to second order in the order parameter of the perturbation expansion[10].

$$\langle r \rangle = r_{\text{eff}} \tag{2.28}$$

In order to find the expansion point, one can minimize the energy functional in Eq.(2.25), this is, however, rather heavy computationally. A second method for finding the effective geometry can be gleaned by considering how the expansion point was chosen as the vibrationally averaged geometry[10]. If instead, the vibrationally averaged geometry is expressed in terms of the equilibrium it can be shown that[10]:

$$\langle r \rangle = r_e - \sum_{j,m=1}^{N} \frac{1}{4\omega_j^2} \frac{V_{\text{e},jmm}^{(3)}}{\omega_m} \tag{2.29}$$

Combining Eq.(2.28) and Eq.(2.29) we get the following equality:

$$r_{\text{eff}} = r_e - \sum_{j,m=1}^{N} \frac{1}{4\omega_j^2} \frac{V_{\text{e},jmm}^{(3)}}{4\omega_m} \tag{2.30}$$

It is now established that in order to find the effective geometry, all that is needed is the second and part of the third derivative of the potential energy at the equilibrium geometry, referred to as the Hessian and the cubic force field[10].

2.7 Finding the expression for $\Psi^{(1)}$

The first order perturbation of the wavefunction will be found by minimizing the energy. We start by setting up an expression for the energy in terms of the wavefunction, and find the minima of this expression. In this manner, the coefficients making up the wavefunction will be attained.

2.7.1 The $E^{(1)}$ expression

Starting with the first order perturbation to the energy, this can be written out as:

$$E^{(1)} = \left\langle \Psi^{(0)} | H^{(1)} | \Psi^{(0)} \right\rangle \tag{2.31}$$

Inserting the value of $H^{(1)}$ defined in Eq. 2.23 and employing a more compact notation where $\left\langle \Psi^{(0)} | q_i | \Psi^{(0)} \right\rangle = \langle q_i \rangle_{00}$:

$$E^{(1)} = \sum_{i=1}^{N} V_i^{(1)} \langle q_i \rangle_{00} + \frac{1}{6} \sum_{i,j,k=1}^{N} V_{ijk}^{(3)} \langle q_i q_j q_k \rangle_{00}$$

This expression will always be zero as both the terms making up $E^{(1)}$ are zero, according to rules governing which values of gaussian integrals survive.

$$E^{(1)} = 0 \tag{2.32}$$

This expression can therefore not be used in attaining an expression for $\Psi^{(1)}$ and it will neither contribute with any expansion coefficients. We therefore turn to the next perturbation, namely $E^{(2)}$.

2.7.2 The $E^{(2)}$ expression

In the following section, the work of Åstrand et al.[10] will be followed closely. The derivation of the expressions will be gone through more thoroughly in order to make the work accessible to wider audience with less background knowledge in the field. The expression for $E^{(2)}$ is deduced from a formula giving the expression for the energy perturbation of an even order of perturbation[56]:

$$\begin{aligned} E^{(2n)} &= \langle\Psi^{(0)}|H^{(2n)}|\Psi^{(0)}\rangle + 2\langle\Psi^{(n)}|H^{(1)} - E^{(1)}|\Psi^{(n-1)}\rangle \\ +2\sum_{m=2}^{n}\langle\Psi^{(n)}|H^{(m)} - E^{(m)}|\Psi^{(n-m)}\rangle &+ \langle\Psi^{(n)}|H^{(0)} - E^{(0)}|\Psi^{(n)}\rangle \end{aligned} \tag{2.33}$$

Inserting for $n = 1$ gives:

$$\begin{aligned} E^{(2)} = \langle\Psi^{(0)}|H^{(2)}|\Psi^{(0)}\rangle &+ 2\langle\Psi^{(0)}|H^{(1)}|\Psi^{(1)}\rangle \\ &+\langle\Psi^{(1)}|H^{(0)} - E^{(0)}|\Psi^{(1)}\rangle \end{aligned} \tag{2.34}$$

Before commencing the task of inserting expressions and solving the equation it is advantageous to find a general expression "$- < H^0 - E^{(0)} >_{rr}$ ". This expression will crop up as a denominator for all the expansion coefficients, it is therefore practical to find an expression for this early on.

$$\begin{aligned} - < H^0 - E^{(0)} >_{rr} &= \int \psi_r^* E^{(0)} \psi_r d\tau - \int \psi_r^* H^{(0)} \psi_r d\tau \\ &= -r\omega \end{aligned} \tag{2.35}$$

The values for the wavefunctions, Hamiltonians and energies are now inserted into the expression for $E^{(2)}$, we also substiitute $- < H^0 - E^{(0)} >_{rr}$ with $-r\omega$:

$$\begin{aligned} E^{(2)} = &\frac{1}{24}\sum_{ijk=1}^{N} V_{ijkl}^{(4)} < q_i q_j q_k q_l >_{00} + \sum_{i=1}^{N}\sum_{r=1}^{\infty}\Bigg[2V_i^{(1)} < q_i >_{0r} a_{r,i}^{(1)} \\ &+ \frac{1}{3}V_{iii}^{(3)} < q_i^3 >_{0r} a_{r,i}^{(1)} + \sum_{m=1;m\neq i}^{N}[V_{imm}^{(3)} < q_i^2 >_{00} < q_i >_{0r} a_{r,i}^{(1)}] + a_{r,i}^{(1)}\omega_i a_{r,i}^{(1)}\Bigg] \\ &+ \sum_{ij=1;i\neq j}^{N}\sum_{rs=1}^{\infty} b_{rs,ij}^{(1)}\Bigg[V_{iij}^{(3)} < q_i^2 >_{0r} < q_j >_{0s} + b_{rs,ij}^{(1)}(r\omega_i + s\omega_j)\Bigg] \\ &+ \sum_{ijk=1;i\neq j\neq k}^{N}\sum_{rst=1}^{\infty} c_{rst,ijk}^{(1)}\Bigg[\frac{1}{3}V_{ijk}^{(3)} < q_i >_{0r} < q_j >_{0s} < q_k >_{0t} + c_{rst,ijk}^{(1)}(r\omega_i + s\omega_j + t\omega_j)\Bigg] \end{aligned} \tag{2.36}$$

Beginning with $a^{(1)}_{r,i}$, Eq.(2.36) is differentiated with respect to this expansion coefficient to find the minima:

$$\frac{\partial E^{(2)}}{\partial a^{(1)}_r} = \sum_{i=1}^{N} \Bigg[2V^{(1)}_i < q_i >_{0r} + \frac{1}{3} V^{(3)}_{iii} < q^3_i >_{0r} + \sum_{m=1;m\neq i}^{N} [V^{(3)}_{imm} < q^2_i >_{00} < q_i >_{0r}] + 2r\omega \Bigg] \tag{2.37}$$

Setting this to zero and solving for $a^{(1)}_{r,i}$ gives:

$$a^{(1)}_{r,i} = -\frac{V^{(1)}_i < q_i >_{0r} + \frac{1}{6} V^{(3)}_{iii} < q^3_i >_{0r} + \frac{1}{2} \sum_{m=1;m\neq i}^{N} V^{(3)}_{imm} < q^2_m >_{00} < q_i >_{0r}}{r\omega} \tag{2.38}$$

Attention is directed towards the second term in Eq.(2.36). The ability to bring in extra terms including m arises from the fact that we can create expressions on the form $< q^n >_{00} < q^m >_{0r}$, these would still be under the coefficient $a^{(1)}_r$ as no new subscript is introduced. This n can only be "2" for terms including V^3_{iii} and "2" or "4" for terms including V^4_{iiij} as a consequence of the symmetry of gaussian functions.

When inserting the correct values for the wavefunctions, Hamiltonians and energies, the only expansion coefficients surviving for $\Psi^{(1)}$ are $r = 1$ and $r = 3$:

For $r = 1$:

$$a^{(1)}_{1,i} = -\frac{V^{(1)}_i < q_i >_{01} + \frac{1}{6} V^{(3)}_{iii} < q^3_i >_{01} + \frac{1}{2} \sum_{m=1;m\neq i}^{N} V^{(3)}_{imm} < q^2_m >_{00} < q_i >_{01}}{\omega_i} \tag{2.39}$$

The solutions for the non-zero integrals are found by solving the respective differential equation. This is a cumbersome task, so the known solutions will be employed directly, and can be found in table A.1.

Simplifying this expression gives:

$$a^{(1)}_{1,i} = \frac{V^{(1)}_i}{\sqrt{2}\omega_i^{3/2}} - \frac{1}{4\sqrt{2}\omega_i^{3/2}} \sum_{m=1}^{N} \frac{V^{(3)}_{imm}}{\omega_m} \tag{2.40}$$

For $r = 3$:

$$a_{3,i}^{(1)} = -\frac{V_i^{(1)} < q_i >_{03} + \frac{1}{6}V_{iii}^{(3)} < q_i^3 >_{03} + \frac{1}{2}\sum_{m=1;m\neq i}^{N} V_{imm}^{(3)} < q_m^2 >_{00} < q_i >_{03}}{3\omega_i} \tag{2.41}$$

Simplifying this expression gives:

$$a_{3,i}^{(1)} = -\frac{\sqrt{3}V_{iii}^{(3)}}{36\omega_i^{5/2}} \tag{2.42}$$

Likewise for $b_{rs,ij}^{(1)}$, we obtain:

$$\frac{\partial E^{(2)}}{\partial b_{rs,ij}^{(1)}} = \sum_{ij=1;i\neq j}^{N}\left[V_{iij}^{(3)} < q_i^2 >_{0r} < q_j >_{0s} + 2b_{rs,ij}^{(1)}\big(r\omega + s\omega\big)\right] = 0 \tag{2.43}$$

Giving:

$$b_{rs,ij}^{(1)} = -\frac{\frac{1}{2}V_{iij}^{(3)} < q_i^2 >_{0r} < q_j >_{0s}}{r\omega + s\omega} \tag{2.44}$$

The only non-zero expansion coefficient is $b_{21,ij}^{(1)}$, inserting the values of $< q_i^2 >_{02}$ and $< q_j >_{01}$:

$$b_{21,ij}^{(1)} = -\frac{V_{iij}^{(3)}}{4\omega_i\sqrt{\omega_j}(2\omega_i + \omega_j)} \tag{2.45}$$

Lastly, for $c_{rst,ijk}^{(1)}$:

$$\frac{\partial E^{(2)}}{\partial c_{rst,ijk}^{(1)}} = \sum_{ijk=1;i\neq j\neq k}^{N}\sum_{rst=1}^{\infty}\Bigg[\frac{1}{3}V_{ijk}^{(3)} < q_i >_{0r} < q_j >_{0s} < q_k >_{0t} + 2c_{rst,ijk}^{(1)}(r\omega + s\omega + t\omega)\Bigg] \tag{2.46}$$

Giving:

$$c^{(1)}_{rst,ijk} = -\frac{\frac{1}{6}V^{(3)}_{ijk} < q_i >_{0r} < q_j >_{0s} < q_k >_{0t}}{r\omega + s\omega + t\omega} \tag{2.47}$$

When inserting the correct values for the wavefunctions, Hamiltonians and energies, the only expansion coefficient surviving is $c^{(1)}_{111,ijk}$:

$$c^{(1)}_{111,ijk} = -\frac{\sqrt{2}V^{(3)}_{ijk}}{4\omega_i\sqrt{\omega_i\omega_j\omega_k}(\omega_i + \omega_j + \omega_k)} \tag{2.48}$$

2.7.3 The expression for $\Psi^{(1)}$

Inserting the coefficients evaluated, the first order perturbation of the wavefunction $\Psi^{(1)}$ becomes:

$$\begin{aligned}\Psi^{(1)} = \sum_{i=1}^{N} -\frac{\sqrt{3}V^{(3)}_{iii}}{36\omega_i^{5/2}}\phi_{3,i} + \left(\frac{V^{(1)}_i}{\sqrt{2}\omega_i^{3/2}} - \frac{1}{4\sqrt{2}\omega_i^{3/2}}\sum_{m=1}^{N}\frac{V^{(3)}_{imm}}{\omega_m}\right)\phi_{1,i} \\ + \sum_{\substack{i,j=1\\ i\neq j}}^{N} -\frac{V^{(3)}_{iij}}{4\omega_i\sqrt{\omega_j}(2\omega_i + \omega_j)}\phi_{21,ij} \\ + \sum_{\substack{i,j,k=1\\ i\neq j\neq k}}^{N} -\frac{\sqrt{2}V^{(3)}_{ijk}}{4\omega_i\sqrt{\omega_i\omega_j\omega_k}(\omega_i + \omega_j + \omega_k)}\phi_{111,ijk}\end{aligned} \tag{2.49}$$

With this, the accuracy of the wavefunction is in line with the one found in Ref [10]. The wavefunction will now be perturbed one step further in order to include a higher order of perturbation when finding expressions for the vibrational averaging of the properties.

2.8 Finding the expression for $\Psi^{(2)}$

2.8.1 The $E^{(3)}$ expression

Employing the same method as previously, the next energy perturbation serves as the starting point. The general expression for the energy perturbation of odd

potential is [56]:

$$\begin{aligned} E^{(2n+1)} = &\left\langle \psi^{(n)} | H^{(1)} - E^{(1)} | \psi^{(n)} \right\rangle + \langle \psi^{(0)} | H^{(2n+1)} | \psi^{(0)} \rangle \\ &+ \sum_{m=2}^{n+2} \sum_{k=n+1-m}^{n} \langle \psi^{(k)} | H^{(m)} - E^{(m)} | \psi^{(2n+1-k-m)} \rangle \end{aligned} \tag{2.50}$$

Inserting for $n = 1$:

$$\begin{aligned} E^{(3)} = \left\langle \psi^{(1)} | H^{(1)} - E^{(1)} | \psi^{(1)} \right\rangle + \langle \psi^{(0)} | H^{(3)} | \psi^{(0)} \rangle + 2\langle \psi^{(0)} | H^{(2)} - E^{(2)} | \psi^{(1)} \rangle \\ +2\langle \psi^{(1)} | H^{(2)} - E^{(2)} | \psi^{(0)} \rangle \end{aligned} \tag{2.51}$$

The third and fourth term cancel each other out. Recalling that $E^{(1)}$ is zero gives:

$$E^{(3)} = \left\langle \psi^{(1)} | H^{(1)} | \psi^{(1)} \right\rangle + \langle \psi^{(0)} | H^{(3)} | \psi^{(0)} \rangle \tag{2.52}$$

We insert the appropriate values into the expression:

$$\begin{aligned} E^{(3)} = &\sum_{i=1}^{N} a_{r,i}^{(1)} \left(V_i^{(1)} \langle q_i \rangle_{11} + \frac{1}{6} V_{iii}^{(3)} \langle q_i \rangle_{11} \langle q_j \rangle_{11} \langle q_k \rangle_{11} + \frac{1}{120} V_{iiiii}^{(5)} < q_i^5 >_{00} \right) \\ &+ \frac{1}{6} \sum_{ij=1}^{N} b_{rs,ij}^{(1)} \left(V_{iij}^{(3)} \left\langle q_i^2 \right\rangle_{11} \langle q_j \rangle_{11} + \frac{1}{120} V_{iiiij}^{(5)} < q_i^4 >_{00} < q_j >_{00} \right. \\ &\left. + \frac{1}{120} V_{iiijj}^{(5)} < q_i^3 >_{00} < q_j^2 >_{00} \right) \\ &+ \frac{1}{6} \sum_{i,j,k=1}^{N} c_{rst,ijk}^{(1)} \left(V_{ijk}^{(3)} \langle q_i \rangle_{11} \langle q_j \rangle_{11} \langle q_k \rangle_{11} \right. \\ &+ \frac{1}{120} V_{iiijk}^{(5)} < q_i^3 >_{00} < q_j >_{00} < q_k >_{00} \\ &\left. + \frac{1}{120} V_{iijjk}^{(5)} < q_i^2 >_{00} < q_j^2 >_{00} < q_k >_{00} \right) \end{aligned} \tag{2.53}$$

Each of these terms have at least one integral which evaluates to zero, therefore:

$$E^{(3)} = 0 \tag{2.54}$$

We are not left with any $\psi^{(2)}$ terms, $E^{(3)}$ can therefore not be used to find an expression for $\psi^{(2)}$, neither does $E^{(3)}$ contribute with any new values to the coefficients of $\psi^{(1)}$. We therefore progress to the fourth energy perturbation, denoted $E^{(4)}$.

2.8.2 The $E^{(4)}$ expression

The general form of the energy perturbations of an even order was:

$$\begin{aligned} E^{(2n)} &= \langle\Psi^{(0)}|H^{(2n)}|\Psi^{(0)}\rangle + 2\langle\Psi^{(n)}|H^{(1)} - E^{(1)}|\Psi^{(n-1)}\rangle \\ +2\sum_{m=2}^{n}\langle\Psi^{(n)}|H^{(m)} - E^{(m)}|\Psi^{(n-m)}\rangle &+ \langle\Psi^{(n)}|H^{(0)} - E^{(0)}|\Psi^{(n)}\rangle \end{aligned} \tag{2.55}$$

Inserting for $n = 2$, results in the following expression:

$$\begin{aligned} E^{(4)} &= \langle\Psi^{(0)}|H^{(4)}|\Psi^{(0)}\rangle + 2\langle\Psi^{(2)}|H^{(1)}|\Psi^{(1)}\rangle \\ +2\langle\Psi^{(2)}|H^{(2)}|\Psi^{(0)}\rangle &+ \langle\Psi^{(2)}|H^{(0)} - E^{(0)}|\Psi^{(2)}\rangle \end{aligned} \tag{2.56}$$

We start by filtering out the terms which include $a_{s,i}^{(2)}$ i.e. the parts of the $E^{(4)}$ expression involving $\Psi^{(2)}$ in equation 2.22.

$$\begin{aligned} E^{(4)}(a_{s,i}^{(2)}) = 2\sum_{i=1}^{N}\sum_{r,s=1}^{\infty} a_{s,i}^{(2)}a_{r,i}^{(1)}V_i^{(1)} < q_i >_{sr} + \frac{1}{3}\sum_{i=1}^{N}\sum_{r,s=1}^{\infty} a_{s,i}^{(2)}a_{r,i}^{(1)}V_{iii}^{(3)} < q_i^3 >_{sr} \\ + \frac{1}{12}\sum_{ijkl=1}^{N}\sum_{s=1}^{\infty} a_{s,i}^{(2)}V_{iiii}^{(4)} < q_i^4 >_{s0} + \sum_{i=1}^{N}\sum_{s=1}^{\infty} a_{s,i}^{(2)}a_{s,i}^{(2)} < H^0 - E^{(0)} >_{ss} \end{aligned} \tag{2.57}$$

We take the first derivative with respect to $a_{s,i}^{(2)}$ and set the expression to zero in order to find the minima for $a_{s,i}^{(2)}$,

$$\begin{aligned} 0 = 2\sum_{r}^{\infty} a_{r,i}^{(1)}V_i^{(1)} < q_i >_{sr} + \frac{1}{3}\sum_{r}^{\infty} a_{r,i}^{(1)}V_{iii}^{(3)} < q_i^3 >_{sr} \\ + \frac{1}{12}V_{iiii}^{(4)} < q_i^4 >_{s0} + 2\sum_{s=1}^{\infty} a_{s,i}^{(2)} < H^0 - E^{(0)} >_{ss} \end{aligned} \tag{2.58}$$

Only two values of $a^{(1)}_{r,i}$ survived: Namely $r = 1$, see Eq. 2.40 and $r = 3$, see Eq.(2.42). Rearranging the equation to obtain an expression for $a^{(2)}_{s,1}$ in addition to reducing to the correct number of values for r gives:

$$\begin{aligned} a^{(2)}_{s,i} = &-\frac{1}{s\omega_i}\Bigg(\sum_{r=1,3}(a^{(1)}_{r,i}V^{(1)}_i < q_i >_{sr} + \frac{1}{6}a^{(1)}_{r,i}V^{(3)}_{iii} < q^3_i >_{sr} \\ &+ \frac{1}{2}a^{(1)}_{r,i}\sum_{m=1,m\neq i}^{N} V^{(3)}_{imm} < q_i >_{sr} < q^2_m >_{00}) + \frac{1}{24}V^{(4)}_{iiii} < q^4_i >_{s0} \\ &+ \sum_{m=1,m\neq i}^{N} V^{(4)}_{iimm} < q^2_i >_{20} < q^2_m >_{00} \Bigg) \end{aligned} \tag{2.59}$$

The subscripts for s will now be evaluated. The non-zero terms for $a^{(2)}_{s,i}$ are: $a^{(2)}_{2,i}$, $a^{(2)}_{4,i}$, and $a^{(2)}_{6,i}$. We start by inserting the values of s for $a^{(2)}_{2,i}$. The expression becomes:

$$\begin{aligned} a^{(2)}_{2,i} = &\frac{1}{2\omega_i}\Bigg(- a^{(1)}_{1,i}V^{(1)}_i < q_i >_{21} + \frac{1}{6}a^{(1)}_{1,i}V^{(3)}_{iii} < q^3_i >_{21} + \frac{1}{2}a^{(1)}_{1,i}\sum_{m=1,m\neq i}^{N} V^{(3)}_{imm} < q_i >_{21} < q^2_m >_{00} \\ &- a^{(1)}_{3,i}V^{(1)}_i < q_i >_{23} + \frac{1}{6}a^{(1)}_{3,i}V^{(3)}_{iii} < q^3_i >_{23} + \frac{1}{2}\sum_{m=1,m\neq i}^{N} a^{(1)}_{3,i}V^{(3)}_{imm} < q_i >_{23} < q^2_m >_{00} \\ &- \frac{1}{24}V^{(4)}_{iiii} < q^4_i >_{20} + \sum_{m=1,m\neq i}^{N} V^{(4)}_{iimm} < q^2_i >_{20} < q^2_m >_{00} \Bigg) \end{aligned} \tag{2.60}$$

Inserting for the solutions to the hermite polynomial integrals:

$$\begin{aligned} a^{(2)}_{2,i} = &\frac{1}{2\omega}\Bigg[a^{(1)}_{1,i}\left(V^{(1)}_i(\frac{1}{\omega})^{\frac{1}{2}} + \frac{1}{6}V^{(3)}_{iii}\frac{3}{\omega^{3/2}} + \frac{1}{2}\sum_{m=1,m\neq i}^{N} V^{(3)}_{imm}(\frac{1}{\omega})^{\frac{1}{2}}\frac{1}{2\omega_m}\right) \\ &- a^{(1)}_{3,i}\left(V^{(1)}_i(\frac{3}{2\omega})^{\frac{1}{2}} + V^{(3)}_{iii}\frac{1}{2}(\frac{27}{8\omega^3})^{\frac{1}{2}} + \frac{1}{2}\sum_{m=1,m\neq i}^{N} a^{(1)}_{3,i}V^{(3)}_{imm}(\frac{3}{2\omega_i})^{\frac{1}{2}}\frac{1}{2\omega_m}\right) \\ &- V^{(4)}_{iiii}\frac{\sqrt{2}}{16\omega^2}2\omega + \sum_{m=1,m\neq i}^{N} V^{(4)}_{iimm}\frac{\sqrt{2}}{2\omega_i}\frac{1}{2\omega_m}\Bigg] \end{aligned} \tag{2.61}$$

Which is simplified in order to find the final expression. All expressions are simplified using the software *Scientific Workplace, MacKichan Software, Inc.*:

$$
\begin{aligned}
a_{2,i}^{(2)} =& - a_{1,i}^{(1)} \left(V_i^{(1)} \frac{1}{2\sqrt{\omega_i^3}} + V_{iii}^{(3)} \frac{1}{4\omega_i^{3/5}} + \frac{1}{8} \sum_{m=1,m\neq i}^{N} V_{imm}^{(3)} \frac{1}{\omega_m \sqrt{\omega_i^3}} \right) \\
& - a_{3,i}^{(1)} \left(V_i^{(1)} \frac{1}{2} (\frac{3}{2\omega_i^3})^{\frac{1}{2}} + V_{iii}^{(3)} \frac{1}{4} (\frac{27}{8\omega_i^5})^{\frac{1}{2}} + \frac{1}{8} \sum_{m=1,m\neq i}^{N} V_{imm}^{(3)} \frac{\sqrt{3}}{\omega_m \sqrt{2\omega_i^3}} \right) \\
& - V_{iiii}^{(4)} \frac{\sqrt{2}}{32\omega_i^3} + \sum_{m=1,m\neq i}^{N} V_{iimm}^{(4)} \frac{\sqrt{2}}{8\omega_m \omega_i^2}
\end{aligned} \tag{2.62}
$$

Moving onto the expansion coefficient $a_{4,i}^{(2)}$, we again start by replacing s, this time with 4. In the next step, the values for the hermite polynomials are added, the expression is then simplified:

$$
\begin{aligned}
a_{4,i}^{(2)} =& \frac{1}{4\omega_i} \Bigg(- \frac{1}{6} a_{1,i}^{(1)} V_{iii}^{(3)} < q_i^3 >_{41} + a_{3,i}^{(1)} V_i^{(1)} < q_i >_{43} - \frac{1}{6} a_{3,i}^{(1)} V_{iii}^{(3)} < q_i^3 >_{43} \\
& + \frac{1}{2} \sum_{m=1,m\neq i}^{N} a_{3,i}^{(1)} V_{imm}^{(3)} < q_i >_{43} < q_m^2 >_{00}) + \frac{1}{24} V_{iiii}^{(4)} < q_i^4 >_{40} \Bigg) \\
=& \frac{1}{4\omega_i} \Bigg(- \frac{1}{6} a_{1,i}^{(1)} V_{iii}^{(3)} \frac{\sqrt{3}}{\omega_i^{3/2}} + a_{3,i}^{(1)} V_i^{(1)} (\frac{2}{\omega_i})^{\frac{1}{2}} + \frac{1}{6} a_{3,i}^{(1)} V_{iii}^{(3)} 3 (\frac{4^3}{8\omega_i^3})^{\frac{1}{2}} \\
& - \frac{1}{2} \sum_{m=1,m\neq i}^{N} a_{3,i}^{(1)} V_{imm}^{(3)} \frac{\sqrt{2}}{2\omega_m \sqrt{\omega_i}} + \frac{1}{24} V_{iiii}^{(4)} \left(\frac{\sqrt{6}}{2\omega_i^2} \right) \Bigg) \\
=& - \frac{1}{24} a_{1,i}^{(1)} V_{iii}^{(3)} \frac{\sqrt{3}}{\omega_i^{3/5}} + a_{3,i}^{(1)} \left(V_i^{(1)} \frac{\sqrt{2}}{4\sqrt{\omega_i^3}} + V_{iii}^{(3)} \frac{1}{\sqrt{8\omega_i^3}} - \frac{1}{8} \sum_{m}^{N} V_{iii}^{(3)} \frac{\sqrt{2}}{2\omega_m \sqrt{\omega_i^3}} \right) \\
& + V_{iiii}^{(4)} \frac{\sqrt{6}}{192\omega_i^3}
\end{aligned} \tag{2.63}
$$

Lastely, the expression for $a_{6,i}^{(2)}$ will be evaluated, the same steps as for the first two expansion coefficients will be written out:

$$
\begin{aligned}
a_{6,i}^{(2)} &= - \frac{\frac{1}{6} a_{3,i}^{(1)} V_{iii}^{(3)} < q_i^3 >_{63}}{6\omega_i} \\
&= - \frac{\frac{1}{6} a_{3,i}^{(1)} V_{iii}^{(3)} (\frac{120}{8\omega_i^3})^{\frac{1}{2}}}{6\omega_i} \\
&= - \frac{\sqrt{15}}{36\omega_i^{5/2}} V_{iii}^{(3)} a_{3,i}^{(1)}
\end{aligned} \tag{2.64}
$$

All the non-zero constants $a^{(2)}_{s,i}$ have now been found. Next in turn are the $b^{(2)}_{rs,ij}$ expansion coefficients. For the first order wavefunction, there is only one non-zero $b^{(1)}_{rs,ij}$ coefficient, namely $b_{21,ij}$. This value can be inserted directly into the expression for $b^{(2)}_{rs,ij}$, with no need for sums and extra subscripts. Just as with $a^{(2)}_{s,i}$, we begin by isolating the terms containing $b^{(2)}_{rs,ij}$ from the general expression for $E^{(4)}$:

$$\begin{aligned} E^{(4)}(b^{(2)}_{rs,ij}) =& \frac{1}{3}\sum_{i,j=1}^{N} b^{(2)}_{rs,ij} b^{(1)}_{21,ij} V^{(3)}_{iij} < q_i^2 >_{r2} < q_j >_{s1} \\ &+ \frac{1}{12}\sum_{ij=1}^{N} b^{(2)}_{rs,ij} V^{(4)}_{iijj} < q_i^2 >_{s0} < q_j^2 >_{r0} \\ &+ \frac{1}{12}\sum_{ij=1}^{N} b^{(2)}_{rs,ij} V^{(4)}_{iiij} < q_i^3 >_{s0} < q_j >_{r0} \\ &+ \sum_{ij=1}^{N} b^{(2)}_{rs,ij} b^{(2)}_{rs,ij} (< H^0 - E^{(0)} >_{rr} + < H^0 - E^{(0)} >_{ss}) \end{aligned} \tag{2.65}$$

This expression is differentiated with respect to $b^{(2)}_{rs,ij}$ for a given ij, giving:

$$\begin{aligned} \frac{\partial E}{\partial b^{(2)}_{sr,ij}} =& 2 b^{(1)}_{21,ij} V^{(1)}_i < q_i >_{sr} + \frac{1}{3} b^{(1)}_{21,ij} V^{(3)}_{iij} < q_i^2 >_{r2} < q_j >_{s1} \\ &+ \frac{1}{12} b^{(2)}_{rs,ij} V^{(4)}_{iijj} < q_i^2 >_{s0} < q_j^2 >_{r0} \\ &+ \frac{1}{12} b^{(2)}_{rs,ij} V^{(4)}_{iiij} < q_i^3 >_{s0} < q_j >_{r0} + 2(b^{(2)}_{rs,ij} r\omega + s\omega) \end{aligned} \tag{2.66}$$

This expression is set to zero, the expression is then rearranged in order to find the minima for $b^{(2)}_{rs,ij}$:

$$\begin{aligned} b^{(2)}_{rs,ij} =& \frac{1}{r\omega_i + s\omega_j} \Bigg(-\frac{1}{6} b^{(1)}_{21,ij} V^{(3)}_{iij} < q_i^2 >_{2r} < q_j >_{s1} + \frac{1}{24} V^{(4)}_{iijj} < q_i^2 >_{r0} < q_j^2 >_{s0} \\ &- \frac{1}{24} V^{(4)}_{iiij} < q_i^3 >_{r0} < q_j >_{s0} + \frac{1}{8} \sum_{m=1, m\neq i}^{N} V^{(4)}_{iiij} < q_i >_{r0} < q_m^2 >_{00} < q_j >_{s0} \Bigg) \end{aligned} \tag{2.67}$$

There is a total of three non-zero values for $b^{(2)}_{rs,ij}$. At first glance there might seem to be more possibilities, but the fact that terms with different subscripts are

multiplied together results in only terms where all the hermitian polynomials are non-zero survive. All possible values for s are: $0, 1, 2$ and the possibilities for r are $0, 1, 2, 3$. The expansion coefficients $b^{(2)}_{10,ij}$, $b^{(2)}_{20,ij}$. and $b^{(2)}_{12,ij}$ become zero, as one of the values in every term is zero. The remaining expansion coefficients are : $b^{(2)}_{11,ij}$, $b^{(2)}_{22,ij}$, and $b^{(2)}_{31,ij}$. Starting with the expression for $b^{(2)}_{11,ij}$ and following the same steps as for $a^{(2)}_i$ we get:

$$\begin{aligned} b^{(2)}_{11,ij} =& \frac{1}{\omega_i + \omega_j} \Bigg(-\frac{1}{6} b^{(1)}_{21,ij} V^{(3)}_{iij} < q_i^2 >_{21} < q_j >_{11} + \frac{1}{24} V^{(4)}_{iijj} < q_i^2 >_{10} < q_j^2 >_{10} \\ & - \frac{1}{24} V^{(4)}_{iiij} < q_i^3 >_{10} < q_j >_{10} + \frac{1}{8} \sum_{m=1, m\neq i}^{N} V^{(4)}_{iiij} < q_i >_{10} < q_m^2 >_{00} < q_j >_{10} \Bigg) \end{aligned} \tag{2.68}$$

The first terms in this expression vanishes as both $< q_i^2 >_{21}$, and $< q_j >_{11}$ evaluates to zero. Similarily, both values in the second term, namely $< q_i^2 >_{01}$ and $< q_j^2 >_{01}$ are also zero, this leaves only the third and fourth term intact:

$$b^{(2)}_{11,ij} = -\frac{\frac{1}{24} V^{(4)}_{iiij} < q_i^3 >_{10} < q_j >_{10} + \frac{1}{8} \sum_{m=1, m\neq i}^{N} V^{(4)}_{iiij} < q_i >_{10} < q_m^2 >_{00} < q_j >_{10}}{\omega_i + \omega_j} \tag{2.69}$$

Inserting the appropriate solutions for the integrals and simplifying gives the final expression:

$$\begin{aligned} b^{(2)}_{11,ij} &= -\frac{\frac{1}{24} V^{(4)}_{iiij} \frac{3}{2\sqrt{2}\omega_i^{3/2}} \frac{1}{\sqrt{2}\omega_j^{1/2}} + \sum_{m=1, m\neq i}^{N} V^{(4)}_{iiij} \frac{1}{\sqrt{2}\omega_i^{1/2}} \frac{1}{2\omega_m} \frac{1}{\sqrt{2}\omega_j^{1/2}}}{\omega_i + \omega_j} \\ &= -\frac{V^{(4)}_{iiij}}{32\omega_i^{3/2}\omega_j^{1/2}(\omega_i + \omega_j)} + \sum_{m=1, m\neq i}^{N} \frac{V^{(4)}_{iiij}}{\sqrt{2}\omega_m 2\omega_i^{1/2} \sqrt{2}\omega_j^{1/2} (\omega_i + \omega_j)} \end{aligned} \tag{2.70}$$

Setting up the expression for the second expansion coefficient for $b^{(2)}$, namely $b^{(2)}_{22,ij}$, the equation becomes:

$$\begin{aligned} b^{(2)}_{22,ij} =& -\frac{\frac{1}{6} b^{(1)}_{21,ij} V^{(3)}_{iij} < q_i^2 >_{22} < q_j >_{12} + \frac{1}{24} V^{(4)}_{iijj} < q_i^2 >_{02} < q_j^2 >_{02}}{< H^0 - E^{(0)} >_{22} + < H^0 - E^{(0)} >_{22}} \\ & - \frac{\frac{1}{24} V^{(4)}_{iiij} < q_i^3 >_{02} < q_j >_{02}}{< H^0 - E^{(0)} >_{22} + < H^0 - E^{(0)} >_{22}} \end{aligned} \tag{2.71}$$

The third term vanishes as both $< q_i^3 >_{02}$ and $< q_j >_{02}$ are zero. Inserting the values of the remaining integrals, the expression is solved and simplified, yielding:

$$\begin{aligned} b_{22,ij}^{(2)} &= -\frac{\frac{1}{6}b_{21,ij}^{(1)}V_{iij}^{(3)}\frac{5}{2\omega_i}\frac{1}{\sqrt{\omega_j}} + \frac{1}{24}V_{iijj}^{(4)}\frac{\sqrt{2}}{2\omega_i}\frac{\sqrt{2}}{2\omega_j}}{2(\omega_i+\omega_j)} \\ &= -\frac{5b_{21,ij}^{(1)}V_{iij}^{(3)}}{24\omega_i\omega_j(\omega_i+\omega_j)} - \frac{V_{iijj}^{(4)}}{96\omega_i\omega_j(\omega_i+\omega_j)} \end{aligned} \tag{2.72}$$

The expression for $b_{31,ij}^{(2)}$ is:

$$b_{31,ij}^{(2)} = -\frac{\frac{1}{24}V_{iiij}^{(4)} < q_i^3 >_{03} < q_j >_{01}}{< H^0 - E^{(0)} >_{11} + < H^0 - E^{(0)} >_{33}} \tag{2.73}$$

$$= -\frac{\frac{1}{24}V_{iiij}^{(4)}(\frac{6}{8\omega_i^3})^{\frac{1}{2}}\frac{1}{\sqrt{2}\omega^{1/2}}}{3\omega_i+\omega_j} \tag{2.74}$$

$$= -\frac{\sqrt{6}V_{iiij}^{4}}{96\sqrt{\omega_i^3}\sqrt{\omega_j}(3\omega_i+\omega_j)} \tag{2.75}$$

The expression for $c_{rst,ijk}^{(2)}$ is found in the same manner as before. By setting the derivative of the expression to zero, these steps will be skipped and the equation for $c_{rst,ijk}^{(2)}$ is plainly written out:

$$\begin{aligned} c_{rst,ijk}^{(2)} = &-\frac{\frac{1}{6}c_{111,ijk}^{(1)}V_{ijk}^{(3)} < q_i >_{1r} < q_j >_{1s} < q_j >_{1t}}{< H^0 - E^{(0)} >_{rr} + < H^0 - E^{(0)} >_{ss} + < H^0 - E^{(0)} >_{tt}} \\ &-\frac{\frac{1}{24}V_{iijk}^{(4)} < q_i^2 >_{1r} < q_j >_{1s} < q_j >_{1t}}{< H^0 - E^{(0)} >_{rr} + < H^0 - E^{(0)} >_{ss} + < H^0 - E^{(0)} >_{tt}} \end{aligned} \tag{2.76}$$

The possible values for the subscripts of $c_{rst,ijk}^{(2)}$ are: $r = 0, 1, 2, 3$, $s = 0, 2$ and $t = 0, 2$, and all combinations of these. Some of these values will still disappear within the expression for $c_{rst,ijk}^{(2)}$, the r can not be 1 or 3. Thus the non-zero terms become: $c_{200,ijk}^{(2)}$, $c_{220,ijk}^{(2)}$,and $c_{222,ijk}^{(2)}$.

$$c^{(2)}_{200,ijk} = -\frac{\frac{1}{6}c^{(1)}_{111,ijk}V^{(3)}_{ijk} < q_i >_{12} < q_j >_{10} < q_j >_{10}}{< H^0 - E^{(0)} >_{00} + < H^0 - E^{(0)} >_{00} + < H^0 - E^{(0)} >_{00}} - \frac{\frac{1}{24}V^{(4)}_{iijk} < q_i^2 >_{12} < q_j >_{10} < q_j >_{10}}{< H^0 - E^{(0)} >_{22} + < H^0 - E^{(0)} >_{00} + < H^0 - E^{(0)} >_{00}} \tag{2.77}$$

The $< q_i^2 >_{12}$ integral is zero. The second terms will therefore disappear for all the values of the superscripts.

$$c^{(2)}_{200,ijk} = \frac{\frac{1}{6}c^{(1)}_{111,ijk}V^{(3)}_{ijk} < q_i >_{12} < q_j >_{10} < q_j >_{10}}{< H^0 - E^{(0)} >_{22} + < H^0 - E^{(0)} >_{00} + < H^0 - E^{(0)} >_{00}} \tag{2.78}$$

Inserting the correct terms we obtain:

$$c^{(2)}_{200,ijk} = \frac{\frac{1}{6}c^{(1)}_{111,ijk}V^{(3)}_{ijk}\frac{1}{\omega_i^{1/2}}\frac{1}{\sqrt{2}\omega_j^{1/2}}\frac{1}{\sqrt{2}\omega_k^{1/2}}}{2\omega_i} = \frac{c^{(1)}_{111,ijk}V^{(3)}_{ijk}}{24(\omega_i^{3/2})(\omega_j\omega_k)^{1/2}} \tag{2.79}$$

The other two terms are found similarly:

$$c^{(2)}_{220,ijk} = -\frac{\frac{1}{6}c^{(1)}_{111,ijk}V^{(3)}_{ijk} < q_i >_{12} < q_j >_{12} < q_k >_{10}}{< H^0 - E^{(0)} >_{22} + < H^0 - E^{(0)} >_{22} + < H^0 - E^{(0)} >_{00}} \tag{2.80}$$

$$= -\frac{\frac{1}{6}c^{(1)}_{111,ijk}V^{(3)}_{ijk}\frac{1}{\omega_i^{1/2}}\frac{1}{\omega_j^{1/2}}\frac{1}{\sqrt{2}\omega_k^{1/2}}}{2(\omega_i+\omega_j)} = -\frac{\frac{1}{6}c^{(1)}_{111,ijk}V^{(3)}_{ijk}}{12\sqrt{2}(\omega_i+\omega_j)(\omega_i\omega_j\omega_k)^{1/2}} \tag{2.81}$$

$$c^{(2)}_{222,ijk} = -\frac{\frac{1}{6}c^{(1)}_{111,ijk}V^{(3)}_{ijk} < q_i >_{12} < q_j >_{12} < q_j >_{12}}{< H^0 - E^{(0)} >_{22} + < H^0 - E^{(0)} >_{22} + < H^0 - E^{(0)} >_{22}} \tag{2.82}$$

$$= -\frac{\frac{1}{6}c^{(1)}_{111,ijk}V^{(3)}_{ijk}\frac{1}{\omega_1^{1/2}}\frac{1}{\omega_j^{1/2}}\frac{1}{\omega_k^{1/2}}}{2(\omega_i+\omega_j+\omega_j)} = -\frac{c^{(1)}_{111,ijk}V^{(3)}_{ijk}}{12(\omega_i+\omega_j+\omega_j)(\omega_i\omega_j\omega_j)^{1/2}} \tag{2.83}$$

Finding $d^{(2)}_{rstu,ijkl}$:

$$\frac{dE}{dd^{(2)}_{rstu,ijkl}} = \frac{1}{12}\sum_{ijkl=1}^{N} d^{(2)}_{rstu,ijkl}V^{(4)}_{ijkl} < q_i >_{r0} < q_j >_{s0} < q_k >_{t0} < q_l >_{u0} \\ +2\sum_{ijkl=1}^{N} d^{(2)}_{rstu,ijkl}d^{(2)}_{rstu,ijkl} < H^0 - E^{(0)} >_{ss} \tag{2.84}$$

Solving for $d^{(2)}_{rstu,ijkl}$:

$$d^{(2)}_{rstu,ijkl} = \frac{\frac{1}{24}V^{(4)}_{ijkl} < q_i >_{r0} < q_j >_{s0} < q_k >_{t0} < q_l >_{u0}}{< H^0 - E^{(0)} >_{rr} + < H^0 - E^{(0)} >_{ss} + < H^0 - E^{(0)} >_{tt} + < H^0 - E^{(0)} >_{uu}} \tag{2.85}$$

There is only one non-zero value for $d^{(2)}_{rstu,ijkl}$, namely $r = 1, s = 1, t = 1, u = 1$.

Inserting the correct values into the subscripts gives:

$$d^{(2)}_{1111,ijkl} = -\frac{\frac{1}{24}V^{(4)}_{ijkl} < q_i >_{10} < q_j >_{10} < q_k >_{10} < q_l >_{10}}{\omega_r + \omega_s + \omega_t + \omega_u} \tag{2.86}$$

The differential equations above have the following solutions:

$$d^{(2)}_{1111,ijkl} = -\frac{\sqrt{2}V^{(4)}_{ijkl}}{48(\omega_r\omega_s\omega_t\omega_u)^{1/2}(\omega_r + \omega_s + \omega_t + \omega_u)} \tag{2.87}$$

2.8.3 The expression for $\Psi^{(2)}$

The whole second order wavefunction has now been found. In all, there are nine expansion coefficients. These will not be inserted into the equation for $\Psi^{(2)}$, as the result will appear cluttered, but are summarized in the table 2.1.

2.9 Vibrationally averaged molecular properties

For an introduction to this topic, a review article written by C.J Jameson [53] is referred to, which gives a clear introductory account of the topic.

Table 2.1: The expansion coefficients found for the second order wavefunction $\Psi^{(2)}$

$a^{(2)}_{r,i}$	$a^{(2)}_{2,i} = -(a_{1,i}(\frac{1}{4\omega^{\frac{5}{2}}}V^3_{i^3} + \frac{1}{2\omega^{3/2}}V_i) + a_{3,i}(\frac{\sqrt{3}}{2\sqrt{2}\omega^{3/2}}V_i + \frac{\sqrt{27}}{8\sqrt{2}\omega^{5/2}}V^3_{i^3}) + \frac{\sqrt{2}}{32\omega^3}V^4_{i^4})$
	$a^{(2)}_{4,i} = -(\frac{1}{192}\frac{\sqrt{6}}{\omega^3}V^4_{i^4} + a_{1,i}\frac{1}{24}\frac{\sqrt{3}}{\omega^{\frac{5}{2}}}V^3_{i^3} + a_{3,i}(\frac{1}{4\omega}V_i\sqrt{\frac{2}{\omega}} + \frac{1}{8\omega}V^3_{i^3}\sqrt{\frac{8}{\omega^3}}))$
	$a^{(2)}_{6,i} = -\frac{\sqrt{15}}{36\omega^{5/2}}V^3_{iii}a_{3,i}$
$b^{(2)}_{rs,ij}$	$b^{(2)}_{11,ij} = \frac{V^4_{iiij}}{32\omega_i^{\frac{3}{2}}\sqrt{\omega_j}(r\omega_i+r\omega_j)}$
	$b^{(2)}_{22,ij} = -\frac{V^4_{iijj}}{96(r\omega_i^2\omega_j+r\omega_i\omega_j^2)} - \frac{b_{21,ij}5V^3_{iij}}{24\left(r\omega_i^2\omega_j+r\omega_i\omega_j^2\right)}$
	$b^{(2)}_{31,ij} = -\frac{\sqrt{6}V^4_{iiij}}{96\sqrt{\omega_i^3}\sqrt{\omega_j}(3\omega_i+\omega_j)}$
$c^{(2)}_{rst,ijk}$	$c^{(2)}_{200,ijk} = -\frac{c^{(1)}_{111,ijk}V^{(3)}_{ijk}}{24(\omega_i^{3/2})(\omega_j\omega_k)^{1/2}}$
	$c^{(2)}_{220,ijk} = -\frac{c_{111,ijk}\sqrt{2}V^3_{ijk}}{144(\omega_i+\omega_j)\sqrt{\omega_i\omega_j\omega_k}}$
	$c^{(2)}_{222,ijk} = -\frac{c_{111,ijk}V^3_{ijk}}{12(\omega_i+2\omega j)\sqrt{\omega_i\omega_j^2}}$
$d^{(2)}_{rstu,ijkl}$	$d^{(2)}_{1111,ijkl} = -\frac{\sqrt{2}V^{(4)}_{ijkl}}{48(\omega_r\omega_s\omega_t\omega_u)^{1/2}(\omega_r+\omega_s+\omega_t+\omega_u)}$

The property surface is extended by a Taylor series, analogous to the potential energy surface:

$$P = P^{(0)}_{\text{exp}} + \sum_{i}^{N} P^{(1)}_{i,\text{exp}} q_i + \sum_{ij}^{N} \frac{1}{2!} P^{(2)}_{ij,\text{exp}} q_i q_j + \sum_{ijk}^{N} \frac{1}{3!} P^{(3)}_{ijk,\text{exp}} q_i q_j q_k + ... \tag{2.88}$$

The property surface reflects the sensitivity of the electron distribution of the molecule. The $P_{ij,\text{exp}}$ denotes the derivative of the property surface, and can be thought of as the sensitivity of P to displacements of the nuclei away from the equilibrium, the "exp" subscript is referring to being at an arbitrary expansion point.

The expectation value for a property is found by using the following expression:

$$\langle P \rangle = \frac{\langle \Psi | P | \Psi \rangle}{\langle \Psi | \Psi \rangle} \tag{2.89}$$

In order to find $\langle P \rangle$, perturbation theory can be used as was first done by M. Toyama et al. [78]. Another alternative would be to use contact transformations [1], or Hellmann-Feynman theorem based methods [38]. Due to time constraint, only the Rayleigh Schrödinger perturbation theory based approach will be explored.

We start by performing a Taylor expansion of the zeroth order perturbation of the property, the first few terms are defined:

$$\begin{aligned}
T^{(0)} &= P^{(0,0)}_{\text{exp}} \\
T^{(1)} &= \sum_{i=1}^{N} P^{(0,1)}_{i,\text{exp}} q_i \\
T^{(2)} &= \frac{1}{2} \sum_{i,j=1}^{N} P^{(0,2)}_{ij,\text{exp}} q_i q_j \\
T^{(3)} &= \frac{1}{6} \sum_{i,j,k=1}^{N} P^{(0,3)}_{ijk,\text{exp}} q_i q_j q_k
\end{aligned} \tag{2.90}$$

Where the first of the superscripts denotes that we are at the zero order perturbation of the wavefunction, the second denotes the derivative of the property surface. Using the notation above, we set up the molecular electronic property surface, analogous to the to the potential energy surface.

$$P^{(0)}(q_1, q_2, ..., q_N) = \sum_{n}^{\infty} P^{(0,n)} = T^{(0)} + T^{(1)} + T^{(2)} + T^{(3)} + [...] \tag{2.91}$$

The property expectation value near equilibrium can be expressed as a multidimensional power series. Both the numerator and the denominator is expanded about $\Psi^{(0)}$. For the numerator this becomes:

$$\left\langle P^{(m,n)}_{\text{numerator}} \right\rangle = \left[\sum_{k=0}^{m} \left\langle \Psi^{(k)} | T^{(n)} | \Psi^{(m-k)} \right\rangle \right] \tag{2.92}$$

The first value in the subscript denotes perturbation order, while the second denotes the derivation order. For the denominator we start by writing out the general expression:

$$\left\langle P^{(m,n)}_{\text{denominator}} \right\rangle = \frac{1}{\langle \Psi^{(0)} + \lambda\Psi^{(1)} + \lambda^2\Psi^{(2)} + ... | \Psi^{(0)} + \lambda\Psi^{(1)} + \lambda^2\Psi^{(2)} + ... \rangle} \tag{2.93}$$

For the zeroth order perturbation, the denominator evaluates to:

$$\left\langle P^{(0,n)}_{\text{denominator}} \right\rangle = \frac{1}{\langle \Psi^{(0)} | \Psi^{(0)} \rangle} = 1 \tag{2.94}$$

For the first order:

$$\begin{aligned} \left\langle P^{(1,n)}_{\text{denominator}} \right\rangle =& \frac{1}{\langle \Psi^{(0)} + \Psi^{(1)} | \Psi^{(0)} + \Psi^{(1)} \rangle} \\ =& \frac{1}{\langle \Psi^{(0)} | \Psi^{(0)} \rangle + 2 \langle \Psi^{(1)} | \Psi^{(0)} \rangle + \langle \Psi^{(1)} | \Psi^{(1)} \rangle} \end{aligned} \tag{2.95}$$

The $\langle \Psi^{(0)} | \Psi^{(0)} \rangle$ equals to 1 and $\Psi^{(0)}$ is orthogonal to $\Psi^{(1)}$, the equation can be simplified to:

$$\left\langle P^{(1,n)}_{\text{denominator}} \right\rangle = 1 + \frac{1}{\langle \lambda\Psi^{(1)} | \lambda\Psi^{(1)} \rangle} = 1 + \frac{1}{1-x} \tag{2.96}$$

Taylor expanding $\frac{1}{1-x}$ gives:

$$\left\langle P^{(1,n)}_{\text{denominator}} \right\rangle = 1 + x - (x-1)\frac{1}{(1-x)^2} = 1 \tag{2.97}$$

The denominator for the second perturbation is:

$$\begin{aligned}\left\langle P^{(2,n)}_{\text{denominator}} \right\rangle =& \frac{1}{\langle \Psi^{(0)} + \lambda\Psi^{(1)} + \lambda^2\Psi^{(2)} | \Psi^{(0)} + \lambda\Psi^{(1)} + \lambda^2\Psi^{(2)} \rangle} \\ =& 1 + \frac{1}{\langle \lambda^2\Psi^{(2)} | \lambda^2\Psi^{(2)} \rangle} \\ =& 1 + \frac{1}{(1-x-x^2)^2}\end{aligned} \tag{2.98}$$

A Taylor expansion of both the numerator and the denominator of Eq.(2.89) up to second order has now been made. The zeroth order perturbation will closely follow the procedure of Åstrand et al. [10], but the perturbation will be taken one step further so as to utilize the analytical cubic and quartic force field available.

2.9.1 Zeroth order perturbation

The zeroth order perturbation will have the following form:

$$\left\langle P^{(0,n)} \right\rangle = \left\langle \Psi^{(0)} | T^{(n)} | \Psi^{(0)} \right\rangle \tag{2.99}$$

Expanding this for values of n gives:

$$\sum_{n=0}^{\infty} \left\langle P^{(0,n)} \right\rangle = \left\langle T^{(0)} \right\rangle + \left\langle T^{(1)} \right\rangle + \left\langle T^{(2)} \right\rangle + ... \tag{2.100}$$

The term $\left\langle T^{(1)} \right\rangle$ is zero as this evaluates to $\left\langle \sum_{i=1}^{\infty} P^{(1)} q_i \right\rangle_{00} = 0$. The other terms have the following values:

$$\sum_{n=0}^{\infty} \left\langle P^{(0,n)} \right\rangle = P^{(0)}_{\text{exp}} + \frac{1}{4}\sum_{i=1}^{N} \frac{P^{(2)}_{\text{exp}}}{\omega_i} + [...] \tag{2.101}$$

It is sufficient to expand up to $P^{(2)}_{\text{exp}}$, as we shall truncate at this Taylor expansion of the property.

2.9.2 First order perturbation

Finding the first order term with use of Eq (2.97):

$$\begin{aligned}\left\langle P^{(1,n)}\right\rangle &= \left\langle \Psi^{(0)}|T^{(n)}|\Psi^{(1)}\right\rangle + \left\langle \Psi^{(1)}|T^{(n)}|\Psi^{(0)}\right\rangle \\ &= 2\left\langle \Psi^{(0)}|T^{(n)}|\Psi^{(1)}\right\rangle \end{aligned} \tag{2.102}$$

The terms needed are therefore:

$$\sum_{n=0}^{\infty}\left\langle P^{(1,n)}\right\rangle = 2\left\langle T^{(0)}\right\rangle_{01} + 2\left\langle T^{(1)}\right\rangle_{01} + 2\left\langle T^{(2)}\right\rangle_{01} + 2\left\langle T^{(3)}\right\rangle_{01} + ... \tag{2.103}$$

The first term is evaluated to $2P^{(0)}$. The third term is evaluated to $P_{ii}^{(2)}\left\langle q_i^2\right\rangle_{01}$ and is thus zero. These two will therefore not be evaluated further. Writing out $2\left\langle T^{(1)}\right\rangle_{01}$ gives:

$$\begin{aligned}2\left\langle T^{(1)}\right\rangle_{01} &= 2\sum_{i=1}^{N} P_{i,\mathrm{exp}}^{(1)}\left\langle q_i\right\rangle_{01} \\ &= \sqrt{2}\sum_{i=1}^{N}\frac{P_{i,\mathrm{exp}}^{(1)}a_{1,i}^{(1)}}{\sqrt{\omega_i}}\end{aligned} \tag{2.104}$$

2.9.3 Second order perturbation

Next, the second order contribution will be found. We are able to find up to the second order contribution as we have expressions for up to the second order perturbation of the wavefunction.

$$\begin{aligned}\left\langle P^{(2,n)}\right\rangle = &\left[\left\langle \Psi^{(0)}|T^{(n)}|\Psi^{(2)}\right\rangle + \left\langle \Psi^{(1)}|T^{(n)}|\Psi^{(1)}\right\rangle + \left\langle \Psi^{(2)}|T^{(n)}|\Psi^{(0)}\right\rangle\right] \\ &\times\left[1+\sum_{p=1}^{m}\sum_{l=0}^{m}(-1)^n\left(\left\langle \Psi^{(l)}|T^{(n)}|\Psi^{(l)}\right\rangle\right)^n\right]\end{aligned} \tag{2.105}$$

Expanding the equation:

$$\begin{aligned}\left\langle P^{(2,n)}\right\rangle = &\left[2\left\langle\Psi^{(0)}|T^{(n)}|\Psi^{(2)}\right\rangle + \left\langle\Psi^{(1)}|T^{(n)}|\Psi^{(1)}\right\rangle\right] \\ &\times\left[\sum_{p=1}^{m}\sum_{l=0}^{m}(-1)^n\left(\left\langle\Psi^{(l)}|T^{(n)}|\Psi^{(l)}\right\rangle\right)^n\right]\end{aligned} \tag{2.106}$$

Evaluating the normalization factor, $P_m^{(2)}$ becomes:

$$\left\langle P_m^{(2)}\right\rangle = 2\left\langle\Psi^{(0)}|T^{(n)}|\Psi^{(2)}\right\rangle + \left\langle\Psi^{(1)}|T^{(n)}|\Psi^{(1)}\right\rangle \tag{2.107}$$

We have access to both the first and the second derivative of P, we therefore want to find expression for $P_0^{(2)}$, $P_1^{(2)}$ and $P_2^{(2)}$. Starting by writing out the expression for $P_0^{(2)}$:

$$\left\langle P_0^{(2)}\right\rangle = 2\left\langle\Psi^{(0)}|T^{(0)}|\Psi^{(2)}\right\rangle + \left\langle\Psi^{(1)}|T^{(0)}|\Psi^{(1)}\right\rangle - \left\langle\Psi^{(0)}|T^{(0)}|\Psi^{(0)}\right\rangle \tag{2.108}$$

As a result of the orthonormality properties of the wavefunction, the first term is zero. The second and third terms both evaluate to $P_0 \times 1$, and thereby cancel each other out. As we remain with no non-zero terms we conclude with:

$$\left\langle P_0^{(2)}\right\rangle = 0 \tag{2.109}$$

Next, the expression for $P_1^{(2)}$ is written out:

$$\left\langle P_1^{(2)}\right\rangle = 2\left\langle\Psi^{(0)}|P_1|\Psi^{(2)}\right\rangle + \left\langle\Psi^{(1)}|P_1|\Psi^{(1)}\right\rangle - \left\langle\Psi^{(0)}|P_1|\Psi^{(0)}\right\rangle \tag{2.110}$$

Inserting the expression of P_1, found in equation(2.91) gives:

$$\begin{aligned}\left\langle P_1^{(2)}\right\rangle = 2\left\langle\Psi^{(0)}|\sum_{i=1}^{N}P_i^{(1)}q_i|\Psi^{(2)}\right\rangle + &\left\langle\Psi^{(1)}|\sum_{i=1}^{N}P_i^{(1)}q_i|\Psi^{(1)}\right\rangle \\ &- \left\langle\Psi^{(0)}|\sum_{i=1}^{N}P_i^{(1)}q_i|\Psi^{(0)}\right\rangle\end{aligned} \tag{2.111}$$

According to the symmetry rules we see that all three of these terms evaluate to zero; $\langle q\rangle_{02} = 0$, $\langle q\rangle_{11} = 0$, and $\langle q\rangle_{00} = 0$, therefore concluding with:

$$\left\langle P_1^{(2)}\right\rangle = 0 \tag{2.112}$$

Lastly, writing out the expression for $P_2^{(2)}$:

$$\left\langle P_2^{(2)} \right\rangle = \left\langle \Psi^{(0)} | P_2 | \Psi^{(2)} \right\rangle + \left\langle \Psi^{(1)} | P_2 | \Psi^{(1)} \right\rangle + \left\langle \Psi^{(2)} | P_2 | \Psi^{(0)} \right\rangle \tag{2.113}$$

Inserting the value of $P_2^{(2)}$, found in equation(2.91) gives:

$$\begin{aligned} \left\langle P_2^{(2)} \right\rangle = \sum_{i,j=1}^{N} \Bigg(& \left\langle \Psi^{(0)} | \frac{1}{2} P_{ij}^{(2)} q_i q_j | \Psi^{(2)} \right\rangle \\ & + \left\langle \Psi^{(1)} | \frac{1}{2} P_{ij}^{(2)} q_i q_j | \Psi^{(1)} \right\rangle + \left\langle \Psi^{(2)} | \frac{1}{2} P_{ij}^{(2)} q_i q_j | \Psi^{(0)} \right\rangle \Bigg) \end{aligned} \tag{2.114}$$

Inserting the value of $\Psi^{(2)}$ in the first of the three terms:

$$\begin{aligned} \sum_{i,j=1}^{N} \left\langle \Psi^{(0)} | \frac{1}{2} P_{ij}^{(2)} q_i q_j | \Psi^{(2)} \right\rangle = & \, a_{2,i}^{(2)} \left\langle \Psi^{(0)} | \sum_{i=1}^{N} \frac{1}{2} P_{ii}^{(2)} q_i^2 | \Psi^{(0)} \right\rangle \\ & + a_{4,i}^{(2)} \left\langle \Psi^{(0)} | \sum_{i=1}^{N} \frac{1}{2} P_{ii}^{(2)} q_i^2 | \Psi^{(0)} \right\rangle \\ & + a_{6,i}^{(2)} \left\langle \Psi^{(0)} | \sum_{i=1}^{N} \frac{1}{2} P_{ii}^{(2)} q_i^2 | \Psi^{(0)} \right\rangle \\ & + b_{11,ij}^{(2)} \left\langle \Psi^{(0)} | \sum_{i,j=1, i \neq j}^{N} \frac{1}{2} P_{ij}^{(2)} q_i q_j | \Psi^{(0)} \right\rangle \\ & + b_{22,ij}^{(2)} \left\langle \Psi^{(0)} | \sum_{i,j=1, i \neq j}^{N} \frac{1}{2} P_{ij}^{(2)} q_i q_j | \Psi^{(0)} \right\rangle \\ & + b_{31,ij}^{(2)} \left\langle \Psi^{(0)} | \sum_{i,j=1, i \neq j}^{N} \frac{1}{2} P_{ij}^{(2)} q_i q_j | \Psi^{(0)} \right\rangle \end{aligned} \tag{2.115}$$

Pulling out the constants from the integral, the following expression is obtained:

$$\begin{aligned}\sum_{i,j=1}^{N}\left\langle \Psi^{(0)}|\frac{1}{2}P_{ij}^{(2)}q_iq_j|\Psi^{(2)}\right\rangle &= \sum_{i=1}^{N}a_{2,i}^{(2)}\frac{1}{2}P_{ii}^{(2)}\left\langle q_i^2\right\rangle_{02} \\ &+\sum_{i=1}^{N}a_{4,i}^{(2)}\frac{1}{2}P_{ii}^{(2)}\left\langle q_i^2\right\rangle_{04} \\ &+\sum_{i=1}^{N}a_{6,i}^{(2)}\frac{1}{2}P_{ii}^{(2)}\left\langle q_i^2\right\rangle_{06} \\ &+\sum_{i,j=1,i\neq j}^{N}b_{11,ij}^{(2)}\frac{1}{2}P_{ij}^{(2)}\left\langle q_i\right\rangle_{01}\left\langle q_j\right\rangle_{01} \\ &+\sum_{i,j=1,i\neq j}^{N}b_{22,ij}^{(2)}\frac{1}{2}P_{ij}^{(2)}\left\langle q_i\right\rangle_{02}\left\langle q_j\right\rangle_{02} \\ &+\sum_{i,j=1,i\neq j}^{N}b_{31,ij}^{(2)}\frac{1}{2}P_{ij}^{(2)}\left\langle q_i\right\rangle_{03}\left\langle q_j\right\rangle_{01}\end{aligned} \tag{2.116}$$

Filling in the values for the integrals the final expression for $\left\langle \Psi^{(0)}|\frac{1}{2}P_{ij}^{(2)}q_iq_j|\Psi^{(2)}\right\rangle$ becomes:

$$\begin{aligned}\sum_{i,j=1}^{N}\left\langle \Psi^{(0)}|\frac{1}{2}P_{ij}^{(2)}q_iq_j|\Psi^{(2)}\right\rangle &= \sum_{i=1}^{N}a_{2,i}^{(2)}\frac{1}{2}P_{ii}^{(2)}\frac{\sqrt{2}}{2\omega_i} \\ &+\sum_{i,j=1,i\neq j}^{N}b_{11,ij}^{(2)}\frac{1}{2}P_{ii}^{(2)}\frac{1}{2\omega_i^{1/2}\omega_j^{1/2}} \\ &+\sum_{i,j=1,i\neq j}^{N}b_{31,ij}^{(2)}\frac{1}{2}P_{ij}^{(2)}\frac{\sqrt{2}}{2\omega_j}\end{aligned} \tag{2.117}$$

The second term for $P^{(2)}$, namely $\left\langle \Psi^{(1)}|P_2|\Psi^{(1)}\right\rangle$, will now be evaluated:

$$\begin{aligned}\sum_{i,j=1}^{N}\left\langle\Psi^{(1)}|\frac{1}{2}P_{ij}^{(2)}q_iq_j|\Psi^{(1)}\right\rangle &= \sum_{i=1}^{N}a_{1,i}^{(1)}a_{1,i}^{(1)}\left\langle\Psi^{(0)}|\frac{1}{2}P_{ii}^{(2)}q_i^2|\Psi^{(0)}\right\rangle \\ &+\sum_{i=1}^{N}a_{1,i}^{(1)}a_{3,i}^{(1)}\left\langle\Psi^{(0)}|\frac{1}{2}P_{ii}^{(2)}q_i^2|\Psi^{(0)}\right\rangle \\ &+\sum_{i=1}^{N}a_{3,i}^{(1)}a_{3,i}^{(1)}\left\langle\Psi^{(0)}|\frac{1}{2}P_{ii}^{(2)}q_i^2|\Psi^{(0)}\right\rangle \\ &+\sum_{i,j=1,i\neq j}^{N}b_{21,ij}^{(1)}b_{21,ij}^{(1)}\left\langle\Psi^{(0)}|\frac{1}{2}P_{ij}^{(2)}q_iq_j|\Psi^{(0)}\right\rangle\end{aligned} \tag{2.118}$$

Pulling out the constants from the integral as previously:

$$\begin{aligned}\left\langle\Psi^{(1)}|\frac{1}{2}P_{ij}^{(2)}q_iq_j|\Psi^{(1)}\right\rangle &= \sum_{i=1}^{N}a_{1,i}^{(1)}a_{1,i}^{(1)}\frac{1}{2}P_{ii}^{(2)}\left\langle q_i^2\right\rangle_{11} \\ &+\sum_{i=1}^{N}a_{1,i}^{(1)}a_{3,i}^{(1)}\frac{1}{2}P_{ii}^{(2)}\left\langle q_i^2\right\rangle_{13} \\ &+\sum_{i=1}^{N}a_{3,i}^{(1)}a_{3,i}^{(1)}\frac{1}{2}P_{ii}^{(2)}\left\langle q_i^2\right\rangle_{33} \\ &+\sum_{i,j=1,i\neq j}^{N}b_{21,ij}^{(1)}b_{21,ij}^{(1)}\frac{1}{2}P_{ij}^{(2)}\left\langle q_i\right\rangle_{11}\left\langle q_i\right\rangle_{22}\end{aligned} \tag{2.119}$$

Evaluating gives:

$$\sum_{i,j=1}^{N}\left\langle\Psi^{(1)}|\frac{1}{2}P_{ij}^{(2)}q_iq_j|\Psi^{(1)}\right\rangle = \sum_{i=1}^{N}P_{ii}^{(2)}\frac{1}{2\omega_i}\left(\frac{2}{3}a_{1,i}^{(1)}a_{1,i}^{(1)}+\frac{\sqrt{3}}{2}a_{1,i}^{(1)}a_{3,i}^{(1)}+\frac{2}{5}a_{3,i}^{(1)}a_{3,i}^{(1)}\right) \tag{2.120}$$

The third term for $P_2^{(2)}$ is $-\left\langle\Psi^{(0)}|P_1|\Psi^{(0)}\right\rangle\left\langle\Psi^{(1)}|\Psi^{(1)}\right\rangle$. If the $\Psi^{(1)}$ has been evaluated correctly, $\left\langle\Psi^{(1)}|\Psi^{(1)}\right\rangle$ equals 1.

$$
\begin{aligned}
-\left\langle \Psi^{(0)}|P_2|\Psi^{(0)}\right\rangle &= \sum_{i=1}^{N} P_{ii}^{(2)} \left\langle \Psi^{(0)}|q_i^2|\Psi^{(0)}\right\rangle \\
&= \sum_{i=1}^{N} P_{ii}^{(2)} \left\langle q_i^2 \omega_i e^{-\omega_i q^2}\right\rangle \qquad (2.121)\\
&= -\sum_{i=1}^{N} P_{ii}^{(2)} \frac{\sqrt{\omega_i}}{\sqrt{\pi}} \frac{\sqrt{\pi}}{2\omega^{3/2}} \\
&= -\sum_{i=1}^{N} P_{ii}^{(2)} \frac{1}{2\omega_i} \qquad (2.122)
\end{aligned}
$$

Combining all of the above expressions, we obtain the final expression for $P_2^{(2)}$:

$$
\begin{aligned}
\left\langle P_2^{(2)}\right\rangle = \sum_{i=1}^{N} a_{2,i}^{(2)} \frac{\sqrt{2}P_{ii}^{(2)}}{4\omega_i} + \frac{P_{ii}^{(2)}}{3\omega}\left(a_{1,i}^{(1)}a_{1,i}^{(1)} + a_{1,i}^{(1)}a_{3,i}^{(1)} + a_{3,i}^{(1)}a_{3,i}^{(1)}\right) - \frac{P_{ii}^{(2)}}{2\omega} \\
+ \sum_{i,j=1,i\neq j}^{N} b_{11,ij}^{(2)} \frac{P_{ij}^{(2)}}{4\omega_i^{1/2}\omega_j^{1/2}} + b_{31,ij}^{(2)} \frac{\sqrt{2}P_{ij}^{(2)}}{4\omega_j} \qquad (2.123)
\end{aligned}
$$

2.10 Property corrections at specific geometries

So far, the expressions found are valid for any expansion point, i.e, any geometry. We will now see how these expressions are simplified by considering certain geometries, more concretely, the equilibrium and the effective geometry.

2.10.1 Equilibrium geometry

Recalling that at the equilibrium, $V^{(1)} = 0$, we will therefore set all the gradients to zero. We will only consider the expansion coefficients that changes with the new geometry, i.e. the ones containing $V^{(1)}$. For the first order coefficients there is one of them $a_{1,i}^{(1)}$, for the second order coefficients there are two, namely $a_{2,i}^{(2)}$ and $a_{4,i}^{(2)}$:

Starting with $a_{1,i,}^{(1)}$, the expression at equilibrium becomes:

$$
a_{1,i,\mathrm{eq}}^{(1)} = -\frac{1}{4\sqrt{2}\omega_i^{3/2}} \sum_{m=1}^{N} \frac{V_{imm}^{(3)}}{\omega_m} \qquad (2.124)
$$

This will also effect all the second order coefficients that contain $a^{(1)}_{1,i,}$, simplifying them. For the second order coefficients, we obtain the following simplified coefficients:

$$\begin{aligned} a^{(2)}_{2,i,\mathrm{eq}} =& - a^{(1)}_{1,i,\mathrm{eq}} \left(V^{(3)}_{iii} \frac{1}{4\omega_i^{3/5}} + \frac{1}{8} \sum_{m=1,m\neq i}^{N} V^{(3)}_{imm} \frac{1}{\omega_m \sqrt{\omega_i^3}} \right) \\ & - a^{(1)}_{3,i,\mathrm{eq}} \left(V^{(3)}_{iii} \frac{\sqrt{27}}{\sqrt{32}\omega_i^{\frac{5}{2}}} + \frac{1}{8} \sum_{m=1,m\neq i}^{N} V^{(3)}_{imm} \frac{\sqrt{3}}{\omega_m \sqrt{2\omega_i^3}} \right) \\ & - V^{(4)}_{iiii} \frac{\sqrt{2}}{32\omega_i^3} + \sum_{m=1,m\neq i}^{N} V^{(4)}_{iimm} \frac{\sqrt{2}}{8\omega_m \omega_i^2} \end{aligned} \tag{2.125}$$

and:

$$\begin{aligned} a^{(2)}_{4,i,\mathrm{eq}} =& - \frac{1}{24} a^{(1)}_{1,i,\mathrm{eq}} V^{(3)}_{iii} \frac{\sqrt{3}}{\omega_i^{3/5}} + a^{(1)}_{3,i,\mathrm{eq}} \left(V^{(3)}_{iii} \frac{1}{\sqrt{8\omega_i^3}} - \frac{1}{24} \sum_{m}^{N} V^{(3)}_{iii} \frac{\sqrt{2}}{2\omega_m \sqrt{\omega_i^3}} \right) \\ & + V^{(4)}_{iiii} \frac{\sqrt{6}}{192\omega_i^3} \end{aligned} \tag{2.126}$$

The expression for the vibrationally averaged properties themselves, however, does not change and remains identical to the Eq. (2.123).

2.10.2 Effective geometry

At the effective geometry, the criteria $V^{(1)}_{\mathrm{eff},j} + \frac{1}{4} \sum_{i=1}^{N} \frac{V^{(3)}_{\mathrm{eff},iij}}{\omega_i} = 0$ is valid. With this in mind $a^{(1)}_{1,i}$ can be shown to disappear altogether:

$$a^{(1)}_{1,i} = \frac{1}{\sqrt{2}\omega_i^{3/2}} \left(V^{(1)} - \frac{1}{4} \sum_{m=1}^{N} \frac{V^{(3)}_{imm}}{\omega_m} \right) = 0 \tag{2.127}$$

This also entails that all terms involving $a^{(1)}_{1,i}$ are zero for the effective geometry. The expression for the property correction will therefore also take on a different form for the effective geometry (beyond only the coefficients changing). For the second order coefficients, these reduce to far simpler expressions:

$$a_{2,i}^{(2)} = -a_{1,i}^{(1)} \frac{1}{2\sqrt{\omega_i^3}} \left(V_i^{(1)} + \frac{1}{4} \sum_{m=1,m\neq i}^{N} \frac{V_{imm}^{(3)}}{\omega_m} \right) - a_{1,i}^{(1)} V_{iii}^{(3)} \frac{1}{4\omega_i^{3/5}}$$
$$-a_{3,i}^{(1)} \frac{1}{2} \frac{\sqrt{3}}{\sqrt{2\omega_i^3}} \left(V_i^{(1)} + \frac{1}{4} \sum_{m=1,m\neq i}^{N} \frac{V_{imm}^{(3)}}{\omega_m} \right) - a_{3,i}^{(1)} V_{iii}^{(3)} \frac{1}{4} (\frac{27}{8\omega_i^5})^{\frac{1}{2}}$$
$$-V_{iiii}^{(4)} \frac{\sqrt{2}}{32\omega_i^3} + \sum_{m=1,m\neq i}^{N} V_{iimm}^{(4)} \frac{\sqrt{2}}{8\omega_m \omega_i^2} \tag{2.128}$$

Here we have rearranged the equation to convincingly show that four of the terms in the above equations become zero, two of them as a consequence of containing $a_{1,i}^{(1)}$:

$$a_{2,i,\text{eff}}^{(2)} = -\frac{3\sqrt{3} a_{3,i}^{(1)} V_{iii}^{(3)}}{8\sqrt{2}\omega_i^{5/2}} - V_{iiii}^{(4)} \frac{\sqrt{2}}{32\omega_i^3} + \sum_{m=1,m\neq i}^{N} V_{iimm}^{(4)} \frac{\sqrt{2}}{8\omega_m \omega_i^2} \tag{2.129}$$

Comparing equation Eq.(2.125) and Eq.(2.129), we see that choosing to expand around the effective geometry greatly reduces the complexity of the equation for the second order perturbation. The largest four terms are omitted when perturbating around the effective geometry. For $a_{4,i}^{(2)}$ it can also be shown to reduce to a simpler expression:

$$a_{4,i}^{(2)} = -\frac{1}{24} a_{1,i}^{(1)} V_{iii}^{(3)} \frac{\sqrt{3}}{\omega_i^{3/5}} + \frac{1}{4} \frac{\sqrt{2}}{\sqrt{\omega_i^3}} a_{3,i}^{(1)} \left(V_i^{(1)} - \frac{1}{4} \sum_{m}^{N} \frac{V_{iim}^{(3)}}{\omega_m} \right)$$
$$+ a_{3,i}^{(1)} V_{iii}^{(3)} \frac{1}{\sqrt{8\omega_i^3}} + V_{iiii}^{(4)} \frac{\sqrt{6}}{192\omega_i^3} \tag{2.130}$$

$$a_{4,i,\text{eff}}^{(2)} = a_{3,i}^{(1)} V_{iii}^{(3)} \frac{1}{\sqrt{8\omega_i^3}} + V_{iiii}^{(4)} \frac{\sqrt{6}}{192\omega_i^3} \tag{2.131}$$

The expression for the property correction at the effective geometry is simplified to:

$$\left\langle P_2^{(2)} \right\rangle = \sum_{i=1}^{N} a_{2,i}^{(2)} \frac{\sqrt{2} P_{ii}^{(2)}}{4\omega_i} + \frac{P_{ii}^{(2)}}{5\omega_i} \left(a_{3,i}^{(1)} a_{3,i}^{(1)} \right) - \frac{P_{ii}^{(2)}}{2\omega_i}$$
$$+ \sum_{i,j=1,i\neq j}^{N} b_{11,ij}^{(2)} \frac{P_{ij}^{(2)}}{4\omega_i^{1/2}\omega_j^{1/2}} + b_{31,ij}^{(2)} \frac{\sqrt{2} P_{ij}^{(2)}}{4\omega_j} \tag{2.132}$$

The effective geometry is clearly an improvement over the equilibrium geometry, however, the effective geometry does not simplify the terms of higher order than $V^{(3)}$. This results in a decline of its usefulness as we increase the perturbation order.

2.11 Analytical derivatives

There are several advantages associated with analytical derivatives compared to numerical derivation: it increases the efficiency by a factor proportional to the number of nuclei. In addition, more accurate results are produced[66, 27, 67]. The largest increase in efficiency is gained from the transition of first order numerical derivatives to analytical. Efficiency is also gained for higher derivatives in line with Wigner's 2n+1 rule [75, 66].

The gradient and Hessian of a Hartree-Fock function can be determined analytically with general response theory according to the following equations [44]:

$$\frac{dE}{d\mathbf{R_K}} = \left\langle \left(\frac{dH}{d\mathbf{R_K}} \right) \right\rangle \tag{2.133}$$

$$\frac{d^2E}{d\mathbf{R_K}d\mathbf{R_L}} = \left\langle \left(\frac{d^2H}{d\mathbf{R_K}d\mathbf{R_L}} \right) \right\rangle + \left\langle \left(\frac{dH}{d\mathbf{R_K}}; \left(\frac{dH}{d\mathbf{R_L}} \right)^T \right) \right\rangle \tag{2.134}$$

The nuclear coordinates are denotes $\mathbf{R_K}$. The ";" indicates a response function[44]. These equations are based on the Hellmann-Feynman theorem[47, 37], stating that the derivative of the energy with respect to a parameter R is the expectation value of $\partial H/\partial \mathbf{R}$,:

This is considered the simplest expression of analytical derivatives, but leads to large inaccuracies unless very large basis sets, up to infinite sized, are used.

In order to obtain accurate results without an infinite basis set a force referred to as the Pulay force is added as a correction to the equation. This correction is the trace of the derivated overlap integral $\partial S/\partial \mathbf{R}$ multiplied with the energy weighted density matrix $\mathbf{W}$ [65]. This theory was then generalized to the Lagrangian theorem [45, 46].

The analytical derivatives[70] used in this thesis, are evaluated using atomic orbital energy based derivative theory [77], expressed with the Lagrangian formulation.

2.11.1 Cubic and quartic force field

The geometric derivatives are received as cartesian coordinates and must be transformed into normal coordinates in order to use them in the equations derived. The transformation from cartesian to normal coordinates is done by executing the following equation[64]:

$$V_{ijk}^{(3)} = \sum_{I=1}^{3N}\sum_{J=1}^{3N}\sum_{K=1}^{3N} V_{IJK}^{(3)} N_{iI} N_{jJ} N_{kK} \quad \forall i,j,k \tag{2.135}$$

The N being the transformation matrix found in equation 2.8. The transformation for the quartic force field is similarly:

$$V_{ijkl}^{(4)} = \sum_{I=1}^{3N}\sum_{J=1}^{3N}\sum_{K=1}^{3N}\sum_{L=1}^{3N} V_{IJKL}^{(4)} N_{iI} N_{jJ} N_{kK} N_{lL} \quad \forall i,j,k,l \tag{2.136}$$

2.11.2 First and second property derivatives

Also the derivative of the electric field has been implemented analytically using atomic orbital energy based derivative theory [77]. With the ability of derivating geometrically and electronically one can acquire the derivatives of the dipole moment and the polarizability[39].

When the properties are differentiated, the output obtained is in cartesian coordinates. Generally, for the first derivative, the conversion to normal coordinates is given by:

$$P_i^{(1)} = \sum_{I=1}^{3N} P_I^{(1)} N_{iI} \quad \forall i \tag{2.137}$$

For the second derivative:

$$P_{ij}^{(2)} = \sum_{I=1}^{3N}\sum_{J=1}^{3N} P_{IJ}^{(2)} N_{iI} N_{jJ} \quad \forall i,j \tag{2.138}$$

As the properties we work with are first and second tensor properties, one needs to add an additional loop so as to cover all the elements in the tensor, rendering the transformation equations into:

$$P_{ij,1\_\text{tensor}}^{(1)} = \sum_{I=1}^{3N} P_{Ij}^{(1)} N_{iI} \quad \forall i, \quad j = \{1,2,3\} \tag{2.139}$$

and:

$$P^{(1)}_{ijk,2\_\text{tensor}} = \sum_{I=1}^{3N} P^{(1)}_{Ijk} N_{iI} \quad \forall i, \quad j,k = \{1,2,3\} \tag{2.140}$$

The same applies for the second derivatives:

$$P^{(2)}_{ijk,1\_\text{tensor}} = \sum_{I=1}^{3N}\sum_{J=1}^{3N} P^{(2)}_{IJk} N_{iI} N_{jJ} \quad \forall i,j, \quad k = \{1,2,3\} \tag{2.141}$$

and:

$$P^{(2)}_{ijkl,2\_\text{tensor}} = \sum_{I=1}^{3N}\sum_{J=1}^{3N} P^{(2)}_{IJkl} N_{iI} N_{jJ} \quad \forall i,j \quad k,l = \{1,2,3\} \tag{2.142}$$

2.12 The properties to be investigated

2.12.1 First tensor properties

The only first tensor property that will be investigated is the dipole moment.

The dipole moment denoted μ, can be obtained by taking the first derivative of the electric field, this can be done as V = -$\vec{\mu} \cdot \vec{E}$. The dipole moment is a first tensor property, therefore, it is usually reported by its magnitude:

$$\mu = \sqrt{\mu_x^2 + \mu_y^2 + \mu_z^2} \tag{2.143}$$

2.12.2 Second tensor properties

The polarizabilty denoted α is the second order derivative of the energy of the electric field, and will be calculated analytically. Two other second order properties will used for validation, nuclear magnetic shielding constant and and the molecular quadrupole moment as defined by Buckingham[19].

For water, three components of the second order tensors will be reported, for a generic property p, these components are reported as p_{xx}, p_{yy}, p_{zz}, the other components will be zero. In the literature it is common to report the mean value (Eq. (2.144)) and the anisotropy of the second order tensors (Eq. (2.145)) instead of reporting component wise.

$$\bar{p} = \frac{1}{3}\left(p_{xx} + p_{yy} + p_{zz}\right) \tag{2.144}$$

$$\Delta p = p_{33} - \frac{1}{2}\left(p_{11} + p_{22}\right) \tag{2.145}$$

where $p_{33} \geq p_{22} \geq p_{11}$.

In order to use these equations, care must be taken to orient the molecule in such a way that only the diagonal elements of the second tensor property are non-zero.

Chapter 3

Implementation

The structure of the program will be presented and justified by means of a class UML diagram. The code implementing the equations derived in the Theory chapter will be presented if it has noteworthy attributes, but the helping functions and methods such as those found in read.input and the testing classes will not. The program was written in Python, due to an extensive use of the NumPy and SciPy packages proving advantageous, in addition to being able to write object oriented. As a reference, *A Primer on Scientific Programming with Python*[59] has been used throughout the whole process.

3.1 Overview

The code was written in an object oriented manner. This makes the code readable and more maintainable. The code that is implemented also had obvious candidates for objects, making object oriented code a natural choice. The class UML diagram, fig.3.1, depicts the structure of the program.

There were several reason for choosing to implement a molecule class. Firstly, it makes sense to create a molecule class to enhance the understanding of the code, as molecules are thought of as objects in the real world. One of the advantages with respect to coding is the increased simplicity: When calculating properties the molecule object is sent as a parameter to the function. The function will then have access to all the properties of the molecule. The alternative would be to send along all the properties of the molecule, one would then typically have to send in four parameters to each function. This is more cluttered and it gives a less intuitive understanding of where the parameters come from, and what they mean.

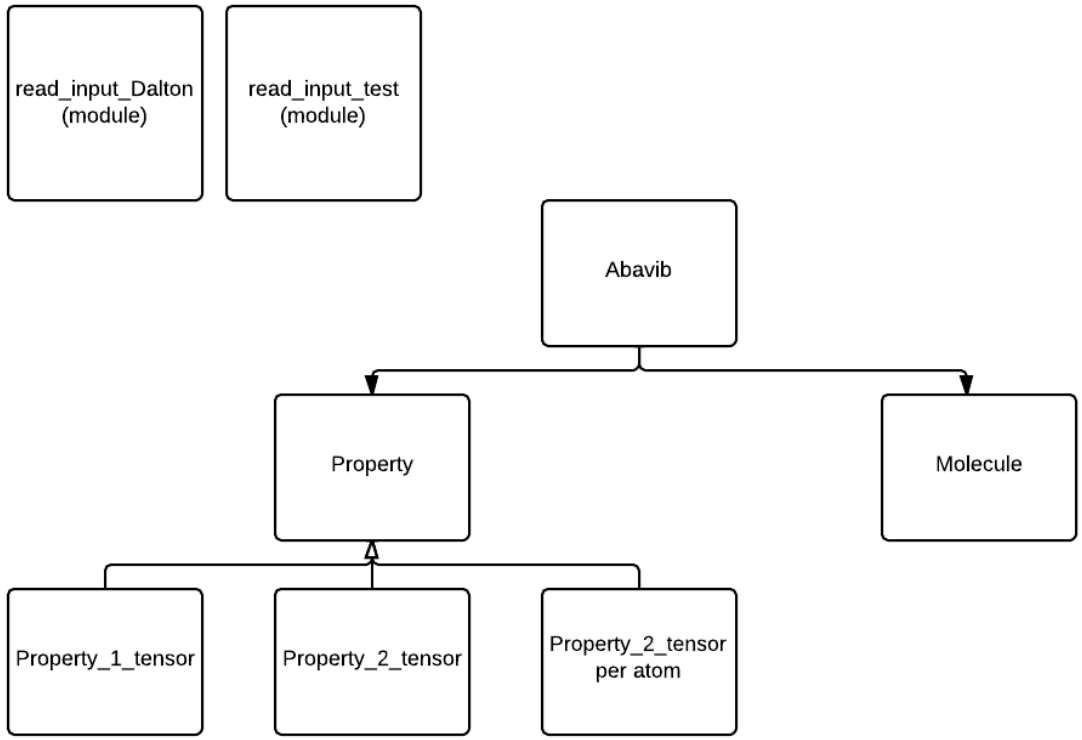

Figure 3.1: The UML diagram of the program

The different properties are also implemented as classes. A super class "Property" has been implemented, which defines what functions are found in the subclasses, and the parameters all properties share. The superclass also includes an initializing method, which initializes a pointer to the molecule object, and also the name of the property. The writet_to_file method is also implemented here. It contains empty callable functions, indicating that the Property class's role is as a template super class and should therefore never be called.

There are three subclasses of Property. These are: "Property_1_Tensor", "Property_2_Tensor", and "Property_2_Tensor_atom". Every property we evaluate falls into one of these subclasses. The subclasses each have a call method which then calculates the property, and writes the results to file. The subclasses also have each their initialization method which inherits from the superclass in addition to initialization the attributes unique to said subclass. In addition to this, there are various helping methods in each subclass. Making properties into objects might be less intuitive then making molecule into objects, yet structuring the program this way makes for several advantages. Much of the code is the same for the three subclasses, and if we did not have a superclass to inherit from, there would be duplication of code. Secondly, having a template superclass imposes certain features on the subclasses, this generally has a stabilizing effect on the program. Introducing property classes also makes the code more readable, as the attributes and methods belonging to the property calculations are grouped within a class.

A read_input_Dalton module and a read_input_test module have also been implemented. The reason for making these modules is that if one wants to use data from another source it is easy to swap the modules as their code is not entangled with the rest of the program. Lastly, the abavib.py file is there to run the program. A simple command line input is chosen, but this is also simple to switch out or expand on if desired.

3.2 Converting to a normal coordinate basis

3.2.1 Evaluating the normal coordinates basis and the fundamental frequencies

In order to calculate the normal coordinates and fundamental frequencies, the Hessian and the equilibrium position of the molecule in Cartesian coordinates are needed, in addition to the masses of all the atoms involved. The Hessian must first be 1. projected, it must then be 2. mass weighted and 3. diagonalized. The code for projecting is found in appendix B code. B.1. The method employs NumPy functions including *linalg.qr* which transforms the input array into a upper quadratic matrix.

The eigenvectors and eigenvalues are found by mass weighting and diagonalizing, executed in the program as seen in Appendix B code B.2. The NumPy function *dot* is responsible for matrix multiplication and *linalg.eig* is used to decompose the matrix into the eigenvectors and eigenvalues.

Because we are at the energy minima, six of the eigenvectors (5 if linear) should be zero. These must be removed, along with their respective eigenvectors. We are, however, not truly at the energy minimum. The six eigenvectors will therefore not be zero, but will be the order of magnitude 10^{-19} or less. Conveniently, the *linalg.eig* function automatically sorts the eigenvalues by magnitude, it is simply just a matter of removing the last six values of the eigenvalues and eigenvectors. Next, the *argsort* function is employed; the argsort function is used in order to sort the eigenvalues and the eigenvectors so that they correspond to each other. The eigenvalues now correspond to the fundamental frequencies, and mass weighting the eigenvectors gives the normal coordinates basis.

3.2.2 Converting the cubic and quartic force field

The cubic force field is recieved from DALTON in cartesian coordinates. It must be converted into normal coordinates before it can be used to calculate the effective geometry. The transformation of the cubic force field from Cartesian to normal coordinates is defined in equation 2.136. The equation is rewritten in order to produce code with fewer nested loops:

$$V_{ijk}^{(3)} = \sum_{I=1}^{3N}\sum_{J=1}^{3N}\sum_{K=1}^{3N} V_{IJK}^{(3)} \times \sum_{I=1}^{3N}\sum_{J=1}^{3N}\sum_{K=1}^{3N} V_{IJK}^{(3)} N_{jJ} \times \sum_{I=1}^{3N}\sum_{J=1}^{3N}\sum_{K=1}^{3N} V_{IJK}^{(3)} N_{kK} \quad \forall i,j,k \tag{3.1}$$

This can be implemented directly as seen in code B.3, and this is how the conversion from cartesian to normal coordinates is implemented in DALTON.

By observing the code corresponding to the nested loops, they appear to be doing the same job as the matrix operation of multiplication. It turns out that by transposing the matrices and multiplying the cubic force field with the normal coordinate basis in a certain order, albeit somewhat arbitrarily, it is possible to transpose the cubic force field using matrix multiplication. The sequence of transposing and multiplying is found in Appendix B, code B.4.

The conversion of the quartic force field is handled likewise.

3.2.3 Converting the first and second derivative of the property surface

The equations to be implemented are the equations: 2.139, 2.140, 2.141, and 2.142.

These can be implemented directly, by substituting the sums for for-loops. The matrix operations corresponding to these sums have been deduced, and are reported in code B.5 and B.6. Only the methods for converting the first tensor gradient and first tensor Hessian are reported, as the there isn't any significant task to add the extra sum for the second tensor.

For the conversion of the Hessian, both the whole property Hessian and the diagonal of said array are returned. The diagonal components are used when evaluating the zeroth order corrections, and using NumPy's *diagonal* function is faster than using a for-loop for this purpose.

3.3 Effective Geometry

The method for calculating the effective geometry has been rewritten in terms of matrix operations B.7, the output of this method is the effective geometry in normal coordinates. From here, the effective geometry must therefore be converted to cartesian coordinates. This is done in the method B.10.

3.4 Property Correction

The property correction methods are as following: The zeroth order correction, the first order correction for molecules at the equilibrium geometry, the second order correction for molecules at the effective geometry, and the second order correction for molecules at the equilibrium geometry. Recalling that the corrections at the effective geometry are just simpler expression for the corrections at the equilibrium geometry, only the implementation at the equilibrium geometry will be discussed, we shall also limit ourselves to corrections to first tensor properties.

On the topic of structure, these correction methods are implemented in their respective Property subclasses. The correct method is automatically chosen for the property of choice, but whether calculations should be done at the effective or equilibrium geometry must be specified. A molecule can have pointers to as many properties and corrections as is desired. The property class gets a pointer to the molecule object and therefore has free access to all the properties of the molecule needed.

The zeroth order correction can be viewed in code B.9, the first order corrections in code B.10; note that the first order correction applies only to the equilibrium geometry. These corrections have been implemented using only matrix operations leading to fast, non-error prone code.

The second order corrections has been by far the hardest part of the program to implement in a reasonable manner, this as a result of operations not having a matrix operation counterpart. The second order correction has therefore been implemented as a combination of for-loops and matrix operations and measures have been taken to produce readable code, as seen in B.11.

The use of for-loops increases the chances of mistakes. This is because certain values must be set to zero, indentation faults can occur, and there is generally a greater number of lines mistakes can crop up in. As opposed to NumPy functions, which have been extensively tested for all types of edge cases, the for-loop can malfunction. There are no values the second order corrections can be compared to. Great care has been taken to make sure this code in in fact on par.

3.5 Version control system

A version control system had been used throughout the project. There are many version control systems to choose from; but the choice ultimately fell on *Git*[25] as it is open source, free, and already installed on most Linux distributions.

A version control system allows for changes to be archived, so one can go back to older versions if needed. The entire project, including the history, is saved both locally and in cloud storage. The project can thereby be accessed for viewing

through the git repository on the candidates GitHub account. To prevent bloating of the thesis, a restricted amount of code documentation is found here, if more extensive viewing is desired, referral is made to said GitHub account.

A useful aspect of the git software is the branching function; in order to try out new features of your program without risking your original program, a branch can be created where new feature may be tried out. If this feature is deemed successful, the branch can then by merged back into the original branch. The main branch is traditionally named *master*. Ideally, this branch should always be operating correctly. It is good practice to always develop code in a different branch, then merge it with master when finished developing. Two examples of branching is displayed over two different time periods in figure 3.2 and figure 3.3.

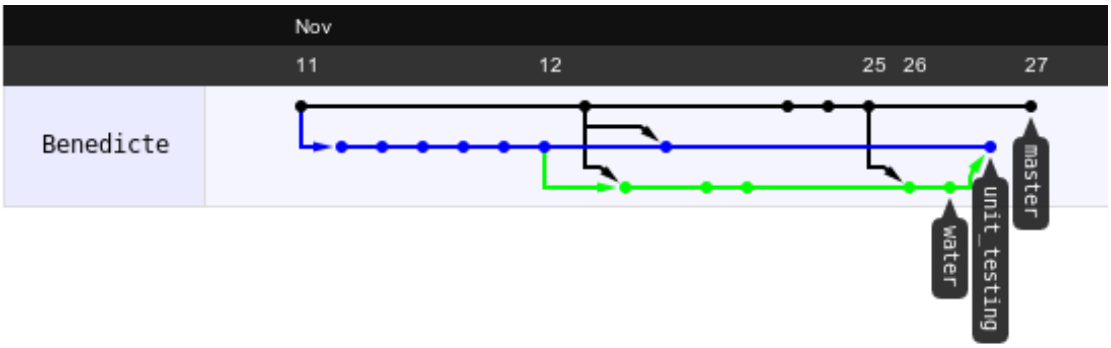

Figure 3.2: An example of the branch history of the project. Here unit testing was developed parallel with generallizing the project in order to take input of any molecule. The second test molecule was water, hence the name of the branch, the first was hydrogen peroxide.

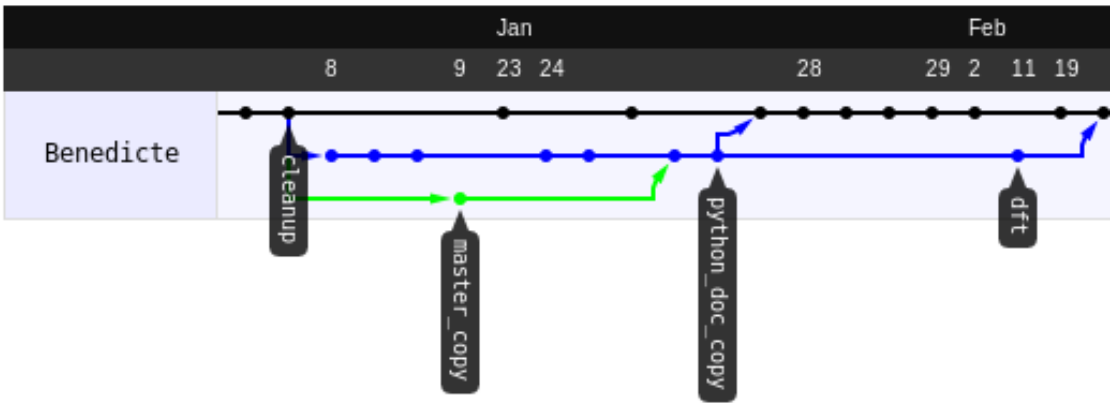

Figure 3.3: In this stage of the program, the structure was rewritten to conform to the object oriented nature of Python, a copy of the original structure (master_copy) was kept for a duration of time in case needed.

3.6 Testing

There were three types of testing done for the program. Firstly, identical input was run through the program in addition to DALTON, and the values were compared. This was always the first step in testing. Secondly, the values produced by the program were compared to the literature. This comparison will be explained in detail in the Validation chapter. Lastly, an attempt has been made in employing unit testing.

Unit testing makes bugs very easy to catch as the program is expanded. It is also used to test edge cases making sure the program does not produce strange results for certain input, for example input with a large amount of zeros. It is good practice to write extensive testing classes, as maintenance generally renders more time demanding than writing the initial code.

The python package *unittest* has been employed, and each method has its own test class. The class accommodates a setup method, where the functions and variables that are to be tested are set up. Various tests are then written and run for each class. The unit tester should ideally be developed before the code is written, and then also appended to as the code is written to meet the unit test requirements. Testing as been done extensively, but not completely.

Chapter 4

Validation

This chapter aims to validate the implementation of the program code as described in the former sections. The effective geometry and zeroth order corrections have been implemented here as well as in DALTON. It is therefore possible to validate against the results obtained with DALTON.

Within this section, the basis sets and electron correlation will be exactly the same as used in the literature[72] in order to show that the program does in fact operate correctly in line with DALTON.

Generally speaking, only calculations at the SCF level with small basis sets have been performed. This is because the purpose of this section is to validate the program against the literature, and as the wavefunctions and optimizations themselves are not part of the program, they do not need to be validated. It is therefore practical to use non-expensive parameters. We will not discuss to what extent the corrected property is a good fit with experimental and other literature in this section. This is because we have used HF without including electron correlation. The discussion of whether or not our calculations are accurate compared to experimental values will therefore be dealt with in the next chapter.

Deviations between the values reported here and in DALTON are to some extent expected. There are several reasons for this: Most importantly, analytical derivatives are employed here, while the values we compare to are obtained using numerical derivatives. Numerical derivatives are not as accurate as analytical, and depend on the step length. The analytical value should fall between the range of values obtained using different step lengths but might not be the exact values reported in the literature. A less important factor contributing to deviations is that certain numerical routines are carried out by NumPy in my program, while DALTON is written in Fortran, this can lead to small differences in the output as a result of round-off error.

4.1 Step lengths

Before embarking on the task of validating the analytical derivatives with the numerical ones, an analysis of the step lengths versus the property correction will be performed. This will give an indication of what variation we can expect to see between the analytical and numerical derivatives. If the correction is very sensitive to the step length we can accept a larger deviation than if the correction is insensitive. The properties which will undergo step length analysis are: The dipole moment, the polarizabilities, and the nuclear shieldings. The reason for the prior two properties is that these are the ones that can be calculated both analytically and numerically. The nuclear shieldings are included as they are known to be very sensitive to the step length, we may therefore expect a deviation from the literature even while using numerical derivatives with a carefully chosen step length. The results for are displayed in table 4.1. The coordinate system chosen is one where the molecule lies in the xy-plane with the x-axis lying along the dipole axis. This leads to only the x-component of the dipole moment being non-zero.

Table 4.1: Variation of the dipole moment and polarizability correction, $\left\langle P_2^{(0)} \right\rangle_{eff}$ for water with respect to step length.

Step length /a.u.	0.001	0.0025	0.0075	0.05
μ_x /a.u.	-0.0017	-0.0019	-0.0019	-0.0011
α_{xx} /a.u.	0.1512	0.1514	0.1515	0.1433
α_{yy} /a.u.	0.0967	0.0972	0.0971	0.0821
α_{zz} /a.u.	0.0200	0.0217	0.0220	0.0145

For the dipole moment we can expect the corrections to be accurate to the second significant figure. The dipole moment appears not to be sensitive to the step length, and it is expected that that the analytical and numerically obtained dipole moments are quite close. For the polarizability there seems to be a larger dependency on the step lengths, especially for α_{yy}, a larger difference can be tolerated for this property.

Table 4.2: Variation of the isotropy and anisotropy of the chemical shielding correction, $\left\langle P_2^{(0)} \right\rangle_{eff}$ for methane with respect to step length. The step lengths reported are taken around the step length found to produce the most accurate values (step length = 0.06).

Step length	0.025	0.05	0.06	0.07
σ_{C} /ppm	-0.47	-0.80	-0.56	-0.85
σ_{H} /ppm	-0.18	-0.20	-0.18	-0.16
$\Delta\sigma_{\mathrm{H}}$ /ppm	-0.18	-0.16	-0.15	-0.16

The chemical shielding's sensitivity with regard to the step length is confirmed in table 4.2, care must be taken in choosing a step length.

4.2 Property corrections for diatomic molecules

Both a numerical and an analytical approach for the derivatives will be taken for a diatomic molecule. Regarding the numerical approach, the same variables will be used as in the article we are validating against [72]. The purpose being to confirm that the Python program produces the correct effective geometry and vibrational corrections. Secondly, we will calculate the cubic force field, Hessian and dipole derivatives analytically in order to validate for the analytical input.

The diatomic molecule chosen is the HF molecule; for all calculations the atomic natural basis set ANO [80, 81] was used with the contraction $[6s5p4d3p]$ for fluoride and $[5s4p3d]$ for hydrogen in line with the publication.

Numerical parameters: For the geometry optimization, a first order optimization was used, the starting point for the Hessian was a model Hessian developed by Pulay and Fogarasi[68], the step length was set to 0.001 a_0. For the effective geometry, only the part of the cubic force field needed, ie. the V_{ijj} values were calculated. This was done by taking the second derivative of the Hessian in normal coordinates using a step length of 0.05 bohr.

Analytical parameters: The analytical Hessian, full analytical cubic force field, and analytical property derivatives were calculated. There are therefore no step lengths to report for the effective geometry or property derivative step.

Table 4.3: Geometry information for HF with a step length of 0.05 bohr

Property	Analytical	Numerical	Literature [72]
r_e /Å	0.8972	0.8972	0.8972
r_{eff} /Å	0.911	0.911	0.911
ω_e /cm^{-1}	4474	4474	4474

In order to gain control and validate all the steps of the property corrections, the optimization step and the calculations of the effective geometry are compared in Table 4.3. We can validate that both the optimization step and the step of finding the effective geometry function correctly, both with regards to using analytical derivatives and to using the python program.

The vibrational averaging is carried out at the effective geometry. The step length is set to 0.05 bohr when finding the second derivatives of the property with numerical derivatives. For the dipole moment and the polarizability analytical derivatives will be used and compared to the numerical ones. For these two properties, a purely analytical approach is taken.

There are three separate methods implemented to carry out the vibrational averaging: One for rank 1 tensors, one for rank 2 tensors, and one for rank 2 tensors where every atom of the molecule has its own tensor. All three of these methods should be validated, thus at least one property of each tensor is reported. The ones chosen are:

Rank 1 tensor: Dipole moment
Rank 2 tensor: Molecular quadrupole moment and polarizability
Rank 2 tensor, values per atom: Nuclear shielding.

The results for these three properties are given in table 4.4.

Table 4.4: Property corrections for HF with a step length of 0.05 bohr.

Property	$\langle P \rangle_{\text{eff}} - \langle P \rangle_{\text{e}}^{\text{a}}$	Literature [72]	$\left\langle P_2^{(0)} \right\rangle_{\text{eff}}^{\text{b}}$	Literature [72]
$\mu_{z,\text{numerical}}$ /a.u.	0.7427	0.7412	-0.0008	-0.0008
$\mu_{z,\text{analytical}}$ /a.u.	0.7427	0.7412	-0.0008	-0.0008
$\alpha_{\text{numerical}}$ /a.u.	0.0671	0.0671	0.0181	0.0181
$\alpha_{\text{analytical}}$ /a.u.	0.0671	0.0671	0.0172	0.0181
Θ_{zz} /a.u.	0.0454	0.0454	0.0080	0.0084
σ_{F} /ppm	-5.75	-5.75	-2.82	-2.91
$\Delta\sigma_{\text{F}}$ /ppm	8.54	8.54	4.44	4.43
σ_{H} /ppm	0.64	0.64	0.28	0.29
$\Delta\sigma_{\text{H}}$ /ppm	0.81	0.81	0.22	0.23

[a]See equation 2.123
[b]See equation 2.123

The molecular quadrupole moments is dependent on the origin of the molecule for polar molecules. Both in the literature[72] and for our calculations the origin is set to the fluorine atom's coordinates.

The second order corrections are close to the literature[72]. The analytical and numerical dipole moments are the same; this is in line with our expectations as the dipole moment was not found to change much with the step length. The difference between the analytical and numerical polarizability is larger with a difference of 0.0009, this is reasonable as was establised with table 4.2.

4.3 Property corrections for polyatomic molecules

The polyatomic molecules to be explored are water, ammonia, and methane, as these are the molecules reported in the literature we validate with[72]. When working with polyatomic molecules, more care must be taken to get the correct symmetry for the coordinate system; this greatly simplifies calculating the tensors that are to be reported. The geometry for water has already been established, for ammonia and methane their geometry are chosen so the center of mass is at origo

and at least one of the hydrogen atoms are in the xy-plane with with the hydrogen atom along the x-axis.

Also for the polyatomic molecules the atomic natural basis set ANO [80, 81] is used with the contraction $[6s5p4d3p]$ for the second row atoms and $[5s4p3d]$ for hydrogen. For the polyatomic molecules only analytical derivatives will be used when finding the effective geometries. The geometries are reported in table 4.5.

Table 4.5: Geometry information for water, ammonia, and methane with analytical derivatives, only the frequency associated with totally symmetric modes are included as this is what is reported in the literature.

	Water	Literature [72]
r_e /Å	0.9398	0.9398
angle_e /°	106.3	106.3
r_{eff} /Å	0.9530	0.9528
$\text{angle}_{\text{eff}}$/°	106.4	106.4
$\omega_{i,e}$ /cm^{-1}	4130	4130
$\omega_{j,e}$ /cm^{-1}	1748	1748
Property	Ammonia	Literature [72]
r_e /Å	0.9978	0.9978
angle_e/°	180.2	180.2
r_{eff} /Å	1.0086	1.0086
$\text{angle}_{\text{eff}}$/°	108.6	108.6
$\omega_{i,e}$ /cm^{-1}	3690.8	3691.0
	Methane	Literature [72]
r_e /Å	1.0814	1.0814
r_{eff} /Å	1.0938	1.0936
$\omega_{i,e}$ /cm^{-1}	3149.4	3149.5

Based on calculations where known input from DALTON is inserted with a known effective geometry, the difference between the effective geometry calculated by the program and DALTON are the same to three significant figures. Any deviation from the literature in the reported results are therefore not affected by the difference in the way python calculates and rounds off.

Table 4.6 depicts the property corrections for water. Again, we see that the dipole moment for both calculated analytically and numerically are in agreement with the literature. The polarizabilities are also within the range of what we expect, as well as the results for molecular quadrupole moment and nuclear shieldings.

From table 4.7 and table 4.8 we can observe that similar results are found for ammonia and methane as for the water molecule. The results for the dipole moment and molecular quadrupole moment are close to the literature, while there are deviations for the polarizablity and the nuclear shielding. For ammonia and methane, the numerical property correction error is larger than the analytical correction for polarizability, illuminating the dependency of the step length. In this

Table 4.6: Property corrections for water with a step length of 0.0075 bohr for the properties with numerical derivatives.

Property	$P_{\text{eff}} - P_{\text{e}}$	Literature [72]	$\left\langle P_2^{(0)} \right\rangle_{\text{eff}}$ [a]	Literature [72]
$\mu_{x,\text{numerical}}$ /a.u.	-0.0039	-0.0039	0.0019	0.0019
$\mu_{x,\text{analytical}}$ /a.u.	-0.0039	-0.0039	0.0019	0.0019
$\alpha_{xx,\text{numerical}}$ /a.u.	-0.0039	-0.0039	0.0971	0.0971
$\alpha_{yy,\text{numerical}}$ /a.u.	-0.0039	-0.0039	0.1515	0.1514
$\alpha_{zz,\text{numerical}}$ /a.u.	-0.0039	-0.0039	0.0220	0.0220
$\alpha_{xx,\text{analytical}}$ /a.u.	0.0627	0.0627	0.0960	0.0971
$\alpha_{yy,\text{analytical}}$ /a.u.	0.0627	0.0627	0.1481	0.1514
$\alpha_{zz,\text{analytical}}$ /a.u.	0.0627	0.0627	0.0220	0.0220
Θ_{xx} /a.u.	-0.0064	-0.0064	0.0047	0.0046
Θ_{yy} /a.u.	0.0386	0.0386	0.0067	0.0068
Θ_{zz} /a.u.	-0.0322	-0.0322	-0.0114	-0.0114
σ_{O} /ppm	0.78	0.80	-4.45	-4.54
$\Delta\sigma_{\text{O}}$ /ppm	0.78	0.80	-1.46	-1.66
σ_{H} /ppm	-0.69	-0.70	0.06	0.06
$\Delta\sigma_{\text{H}}$ /ppm	-0.69	-0.70	-0.21	-0.22

[a]See equation 2.123

Table 4.7: Property corrections for ammonia with a step length of 0.001 bohr for the properties with numerical derivatives. The origin is set to the center of mass.

Property	$P_{\text{eff}} - P_{\text{e}}$	Literature [72]	$\left\langle P_2^{(0)} \right\rangle_{\text{eff}}$ [b]	Literature [72]
$\mu_{z,\text{numerical}}$ /a.u.	0.0107	0.0107	0.0097	0.0097
$\mu_{z,\text{analytical}}$ /a.u.	0.0107	0.0107	0.0095	0.0097
$\bar{\alpha}_{\text{numerical}}$ /a.u.	0.2350	0.2351	0.2391	0.2591
$\bar{\alpha}_{\text{analytical}}$ /a.u	0.2350	0.2351	0.2586	0.2591
Θ_{zz} /a.u.	-0.0322	-0.0322	-0.0114	-0.0114

[a]See equation 2.123

Table 4.8: Property corrections for methane with a step length of 0.06 bohr.

Property	$P_{\text{eff}} - P_{\text{e}}$	Literature [72]	$\left\langle P_2^{(0)} \right\rangle_{\text{eff}}$ [a]	Literature [72]
$\bar{\alpha}_{\text{numerical}}$ /a.u.	0.3757	0.3754	0.5076	0.5257
$\bar{\alpha}_{\text{analytical}}$ /a.u.	0.3757	0.3754	0.5241	0.5257
σ_{C} /ppm	2.55	2.55	-0.56	-0.53
σ_{H} /ppm	-0.42	-0.42	-0.18	-0.18
$\Delta\sigma_{\text{H}}$ /ppm	-0.21	-0.22	-0.15	-0.15

[a]See equation 2.123

regard, the polarizability is a good candidate for the analytical method, as there is a significant uncertainty associated with the numerical derivation.

Chapter 5

Examples

5.1 Calculations up to second order corrections

The dipole moment and polarizability will be calculated and corrected up the second order perturbation of the property surface. The corrections in question are: $P^{(0)}_{2_{\text{eff}}}$ and $P^{(2)}_{2_{\text{eff}}}$ defined in Eq.(2.101) and Eq.(2.123) respectively, recalling that we have truncated at the second derivative of the property.

Calculations will be carried out at DFT level, the basis set aug-cc-pVTZ [55, 82, 83] will be used for calculations of the dipole moment, as this is found to be the basis set limit for these calculations [28].

The aug-cc-pVNZ basis sets are some of the most widely used. The *cc-p* stands for *correlation-consistent polarized*[60]. This is important as the charge distribution about an atom perturbs when bonded to an atom with a different electronegativity. The lowest energies cannot be reached without polarization functions. The polarization functions become more important the larger the electronegativity of the bonded atoms in molecule is. It is also of utmost importance when determining dipole moment and the polarizabity. The N in aug-cc-pVNZ is referred to as double-zeta, triple-zeta, etc. As the N becomes larger, successively larger shells of polarization are added. The *aug* signifies the the presence of diffuse components of the basis sets. These are shallow Gaussian basis functions, improving the tail portion of the atomic orbitals, and are especially important if atoms in the molecule has a significant amount of electron density. The aug-cc-pVNZ basis sets should only be used for first and second order elements, additional functions must be added for third period elements. In this thesis, only second order elements will be used, rendering the aug-cc-pVNZ basis sets a good choice. For the polarizability, the basis set aug-cc-pVDZ has been found to be sufficient [42].

As we are operating with DFT, an exchange-correlation energy functional is needed, this functional will account for electron correlation and exchange interaction[60]. The functional that has been found to give the most accurate results are the hybrid

functionals B3LYP[13, 76] and B3PW91. Hybrid functionals are created by both the exact exchange from Hartree-Fock theory and correlation from empirical or *ab initio* data. Only B3LYP will be used as B3PW91 is not implemented in DALTON for all the required routines, fortunately, this functional was found to be best for property calculations with DFT for OpenRSP[4].

We will continue with the molecules used for the validation; H_2O, NH_3, and CH_4, in addition the molecule D_2O will also be used in order to demonstrate the isotope functionality of the program.

The basis set and functional stated above will be used in the geometry optimization step, the effective geometry step, and when executing the zeroth and second order property correction. All parts of the calculations will be executed with analytical derivatives.

5.1.1 Effective geometry

Table 5.1: Geometry information for H_2O, D_2O, NH_3, and CH_4, at DFT level with analytical derivatives, only the frequency associated with totally symmetric modes are included.

	H_2O	D_2O	NH_3	CH_4
r_e /Å	0.9621	0.9621	1.0134	1.0886
r_{eff} /Å	0.9769	0.9727	1.0255	1.1012
Experiment r_e /Å	0.959[a]	0.956[c]	1.0124[c]	1.087[c]
angle_e/°	105.1	105.1	107.2	109.5
$\text{angle}_{\text{eff}}$/°	104.9	105.1	107.6	109.5
Experiment /°	105.0[a]	105.2[c]	106.6[c]	109.4[c]
$\omega_{i,e}$ /cm^{-1}	3896.1	2855.9	3466.6	3025.9
$\omega_{j,e}$ /cm^{-1}	1626.5	1190.9	-	-
Experiment $\omega_{i,}$/cm^{-1}	3943[b]	2888[b]	3444[c]	2917[c]
Experiment $\omega_{i,}$ /cm^{-1}	1648[b]	1206[b]	-	-

[a]From spectra, see Ref[51]
[b]From spectra, see Ref[14]
[c]From the Computational Chemistry Comparison and Benchmark Database, see Ref[21].

The equilibrium and effective geometries are reported in Table 5.1. If compared with the geometries reported in table 4.5 in the validation section, the bond lengths have increased, while the fundamental frequencies have decreased. The reason for this difference is mainly that electron correlation was not included for the Hartree-Fock calculations, the energy is therefore lower for the DFT calculations, as electron correlation is accounted for. The values reported here are therefore closer to the experimental values than those in table 4.5.

Comparing the H_2O and D_2O molecule, where there has been an isotopic substitution, this has not resulted in a difference in the equilibrium bond length. It is assumed that the potential energy function is not changed by isotopic substitution[48],

so this is as expected. The vibrational frequencies are different for the two molecules, this as a result of the change in mass changes the frequencies of vibration. This effect is especially significant for the substitution of hydrogen with deuterium. The change in the frequency also causes a change in the bond length at the effective geometry, the dipole moment and polarizability as the frequency takes part in evaluating these.

Table 5.2: Property corrections for H_2O at the effective geometry

Property	P_e - P_{eff}	$< P_2^{(0)} >_{eff}$	$< P_2^{(2)} >_{eff}$
μ_x /a.u.	-0.0033	0.0025	0.0012
α_{xx} /a.u.	0.3064	0.1395	-0.0698
α_{yy} /a.u.	0.1999	0.0802	-0.0404
α_{zz} /a.u.	0.0902	0.0093	-0.0048
$\bar{\alpha}$ /a.u.	0.1988	0.0763	-0.0383

Table 5.3: Property corrections for D_2O at the effective geometry

Property	P_e - P_{eff}	$< P_2^{(0)} >_{eff}$	$< P_2^{(2)} >_{eff}$
μ_x /a.u.	-0.0023	-0.0019	0.0009
α_{xx} /a.u.	0.0650	0.1021	-0.0510
α_{yy} /a.u.	-0.3055	0.0580	-0.0290
α_{zz} /a.u.	-0.4632	0.0069	-0.0035
$\bar{\alpha}$ /a.u.	-0.2345	0.0557	0.0278

The property corrections for water are reported in Table 5.2. The corrections obtained by using the effective geometry is the largest, the zeroth order correction is larger than the second order correction. Mathematically, this is as expected, as the second order correction is further out in the Taylor expansion. The further out in the expansion, the smaller the corrections.

The corrections for the polarizability is larger than for the dipole moment, also with respect to % correction. This holds true both for the zeroth order and second order corrections. The corrections cause the value of the proprty to fluctuate around the true value: the zeroth order correction is positive, and over-corrects the property. The second order correction is negative and brings the value of the property closer to the true value. For the dipole moment, however, calculating the dipole moment at the effective geometry initially results in a less accurate value. This has been observed also in previous studies [72], and the error is attributed to the overestimation of the initial dipole moment.

The correction of D_2O are for the most part smaller in magnitide than the corrections for H_2O. Looking to the equation governing the corrections at the $\left\langle P_2^{(0)} \right\rangle_{eff}$ level:

$$\left\langle P_2^{(0)} \right\rangle = \sum_i^N \frac{P_{ii}^{(2)}}{4\omega_i} \tag{5.1}$$

Both the frequencies and the $P_{ii}^{(2)}$ for H_2O and D_2O are the same if calculating in the same geometry, i.e. in r_e. However, r_{eff} is different for the two molecules, resulting in different frequencies and different $P_{ii}^{(2)}$.

From Eq. (5.1) it is seen that the correction is divided by the frequencies. The frequencies of H_2O are larger than those of D_2O, thereby H_2O should be attaining smaller corrections. The smaller magnitude of the D_2O must therefore be a result of a smaller value of $P_{ii}^{(2)}$.

Table 5.4: Property corrections for NH_3 at the effective geometry

Property	P_{eff} - P_{e}	$< P_2^{(0)} >_{\text{eff}}$	$< P_2^{(2)} >_{\text{eff}}$
μ_z /a.u.	0.0246	0.0103	0.0001
$\bar{\alpha}$ /a.u.	-0.3600	0.2430	-0.1224
$\Delta\alpha$ /a.u	0.0248	0.0485	0.0420

Table 5.5: Property corrections for CH_4 at the effective geometry

Property	$P_{\text{e}} - P_{\text{eff}}$	$< P_2^{(0)} >_{\text{eff}}$	$< P_2^{(2)} >_{\text{eff}}$
$\bar{\alpha}$ /a.u.	0.403	0.552	-0.262

For NH_3 in table 5.8 and CH_4 in table 5.9, the second order corrections are smaller than the zeroth order corrections, as was the case for H_2O and D_2O. For NH_3, the dipole moment is corrected by a very small amount in the second order correction, and only correcting to the $\left\langle P_2^{(0)} \right\rangle_{\text{eff}}$ can be justified. For the polarizability the second order corrections are substantial.

Table 5.6: Cumulative property corrections for H_2O at the effective geometry

Property	P_{e}	P_{eff}	$< P_2^{(0)} >_{\text{eff}}$	$< P_2^{(2)} >_{\text{eff}}$	Experimental
μ_x /a.u.	-0.7266	-0.7299	-0.7274	-0.7286	-0.7186[a]
α_{xx} /a.u.	10.1356	10.596	10.736	10.6673	10.314[b]
α_{yy} /a.u.	9.3162	9.963	10.043	10.003	9.906[b]
α_{zz} /a.u.	8.9070	9.523	9.532	9.527	9.546[b]
$\bar{\alpha}$ /a.u.	9.4529	10.027	10.103	10.065	9.922[b]

[a] Molecular beam electric resonance experiment [62]
[b] Rotational Raman spectrum of water vapor [63]

The corrections are added to the original property cumulatively and the resulting values are reported in Table 5.6, 5.7 5.8, and 5.9 for the four molecules. For H_2O, we observe a steady increase in accuracy as we add increasingly higher orders of corrections for the polarizability, although there seems to be an overcorrection.

There aren't any experimental values to compare with regarding the polarizabiliy values of D_2O. The final isotropic polarizability is smaller than the anisotropic polarizability of H_2O. This appears to be as expected when comparing values from similar studies done in the literature [12].

Table 5.7: Cumulative property corrections for D_2O at the effective geometry

Property	P_e	P_{eff}	$< P_2^{(0)} >_{eff}$	$< P_2^{(2)} >_{eff}$	Experimental
μ_x /a.u.	-0.7266	-0.7290	-0.7271	-0.7280	-0.7283[a]
α_{xx} /a.u.	10.286	10.351	10.454	10.403	
α_{yy} /a.u.	9.763	9.457	9.515	9.486	
α_{zz} /a.u.	9.434	8.971	8.978	8.974	
$\bar{\alpha}$ /a.u.	9.828	9.593	9.649	9.621	

[a] Molecular beam electric resonance experiment [26]

Table 5.8: Cumulative property corrections for NH_3 at the effective geometry

Property	P_e	P_{eff}	$< P_2^{(0)} >_{eff}$	$< P_2^{(2)} >_{eff}$	Experimental
μ_z /a.u.	-0.5867	-0.5780	-0.5677	-0.5729	-0.5791[a]
$\bar{\alpha}$ /a.u. 14.597	14.957	14.549	14.795	14.673	14.573[b]
$\Delta\alpha$ /a.u	1.1176	1.1424	1.0538	1.0215	

[a] Laser-microwave double resonance measurements [62]
[b] Quadratic extrapolation of refractive data [85]

5.1.2 Equilibrium geometry

The corrections will now be calculated at the equilibrium geometry. We will therefore employ the corrections $P_{1_e}^{(1)}$ and $P_{2_{e,}}^{(2)}$ defined for the equilibrium geometry in Eq. 2.104 and Eq. 2.123. For the $P_2^{(0)}$ correction,s defined in Eq. 2.101, the same method is used both for the effective and the equilibrium geometry as this method remains unaltered.

The gain in accuracy acquired from carrying out calculations at the effective goemetry is partly compensated through the non-zero first order corrections at the equilibrium geometry as can be seen in table 5.10. The second order correction for the effective and the equilibrium geometry are of similar magnitude although the expression for the second order correction at the effective geometry is much simpler, this speaking in favor for carrying out calculations at the effective geometry.

In table 5.11 one observes the increase of accuracy by including increasing numbers of corrections. We observe that as we add corrections to both the effective and equilibrium corrections, the property values become similar. This as a result of more terms being included in the correction for the equilibrium geometry.

Corrections at the equilibrium geometry produces better results than the correc-

Table 5.9: Cumulative property corrections for CH_4 at the effective geometry

Property	P_e	P_{eff}	$< P_2^{(0)} >_{eff}$	$< P_2^{(2)} >_{eff}$	Experimental
$\bar{\alpha}$ /a.u.	16.042	16.445	16.967	16.705	17.258[a]

[a] Quadratic extrapolations from refractive data [50]

Table 5.10: Comparisson of the property corrections for water between the effective and equilibrium geometry, as P_{eff} encompasses the $\left\langle P_1^{(1)} \right\rangle_e$ corrections, it is natural to compare these.

Property	$< P_1^{(1)} >_{\mathrm{e}}$	$P_{\mathrm{eff}} - P_e$	$< P_2^{(2)} >_{\mathrm{e}}$	$< P_2^{(2)} >_{\mathrm{eff}}$
μ_x /a.u.	0.0009	-0.0033	0.0012	0.0012
α_{xx} /a.u.	0.0744	0.3064	-0.0682	-0.0698
α_{yy} /a.u.	0.0517	0.1999	-0.0403	-0.0404
α_{zz} /a.u.	0.0231	0.0902	-0.0048	-0.0048
$\bar{\alpha}$ /a.u.	0.0497	0.1988	-0.0378	-0.0383

Table 5.11: The cumulative of the property corrections for water at the equilibrium geometry.

Property	P_{e}	$< P_2^{(0)} >_{\mathrm{e}}$	$< P_1^{(1)} >_{\mathrm{e}}$	$< P_2^{(2)} >_{\mathrm{e}}$	$< P_2^{(2)} >_{\mathrm{eff}}$	Experimental
μ_x /a.u.	-0.7266	-0.72921	-0.73006	-0.7306	-0.7305	-0.7186[a]
α_{xx} /a.u.	10.136	10.275	10.349	10.451	10.667	10.314[b]
α_{yy} /a.u.	9.316	9.396	9.448	9.854	10.003	9.906[b]
α_{zz} /a.u.	8.907	8.916	8.940	9.462	9.527	9.546[b]
$\bar{\alpha}$ /a.u.	9.828	9.529	9.579	9.921	10.039	9.922[b]

[a] Molecular beam electric resonance experiment [62]
[b] Rotational Raman spectrum of water vapor [63]

tions at the effective geometry. This as a result of the effective geometry appearing to over-correct, at least for water. The larger correction obtained at the effective geometry can also be viewed as faster convergence. As the perturbation approach is mathematically sound, the non-corrected properties may be too high, as has also been brought up in [72]. If this is the case, the effective geometry produces better results with fewer corrections.

5.2 Water dimer

The equilibrium and effective geometry will be calculated employing DFT and analytical geometric derivatives. The geometries and frequencies will be compared to both the previous work this work is build on [5], and with experimental measurements.

These calculations demonstrate the methods used to find the effective geometry as well as the harmonic frequencies; by doing calculations on the deuterium water dimer we also get to demonstrate the program's ability to work with isotopes. The values that will be reported with respect to the geometry is the equilibrium bond length of the oxygens of the water molecule making up the dimer, the effective bond length between the oxygen atoms, and the two angles denotes α and β depicted in figure 5.1.

The intial configuration for all the dimers was found in *Avogadro*[43] using a Merck molecular force field [41], and a conjugate gradient algorithm as a starting point. For all parts of the calculations, the B3LYP functional will be employed, this has been found to be an adequate functional, producing values with an error within 0.005 Å for the geometry and frequency calculations for the water monomer, reasonable results are also found for the water dimer[84]. Three basis set were used both for the optimization and for calculating the effective geometry: aug-cc-pVDZ, aug-cc-pVTZ, and aug-cc-pVQZ.

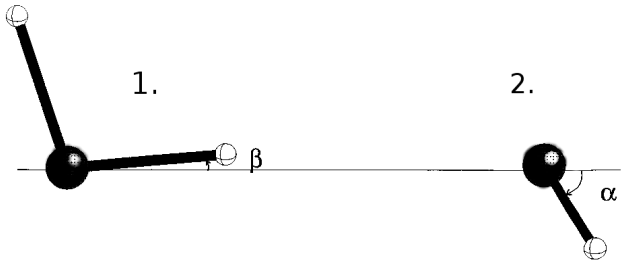

Figure 5.1: From Ref [5], the water molecule underneath the "1" will be referred to as Molecule 1, the other as Molecule 2. The dimer bonding is taking place between the hydrogen of Molecule 1 and the oxygen of Molecule 2.

5.2.1 The $(H_2O)_2$ dimer

The geometry specifications of the water dimer are reported in table 5.12. The equilibrium and effective geometries evaluated at the three successively larger basis sets are compared.

Table 5.12: The structure of the water dimer at the effective geometry vs at the equilibrium geometry

	R_{eq} O-O /Å	R_{eff} O-O/Å	α_{eff} /deg	β_{eff} /deg
aug-cc-pVDZ	2.914	2.928	53.5	5.9
aug-cc-pVTZ	2.920	2.986	57.6	3.8
aug-cc-pVQZ	2.921	2.986	57.5	3.9
Literature[a]	2.851	2.982	64	10.1
Spectra[b]	2.946 ± 0.006		55.2 ± 2.0	5.3± 2.0
Spectra[c]	2.976		57 ± 10	-1 ± 10

[a] Åstrand et al. Ref.[5]

[b] Infrared spectra Ref.[79]

[c] Microwave spectra Ref.[58]

For the equilibrium bond lengths, we see that as the size of the basis set increases from aug-cc-pVDZ to aug-cc-pVTZ to aug-cc-pVQZ, the bond length increases,

and is thereby more in agreement with the literature. The bond lengths of the effective geometry can be concluded to be in decent agreement with the literature. The geometry appears to have converged with respect to the basis set for the bond length at the effective geometry. The difference obtained from changing the basis set is small compared to the difference between the frequencies obtained using the equilibrium and effective geometry, illuminating that the method of employing a variationally determined expansions point is efficient.

Table 5.13: The intermolecular frequencies for the $(H_2O)_2$ dimer reported in cm^{-1} for successively larger basis sets. The subscript found on the basis set marks at which geometry the frequencies are evaluated at. The "eq" subscript stands for the equilibrium geometry, "eff" for the effective geometry.

	Intermolecular frequencies /cm^{-1}					
	ν_1	ν_2	ν_3	ν_4	ν_5	ν_6
aug-cc-pVDZ$_{eq}$	632.4	358.9	180.6	158.1	152.9	130.1
aug-cc-pVTZ$_{eq}$	623.7	361.4	184.0	155.2	153.6	129.7
aug-cc-pVQZ$_{eq}$	622.4	359.5	186.3	157.2	155.1	128.4
Literature[a]	662.1	419.2	222.6	176.3	146.5	120.6
aug-cc-pVDZ$_{eff}$	521.3	510.8	272.2	180.0	123.0	121.8
aug-cc-pVTZ$_{eff}$	534.2	408.7	239.2	176.4	119.8	111.2
aug-cc-pVQZ$_{eff}$	530.6	410.6	238.1	178.8	119.9	113.4
Literature[a]	548.0	301.3	177.1	137.3	76.3i	84.4i
Spectra[b]	522.4	372.6	173.0	150.6	122.2	116.0

[a] Åstrand et al. See Ref.[11]
[b] Matrix isolation using Argon Ref.[24]

There are ($3N$ - 6) 12 non-zero normal mode frequencies. Six of these are of a value higher than 1000 cm^{-1}, the other six are smaller than 1000 cm^{-1}. The six large frequencies are attributed to intramolecular vibrational modes. The six small frequencies are intermolecular modes, three modes per water molecule comprising the water dimer.

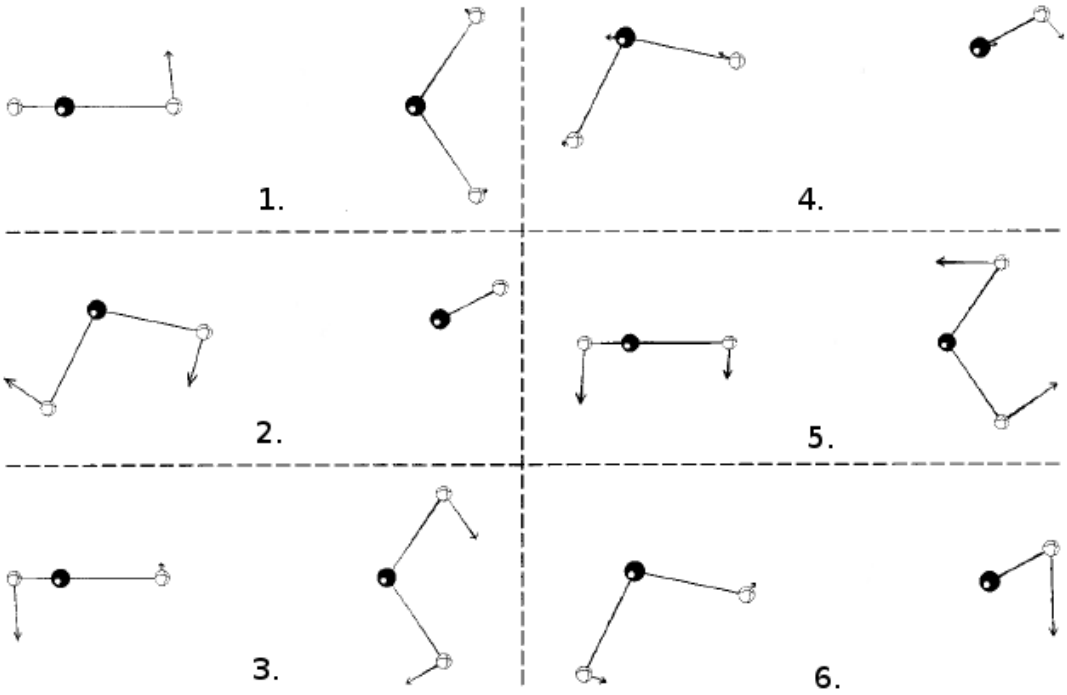

Figure 5.2: The motions of the six intermolecular normal mode frequencies: 1. out of plane shear, 2. in plane shear, 3. out of plane bend, 4. stretch, 5. in plane bend, and 6. torsion, the figure is from Ref.[11]

The intermolecular frequencies are reported in figure 5.13. The vibrational frequencies determined at the equilibrium geometry are all overestimated. This is a common problem with using the harmonic oscillator approximation[29]. There are two main solutions to this problem, the first is to find the anharmonic component by means of perturbation theory, as will be done here. The second is by using a scaling factor[24].

In contrast to the bond lengths and bond angles, the results obtained using aug-cc-pVTZ and aug-cc-pVQZ are not obviously more similar than the frequencies between aug-cc-pVDZ and aug-cc-pVTZ. This holds true both with respect to the equilibrium and the effective frequencies. Yet, there seems to be better agreement with the literature for the largest basis sets. The difference obtained through increasing the size of the basis set is small compared to the difference between the equilibrium and effective energy, as was also the case for the bond lengths. There seems to be good agreement between the frequencies at the effective geometry and the data obtained from the spectra, but there is still some overestimation. This may be a result of basis set superposition error (BSSE) [74]. BSSE leads to frequencies appearing larger than they are. This can be corrected with for example a counterpoise correction, or by using a larger basis set.

All experimental frequencies we compare with were obtained from infrared matrix

isolation experiments. However, caution must be made when comparing to these as the matrix is found to perturb the intermolecular frequencies from their gas phase by up to 20% [17]. This is referred to as the matrix effect.

Table 5.14: The intramolecular frequency shift from the monomer water dimer reported in cm^{-1} for both water molecules constituting the dimer at different basis sets

	Intramolecular frequencies /cm^{-1}					
	$2\nu_1$	$1\nu_1$	$2\nu_2$	$1\nu_2$	$2\nu_3$	$1\nu_3$
aug-cc-pVDZ$_{eq}$	3892	3871	3786	3670	1636	1616
aug-cc-pVTZ$_{eq}$	3887	3867	3788	3673	1646	1627
aug-cc-pVQZ$_{eq}$	3894	3875	3796	3684	1648	1629
H_2O_{eq} monomer	3896	3896	3794	3794	1627	1627
	Intramolecular frequencies /cm^{-1}					
	$2\nu_1$	$1\nu_1$	$2\nu_2$	$1\nu_2$	$2\nu_3$	$1\nu_3$
aug-cc-pVDZ$_{eff}$	3767	3754	3643	3641	1614	1603
aug-cc-pVTZ$_{eff}$	3730	3715	3645	3625	1599	1598
aug-cc-pVQZ$_{eff}$	3698	3633	3638	3527	1584	1583
H_2O_{eff} monomer	3710	3710	3605	3605	1659	1659
Spectra[a]	3754	3735	3660	3601	1616	1599

[a]Matrix isolation using Argon Ref.[18]

The intramolecular frequencies are reported in table 5.14. There are six unique intramolecular frequencies calculated for the water dimer. With this we can can conclude that the dimerization of two water molecules is not symmetric with respect to the two water atoms, i.e. the two water atoms are experiencing different potential fields. The smaller vibrational frequencies are attributed to molecule 1, as one of the hydrogen atom in this molecule is intermolecularly bonded to the neighboring water molecule. The pull from the intermolecular bond will then weaken the intramolecular bonds, resulting in a lowering of the frequency. The frequency denoted ν_1 is the asymmetric stretch, ν_2 the symmetric stretch, and ν_3 the bend.

The intramolecular frequencies are compared to the monomer water molecules. Molecule 1 has a large negative shift compared to the water monomer. The largest shift is the one for the symmetric strech, the asymmetric stretch mode and bend mode have comparable shift values of a small magnitude. For Molecule 2, the shifts appear not to be as as large, the largest shift being for the bend, this shift is positive. This is not surprising, as it is Molecule 1 which is affected most by the dimerization. The fact that the hydrogen atom on Molecule 1 has a dimer bond will alter how it moves.

The intermolecular frequencies are known to have a larger anharmonic part than the intramolecular frequencies[24]. The deviation between the frequencies obtained with the equilibrium and the effective geometry is therefore expected to be smaller

for the intramolecular frequencies, and this seems to hold true: The intramolecular frequencies evaluated at the equilibrium geometry are in better agreement with the literature and closer to the values at the effective geometry than that of the intermolecular frequencies.

5.2.2 The HOH-D_2O dimer

The effect of isotopic substitution will now be briefly explored in this section, there has been a great deal of literature of on this subject [11, 23, 33, 35, 57], and will be touched upon here.

Table 5.15: The structure of the HOH-D_2O dimer at the effective geometry vs at the equilibrium geometry

	R_{eq} O-O /Å	R_{eff} O-O/Å	α_{eff} /deg	β_{eff} /deg
aug-cc-pVTZ	2.920	2.949	29.6	9.3
aug-cc-pVQZ	2.920	2.949	29.6	9.3
Literature[a]	-	2.972	29.9	9.2

[a]See Ref.[11]

Table 5.15 contains the geometric information for HOH-D_2O. The two basis sets, aug-cc-pVTZ and aug-cc-pVQZ give the same results. Because of the convergence of the aug-cc-pVTZ basis set, this will be the only one employed further for the The HOH-D_2O dimer.

The O-O bond length is shorter for the deuterium dimer than for the $(H_2O)_2$ dimer, indicating that the deuterium dimer is more strongly bonded.

Table 5.16: The intermolecular frequencies for HOH-D_2O reported in cm^{-1} for different basis sets

	Intermolecular frequencies /cm^{-1}					
	ν_1	ν_2	ν_3	ν_4	ν_5	ν_6
aug-cc-pVTZ$_{eq}$	623.7	361.1	183.7	155.0	153.1	128.5
Literature[a]$_{eq}$	639.8	391.6	125.9	150.6	94.3	205.9
aug-cc-pVTZ$_{eff}$	520.5	304.7	143.7	114.0	60.4	73.5
Literature[a]$_{eff}$	543.6	305.2	148.0	138.4	49.7	58.8
Spectra[b]	519.4	306.6	167.1	100.2	70.6	77.5

[a]Åstrand et al. Ref.[11]
[b]Spectra from krypton matrix isolation Ref.[33]

The intermolecular frequencies are presented in table 5.16. The vibrational frequencies are smaller for the HOH-D_2O dimer than the $(H_2O)_2$. This a a result of

the larger mass of the deuterium atom. The frequencies calculated at the effective geometry seem to be in significantly better agreement with the spectra[33], reflecting the large anharmonic part of the intermolecular frequencies.

Table 5.17: The intramolecular frequencies for HOH-OD_2 reported in cm^{-1} for both water molecules constituting the dimer.

	Intramolecular frequencies /cm^{-1} (H_2O)		
	ν_1	ν_2	ν_3
aug-cc-pVTZ$_{eq}$	3866	3659	1640
aug-cc-pVTZ$_{eff}$	3798	3743	1601
Spectra[a]	3761	3665	1596
	Intramolecular frequencies /cm^{-1} (D_2O)		
	ν_1	ν_2	ν_3
aug-cc-pVTZ$_{eq}$	2816	2606	1185
aug-cc-pVTZ$_{eff}$	2792	2603	1175
Spectra[a]	2712	2672	1179

[a]Spectra from argon matrix isolation Ref.[34]

Lastly, the intramolecular frequencies in table 5.17 will be discussed. The shifts display the same trends as the $(H_2O)_2$ dimer. For Molecule 1, here being the H_2O molecule, exhibits a negative shift compared to the water monomer molecule. The largest shift is experienced for the symmetric stretch mode.

For the intramolecular frequencies, the H_2O are larger than the D_2O, this by a factor of approximately $\sqrt{2}$. The reason for this can be found by gleaning Eq.5.2. The ν is the wavenumber, k can be thought of as the bond enthalpy, and μ is the reduced mass of the dimer. The mass of deuterium is double that of hydrogen, the reduced mass of O-D will therefore be half of the reduced mass of the O-H bond. As the bond enthalpy(k) of H_2O and D_2O are the same, we expect the O-D vibrations to be $\frac{1}{\sqrt{2}}$ smaller than the O-H.

$$\nu = \frac{1}{2\pi c}\sqrt{\frac{k}{\mu}} \tag{5.2}$$

To illustrate this the intramolecular frequencies of D_2O are multiplied with $\sqrt{2}$ and the results are presented in table 5.18. The results are quite similar, albeit with slightly higher values than the ones corresponding to the H_2O frequencies. The reason for the higher values are the negative shift experienced by the HOH species in HOH-OD_2.

There are no experimental data found on the intramolecular frequencies of the HOH-D_2O dimer, but there is nothing to suggest it doesn't follow the same trends as of the $(H_2O)_2$ dimer.

Table 5.18: The intramolecular frequencies for D_2O multiplied with $\sqrt{2}$ to illustrate the mass dependence of frequencies

	Intramolecular frequencies /cm^{-1} (D_2O)		
	ν_1	ν_2	ν_3
aug-cc-pVTZ$_{eq}$	3982	3685	1671
aug-cc-pVTZ$_{eff}$	3823	3670	1656

[a]Spectra from argon matrix isolation Ref.[34]

Chapter 6

Conclusion

6.1 Evaluation

In principal, there are no limits on how much time and effort which can be dedicated to the subject of this thesis. Further questions and potential research areas came up nearly exponentially as the work was conducted. There are, however, time constraints, and not all parts of the field was, or can, be explored in equal depth. The aspiration for this project is that it can stand its ground independently: The equations governing the vibrational motions were derived, they were then implemented and validated, and examples of the program were given.

The objectives were to: include an extra correction to the vibrational property corrections, carry out calculations using DFT, and carry out calculations using analytical property and geometric derivatives. All these objectives have been met with promising results, although the property correction evaluated with DFT lead to over-corrections of the properties for some of the molecules. The extra property correction produced results in better agreement with the literature than with the zeroth order correction alone. The calculation with analytical derivatives have produced results in line with the literature, and proved to be virtually identical to the numerical derivatives.

6.2 Further work

There is much to extend on, some of the possible work that cropped up when working on the thesis will be described.

With respect to the derivation of the vibrational correction, extensions to these can be made in two dimensions, either by means of higher orders of perturbation, or by including higher orders of derivations to each perturbation. In this work, the order of perturbation has been increased from $\left\langle P_2^{(0)} \right\rangle$ to $\left\langle P_2^{(2)} \right\rangle$, the derivations

have only been included up to P_2. Including higher orders of property derivations could therefore be informative. The amount of property derivatives included could be extending to P_3. This is now possible as the OpenRSP contribution to DALTON can evaluate analytical derivative of the property derivatives recursively, ie to any desired order. The correction $\left\langle P_3^{(0)} \right\rangle$ evaluates to zero, so the $\left\langle P_3^{(1)} \right\rangle$ correction would be the logical next correction to implement:

$$\begin{aligned}\left\langle P_3^{(1)} \right\rangle = &\frac{1}{6}\sqrt{\frac{3}{2}}\sum_{i=1}^{N}\frac{P_{iii}^{(3)}}{\omega_i^{3/2}}(\sqrt{3}a_{1,i}^{(1)} + \sqrt{2}a_{3,i}^{(1)}) \\ &+ \frac{1}{4}\sum_{i,j=1,i\neq j}^{N}\frac{P_{iij}^{(3)}}{\omega_i\omega_j^{1/2}}(\sqrt{2}a_{1,i}^{(1)} + 2b_{21,ij}^{(1)}) \\ &+ \frac{1}{6\sqrt{2}}\sum_{i,j,k=1,i\neq j\neq k}^{N}\frac{P_{ijk}^{(3)}c_{111,ijk}^{(1)}}{\sqrt{\omega_i\omega_j\omega_k}}\end{aligned} \tag{6.1}$$

The other dimension it would be possible to extend, is the order of perturbation. This would, however, require the evaluation of the quintic force field $V^{(5)}$, which is very computationally heavy. Expanding for the derivative of the property is therefore the first extension one should attempt.

With respect to the implementation, more testing could definitely be conducted. Edge cases could be checked, and a better system for catching and raising errors should be put in place.

Another area to look into is including the post Born-Oppenheimer correction[3, 4] that has been developed with the purpose of improving the vibrational analysis in DALTON. Just as the corrections in this thesis has, this post Born-Oppenheimer correction could be added in addition to the $P_2^{(2)}$ corrections introduced here.

One of the largest hurdles to future work is that the variationally determined expansion point r_{exp} leads to much faster converging correction for the couple first orders of expansion, especially the $P^{(1)}$ term disappearing makes stopping at $P^{(0)}$ of high returns. The $P^{(2)}$ have shown to be important, however, but the same savings are not made, as $P^{(3)}$ is not zero at the effective geometry. This is proven in the appendix C.

The terms which disappear at the effective geometry are those of $V^{(1)}$ and $V^{(3)}$. At higher perturbations, higher order potential force fields are included, the use of r_{exp} therefore gives diminishing returns. Finding some method of increasing the rate of convergence for higher orders of the potential force field would therefore be highly advantageous.

Appendix A

Solutions for Hermitian Integrals

Table A.1: The solutions for the integrals occurring for the calculations of the fourth order energy perturbation.

$< q >_{10} = \frac{1}{\sqrt{2}\omega^{1/2}}$
$< q >_{12} = \frac{1}{\sqrt{\omega}}$
$< q >_{21} = (\frac{1}{\omega})^{\frac{1}{2}}$
$< q >_{32} = (\frac{3}{2\omega})^{\frac{1}{2}}$
$< q >_{34} = (\frac{2}{\omega})^{\frac{1}{2}}$
$< q^2 >_{02} = \frac{\sqrt{2}}{2\omega}$
$< q^2 >_{22} = \frac{5}{2\omega}$
$< q^2 >_{13} = \frac{\sqrt{3}}{2\omega}$
$< q^3 >_{10} = \frac{3}{2\sqrt{2}\omega^{3/2}}$
$< q^3 >_{21} = \frac{3}{\omega^{3/2}}$

$$< q^3 >_{30} = (\frac{6}{8\omega^3})^{\frac{1}{2}}$$

$$< q^3 >_{32} = 3(\frac{27}{8\omega^3})^{\frac{1}{2}}$$

$$< q^3 >_{34} = 3(\frac{4^3}{8\omega^3})^{\frac{1}{2}}$$

$$< q^3 >_{36} = (\frac{120}{8\omega^3})^{\frac{1}{2}}$$

$$< q^3 >_{41} = \frac{\sqrt{3}}{\omega^{3/2}}$$

$$< q^4 >_{00} = \frac{3}{4a^2}$$

$$< q^4 >_{02} = \frac{3\sqrt{2}}{2\omega^2}$$

$$< q^4 >_{04} = (\frac{\sqrt{6}}{2\omega^2})$$

Appendix B

Python functions

```
trans1 = [1,0,0]
trans2 = [0,1,0]
trans3 = [0,0,1]

trans_rot = zeros((3* n_atoms, 6))

for atom in range(n_atoms):
    ij = atom*3
    trans_rot[ij, 0] = 1.0
    trans_rot[ij + 1, 1] = 1.0
    trans_rot[ij + 2, 2] = 1.0
    trans_rot[ij, 3] = -1* cart_coord[atom, 1]
    trans_rot[ij + 1, 3] = cart_coord[atom, 0]
    trans_rot[ij + 1, 4] = -1* cart_coord[atom, 2]
    trans_rot[ij + 2, 4] = cart_coord[atom, 1]
    trans_rot[ij, 5] = cart_coord[atom, 2]
    trans_rot[ij + 2, 5] = -1* cart_coord[atom, 0]
    ij = ij + 3

trans_rot = linalg.qr(mat(trans_rot), mode = 'economic') [0:1]
trans_rot = -1* mat(trans_rot[0])
trans_rot_proj = -(trans_rot * (trans_rot.T) \
                    - mat(identity(3*n_atoms)))
trans_rot_proj = mat(trans_rot_proj)
hess_proj = (trans_rot_proj * mat(Hessian)) * trans_rot_proj
```

Code B.1: Projecting the Hessian

```
hess_proj = self.Hessian_trans_rot(Hessian, coordinates,
                  self.number_of_normal_modes, n_atoms)
Hessian_proj = dot(M_I.transpose(), hess_proj)
Hessian_proj = dot(Hessian_proj, M_I)
```

```
v, La = linalg.eig(Hessian_proj)
v_reduced = v[:self.number_of_normal_modes]

v_args = v_reduced.argsort()[::-1]
v_reduced = array(v_reduced, double)
v_reduced = v_reduced[v_args]

La = dot(M_I, array(La, double))
La_reduced = La[:,:self.number_of_normal_modes]
La_reduced = La_reduced[:,v_args]
```

Code B.2: Mass weighting and diagonalizing the projected Hessian

```
        for i in range(self.n_coordinates):
            for j in range(self.n_coordinates):
                for k in range(self.n_coordinates):
                    temp = 0
                    for kp in range(self.n_coordinates):
                        temp = temp + cubic_force_field_clone[kp,j,i]*
                            self.eigenvectors_full[kp,k]
                    cff_norm[k,j,i]= temp

        for i in range(self.n_coordinates):
            for j in range(self.n_coordinates):
                for k in range(self.n_coordinates):
                    temp = 0
                    for jp in range(self.n_coordinates):
                        temp = temp + cff_norm[k,jp,i]*
                            self.eigenvectors_full[jp,j]
                    cubic_force_field_clone[k,j,i]= temp

        for i in range(self.number_of_normal_modes):
            for j in range(self.number_of_normal_modes):
                for k in range(self.number_of_normal_modes):
                    temp = 0
                    for ip in range(self.n_coordinates):
                        temp = temp + cubic_force_field_clone[k,j,ip]*
                            self.eigenvectors_full[ip, i]
                    cff_norm[k,j,i]= temp
```

Code B.3: Conversion of the cubic force field to normal coordinates as corresponding to the transformation equation

```
    cubic_force_field = transpose(cubic_force_field)
    cubic_force_field = dot(cubic_force_field, self.eigenvectors_full)
    cubic_force_field = transpose(cubic_force_field, (0,2,1))
```

```
    cubic_force_field = dot(cubic_force_field,self.eigenvectors_full)
    cubic_force_field = transpose(cubic_force_field, (2,1,0))
    eigenvectors_full = self.eigenvectors_full[:,:number_of_normal_modes]
    cubic_force_field =
        cubic_force_field[:number_of_normal_modes,:number_of_normal_modes,:]
    cubic_force_field = dot(cubic_force_field, eigenvectors_full)
    cff_norm = transpose(cubic_force_field, (1,0,2))
```

Code B.4: Conversion of the cubic force field to normal coordinates using matrix mechanics

```
conversion_factor = -1822.8884796 #(a.u to a.m.u)

        grad_norm = zeros((self.molecule.n_coordinates,3))

        grad_norm[:,0] += dot(grad[:,0],self.molecule.eigenvectors_full)
        grad_norm[:,1] += dot(grad[:,1],self.molecule.eigenvectors_full)
        grad_norm[:,2] += dot(grad[:,2],self.molecule.eigenvectors_full)

        grad_norm =
            grad_norm[:self.molecule.number_of_normal_modes,:]*conversion_factor
```

Code B.5: Conversion of the dipole gradient to normal coordinates using matrix mechanics

```
conversion_factor = -1822.8884796 #(a.u to a.m.u)

        hess_norm = zeros((n_coordinates,n_coordinates,3))

        for i in range(3):
            hess_norm[:,:,i] =
                dot(dipole_Hessian[:,:,i],self.molecule.eigenvectors_full)
            hess_norm[:,:,i] =
                dot(transpose(hess_norm[:,:,i]),self.molecule.eigenvectors_full)

        hess_norm =
            hess_norm[:number_of_normal_modes,:number_of_normal_modes,:]
        hess_norm = transpose(hess_norm,(1,0,2))
        hess_diag = hess_norm.diagonal(0,0,1)*conversion_factor
```

Code B.6: Conversion of the dipole Hessian to normal coordinates using matrix mechanics

```
        prefix = -1/(4*sqrt(1822.8884796)*self.frequencies**2)

        molecular_geometry = np.sum(divide(cff_norm.diagonal(0,0,1)\
```

```
        [:self.number_of_normal_modes,:self.number_of_normal_modes]\
        ,self.frequencies), axis=1)

        molecular_geometry = molecular_geometry*prefix
```

Code B.7: Evaluating the effecitve geometry in normal coordinates

```
factor = sqrt(1822.8884796)

cff_norm, cff_norm_reduced = self.to_normal_coordinates_3D\
(ri.read_cubic_force_field(self.get_cubic_force_field_name(),
    self.n_coordinates))
effective_geometry_norm = self.effective_geometry_norm(cff_norm_reduced)

cartessian_coordinates =
    np.sum(factor*effective_geometry_norm*self.eigenvectors, 1)

#instead of reshape() this will fail if it cannot be done efficiently:
cartessian_coordinates.shape = (self.n_atoms, 3)
```

Code B.8: Converting the effective geometry from normal to cartessian coordinates

```
import Molecule as mol
from numpy import array, zeros, absolute, add, sqrt

correction_property = zeros((self.molecule.n_atoms,3,3))
sproperty_derivative = self.get_property_derivative()
self.uncorrected_property = self.get_uncorrected_property()
eigenvalues = self.molecule.eigenvalues

for nm in range(self.molecule.n_atoms):
    factor = 1/(sqrt(eigenvalues[nm]))
    for i in range(3):
        correction_property[atm,j,i] += pre_property[nm,i]*factor

self.correction_property = correction_property*self.prefactor
self.corrected_property = self.correction_property +
    self.uncorrected_property
```

Code B.9: The zeroth order corrections for both the effective and equilibrium geometry

```
factor = np.sum(divide(cff_norm.diagonal(0,0,1)\
        [:self.number_of_normal_modes,:self.number_of_normal_modes],self.freq),
            axis=1)
        first_a1 = -1.0/(4*sqrt(2)*self.freq**(3.0/2))*factor
```

```
        for a in range(3):
            first_order_correction[a] = np.sum((sqrt(2)* prop_deriv[:,a]\
            * first_a1)/sqrt(self.freq), axis=0)
```

Code B.10: The first order corrections for the equilibrium geometry

```
first_a1_factor = np.sum(divide(cff_norm.diagonal(0,0,1)\
        [:self.number_of_normal_modes,:self.number_of_normal_modes],self.freq),
            axis=1)

first_a1 = -1.0/(4*sqrt(2)*self.freq**(3.0/2))*first_a1_factor
first_a3 = (sqrt(3.0)*cff.diagonal(0,0,1).diagonal())/36**(5.0/2)

term_11 =
    -1.0*first_a1*cff.diagonal(0,0,1).diagonal()/(4*self.freq**(3.0/5))
term_12 =
    -1.0*first_a1*np.sum(divide(cff_norm.diagonal(0,0,1),(8*self.freq)),axis=1)/
self.freq**(3.0/2)
term_13 = -1.0*first_a3*sqrt(27)*cff_norm.diagonal(0,0,1).diagonal()/
(sqrt(32)*self.freq**(5.0/2))
term_14 = -1*first_a3*sqrt(3)*np.sum(divide(cff_norm.diagonal(0,0,1),
    (8*sqrt(2)*self.freq)), axis=1) /(self.freq**(3.0/2))
term_15 =
    -1*sqrt(2)*qff_norm.diagonal(0,0,1).diagonal(0,0,1).diagonal()/
(32.0*self.freq**3)
term_16 = sqrt(2)*np.sum(qff_norm.diagonal(0,0,1).diagonal(0,0,1)/
(8*self.freq),axis= 1)/self.freq**2.0

second_a2 = term_11 + term_12 + term_13 + term_14 + term_15 + term_16

for a in range(3):
    second_b11 = zeros((self.molecule.number_of_normal_modes,
        self.molecule.number_of_normal_modes))
    second_b31 = zeros((self.molecule.number_of_normal_modes,
        self.molecule.number_of_normal_modes))

    for i in range(self.molecule.number_of_normal_modes):

        quartic_correction[a] +=
            second_a2[i]*sqrt(2.0)*prop_deriv[i][i][a]/(4*self.freq[i]) \
        + (first_a3[i]**2 + first_a1[i]**2 +
            first_a3[i]*first_a1[i])*prop_deriv[i][i][a]/(3*self.freq[i])\
        -prop_deriv[i][i][a]/(2*self.freq[i])

    for i in range(self.molecule.number_of_normal_modes):
        for j in range(self.molecule.number_of_normal_modes):
```

```
        prefix_1 = 1/(32*self.freq[i]**(3.0/2) *
            self.freq[j]**0.5*(self.freq[i] + self.freq[j]))
        second_b11[i][j] += prefix_1*qff_norm[i][i][i][j]

        prefix_1= sqrt(6.0)/(96*self.freq[i]**(3/2) *
            self.freq[j]**0.5*(3*self.freq[i] + self.freq[j]))
        second_b31[i][j] += prefix_1*qff_norm[i][i][i][j]

        for m in range(self.molecule.number_of_normal_modes):
            prefix_2 = 1/sqrt(2.0)*self.freq[m]*2
                *self.freq[i]**(1.0/2)*sqr(2.0)*self.freq[j]**(1.0/2)
                *(self.freq[i]+self.freq[j])
            second_b11[i][j] += prefix_2*qff_norm[i][i][i][j]

        quartic_correction[a] +=
            second_b11[i][j]*prop_deriv[i][j][a]/(4*self.freq[i]**(1.0/2)\
            *self.freq[j]**(1.0/2)) \
            +second_b31[i][j]*sqrt(2.0)*prop_deriv[i][j][a]/(4*self.freq[j])

    quartic_correction = quartic_correction*self.prefactor
```

Code B.11: The second order corrections for the dipole equilibrium geometry

Appendix C

Showing that $P^{(3)}$ is non-zero

To show that $P^{(3)}$ is non-zero, it is enough to show that the numerator is non-zero, as the denominator can never be zero. The expression for $P^{(3)}$ is found by the equation:

$$\left\langle P^{(m,n)}_{\text{numerator}} \right\rangle = \left[\sum_{k=0}^{m} \left\langle \Psi^{(k)} | T^{(n)} | \Psi^{(m-k)} \right\rangle \right] \tag{C.1}$$

Inserting for $n = 3$ and gives:

$$\left\langle P^{(3,n)}_{\text{numerator}} \right\rangle = 2 \left\langle \Psi^{(0)} | T^{(n)} | \Psi^{(3)} \right\rangle + 2 \left\langle \Psi^{(1)} | T^{(n)} | \Psi^{(2)} \right\rangle \tag{C.2}$$

The expression for $\Psi^{(1)}$ and $\Psi^{(2)}$ are already known, we will therefore work with the second term of Eq C.2.

Considering only the expression with $T^{(2)}$, the second term becomes:

$$\left\langle a^{(1)}_{1,i} + a^{(1)}_{3,i} + b^{(1)}_{11,ij} | P^{(2)} q_i q_j | a^{(2)}_{2,i} + a^{(2)}_{4,i} + a^{(2)}_{6,i} + b^{(2)}_{11,ij} + b^{(2)}_{22,ij} + b^{(2)}_{13,ij} \right\rangle \tag{C.3}$$

Expanding this we embarked on a non-zero term:

$$= b^{(1)}_{11,ij} b^{(2)}_{22,ij} P^{(2)} \left\langle q_i \right\rangle_{12} \left\langle q_j \right\rangle_{12} \tag{C.4}$$

And we have now shown that $P^{(3)}$ is non-zero.

Bibliography

[1] G. Amat, H. H. Nielsen, and G. Tarrago. *Rotation-vibration of polyatomic molecules.* Dekker, New York, 1971.

[2] C. Angeli, K. L. Bak, V. Bakken, O. Christiansen, R. Cimiraglia, S. Coriani, P. Dahle, E. K. Dalskov, T. Enevoldsen, B. Fernandez, L. Ferrighi, L. Frediani, C. Hattig, K. Hald, A. Halkier, H. Heiberg, T. Helgaker, H. Hettema, B. Jansik, H. J. Aa. Jensen, D. Jonsson, P. Jrgensen, S. Kirpekar, W. Klopper, S. Knecht, R. Kobayashi, J. Kongsted, H. Koch, A. Ligabue, O. B. Lutns, K. V. Mikkelsen, C. B. Nielsen, P. Norman, J. Olsen, A. Osted, M. J. Packer, T. B. Pedersen, Z. Rinkevicius, E. Rudberg, T. A. Ruden, K. Ruud, P. Sa lek, C. C. M. Samson, A. Sanchez de Meras, T. Saue, S. P. A. Sauer, B. Schimmelpfennig, A. H. Steindal, K. O. Sylvester-Hvid, P. R. Taylor, O. Vahtras, D. J. Wilson, and H. Ågren. *DALTON2011 Program Manual.*

[3] A. F. C. Arapiraca, D. Jonsson, and J. R. Mohallem. Vibrationally averaged post Born-Oppenheimer isotopic dipole moment calculations approaching spectroscopic accuracy. *J. Chem. Phys.*, 135:244313, 2011.

[4] A.F.C. Arapiraca and J.R. Mohallem. DFT vibrationally averaged isotopic dipole moments of propane, propyne and water isotopologues, *in press. Chem. Phys. Lett.*, 2014.

[5] P.-O. Åstrand, G. Karlström, A. Engdahl, and B. Nelander. Novel model for calculating the intermolecular part of the infrared spectrum for molecular complexes. *J. Chem. Phys.*, 102:3534–3554, 1995.

[6] P.-O. Åstrand and K. V. Mikkelsen. Calculation of nuclear shielding constants and magnetizabilites of the hydrogen fluoride molecule. *J. Chem. Phys.*, 104:648–653, 1996.

[7] P.-O. Åstrand, K. Ruud, K. V. Mikkelsen, and T. Helgaker. The magnetizability anisotropy and rotational g factor of deuterium hydride and the deuterium molecule. *Chem. Phys. Lett.*, 271:163–166, 1997.

[8] P.-O. Åstrand, K. Ruud, K. V. Mikkelsen, and T. Helgaker. Rovibrationally averaged magnetizability, rotational g factor, and indirect spin-spin coupling of the hydrogen fluoride molecule. *J. Chem. Phys.*, 110:9463–9468, 1999.

[9] P.-O. Åstrand, K. Ruud, and D. Sundholm. A modified variation-perturbation approach to zero-point vibrational motion. *Theor. Chem. Acc.*, 103:365–373, 2000.

[10] P.-O. Åstrand, K. Ruud, and P. R. Taylor. Calculation of the vibrational wave function of polyatomic molecules. *J. Chem. Phys.*, 112:2655–2667, 2000.

[11] P.-O. Åstrand, A. Wallqvist, and G. Karlström. Nonempirical intermolecular potentials for urea-water systems. *J. Chem. Phys.*, 100:1262–1273, 1994.

[12] G. Avila. *Ab initio* dipole polarizability surfaces of water molecule: Static and dynamic at 514.5 nm. *J. Chem. Phys.*, 122:144310, 2005.

[13] A.D Becke. *J. Chem. Phys.*, 98:5648–5625, 1993.

[14] W. S. Benedict, N. Gailar, and E. K. Plyler. Rotationvibration spectra of deuterated water vapor. *J. Chem. Phys.*, 24:1139 –1165, 1956.

[15] M. Born and K. Huang. *Dynamical Theory of Crystal Lattices.* Clarendon Press, Oxford, 1954.

[16] M. Born and J. R. Oppenheimer. *Ann. Phys.*, 84:457, 1927.

[17] Y. Bouteillera and J.P. Perchard. The vibrational spectrum of $(H_2O)_2$: comparison between anharmonic ab initio calculations and neon matrix infrared data between 9000 and 90 cm^1. *Chem. Phys.*, 305:1–12, 2004.

[18] U. Buck and F. Huisken. Infrared spectroscopy of size-selected water and methanol clusters. *Chem. Rev.*, 10:3863–90, 2000.

[19] A. D. Buckingham. Permanent and induced molecular moments and long-range intermolecular forces. *Adv. Chem. Phys.*, 12:107–142, 1967.

[20] Edited by M. Quack and F. Merkt. Handbook of high-resolution spectroscopy. *Wiley*, page 2182, 2011.

[21] Edited by Russell D. Johnson III. *NIST Standard Reference Database Number 101.* 2013.

[22] Edited by V. Barone. Computational strategies for spectroscopy: From small molecules to nano systems. *Wiley*, 2011.

[23] J. Ceponkus, P. Uvdal, and B. Nelander. Far-infrared band strengths in the water dimer: Experiments and calculations. *J. Chem. Phys.*, 112:3921–3926, 2008.

[24] J. Ceponkus, P. Uvdal, and B. Nelander. Intermolecular vibrations of different isotopologs of the water dimer: Experiments and density functional theory calculations. *J. Chem. Phys.*, 129:194306, 2008.

[25] S. Chacon. *Pro Git.* 2009.

[26] S. A. Clough, Y. Beers, G. P. Klein, and L. S. Rothman. Dipole moment of water from Stark measurements of H_2O, HDO, and D_2O. *J. Chem. Phys.*, 59:2254–2259, 1973.

[27] A. G. Császár. Anharmonic molecular force fields. *WIREs Comput Mol Sci*, 2:273289, 2012.

[28] F. De Proft, F. Tielens, and P. Geerlings. Performance and basis set dependence of density functional theory dipole and quadrupole moments. *J. Mol. Struct. (THEOCHEM)*, 506:1–8, 2000.

[29] M. E. Dunn, T. M. Evans, K. N. Kirschner, and G. C Shields. Prediction of accurate anharmonic experimental vibrational frequencies for water clusters, $(H_2O)_n$, n=2-5. *J. Phys. Chem. A*, 110:303–9, 2006.

[30] Jr E. Bright Wilson, J.C Decius, and Paul C. Cross. *Molecular Vibrations: The Theory of Infrared and Raman Vibrational Spectra*. Courier Dover Publications, 1955.

[31] C. Eckart. Some studies concerning rotating axes and polyatomic molecules. *Phys. Rev.*, 47:552, 1935.

[32] U. Ekström, L. Visscher, R. Bast, A. J. Thorvaldsen, and K. Ruud. *J. Chem. Theory Comput.*, 6:1971, 2010.

[33] A. Engdahl and B. Nelander. On the relative stability of H- and D-bonded water dimers. *J. Chem. Phys.*, 86:1819–1823, 1987.

[34] A. Engdahl and B. Nelander. The intramolecular vibrations of the ammonia water complex. A matrix isolation study. *J. Chem. Phys.*, 91:6604, 1989. Erratum in *J. Chem. Phys.* **92**, 6336, 1990.

[35] A. Engdahl and B. Nelander. IR induced isomerisation of HDO complexes: a method for the observation of FIR spectra of matrix isolated water complexes. *Chem. Phys.*, 213:333–339, 1996.

[36] S. T. Epstein. *The Variation Method in Quantum Chemistry*, volume 33 of *Physical Chemistry*. Academic Press, 1974.

[37] R. P. Feynman. Forces in molecules. *Phys. Rev.*, 56:340–343, 1939.

[38] P.W. Fowler. Vibration-rotation effects on properties of symmetric tops and linear molecules. *Mol. Phys.*, 43:591, 1981.

[39] B. Gao, M. Ringholm, R. Bast, K. Ruud, A. J. Thorvaldsen, and M. Jaszuński. Analytic density functional theory calculations of pure vibrational hyperpolarizabilities: The first dipole hyperpolarizability of retinal and related molecules. 118:748756, 2014.

[40] B. Gao, A. J. Thorvaldsen, and K. Ruud. *Int. J. Quant. Chem.*, 111:858, 2011.

[41] T. A. Halgren. Merck molecular force field. i. basis, form, scope, parameterization, and performance of MMFF94. *J. Comput. Chem.*, 17:490519, 1996.

[42] J. R. Hammond, J. Autschbach N. Govind, K. Kowalski, and S. S. Xantheas. Accurate dipole polarizabilities for water clusters n = 2 12 at the coupled-cluster level of theory and benchmarking of various density functionals. *J. Chem. Phys.*, 131:214103, 2009.

[43] M. D. Hanwell, D. E. Curtis, D. C. Lonie, T. Vandermeersch, E. Zurek, and G. R. Hutchison. Avogadro: An advanced semantic chemical editor, visualization, and analysis platform. *Journal of Cheminformatics*, 4:17, 2012.

[44] T. Helgaker, S. Coriani, P. Jøgensen, K. Kristensen, J. Olsen, and K. Ruud. Recent advances in wave function-based methods of molecular-property calculations. *Chem. Rev.*, 112:543–631, 2012.

[45] T. Helgaker and P. Jørgensen. Configuration-interaction energy derivatives in a fully variational formulation. *Theor. Chim. Acta*, 75:111–127, 1989.

[46] T. Helgaker, P. Jørgensen, ed. S. Wilson, and G. H. F. Diercksen. *Calculation of geometrical derivatives in molecular electronic-structure theory.* Plenum, New York, 1992.

[47] J. Hellmann. Einführung in die quantenchemie. *Liepzig*, pages 285–286, 1937.

[48] G. Herzberg. *Spectra od Diatomic Molecules.* D Van Nostrand, Company Inc., 2nd edition, 1950.

[49] J. O. Hirschfelder, W. Byers Brown, and S. T. Epstein. Recent developments in perturbation theory. *Adv. Quant. Chem.*, 1:255–374, 1964.

[50] U. Hohm. Dipole polarizability and bond dissociation energy. *J. Chem. Phys.*, 101:6362–6364, 1994.

[51] A. R Hoy and P. R. Bunker. A precise solution of the rotation bending schrdinger equation for a triatomic molecule with application to the water molecule. *J. Mol. Spectrosc.*, 74:18, 1979.

[52] E. Hylleraas. *Z. Phys.*, 65:209, 1930.

[53] C. J. Jameson. Rovibrational averaging of molecular electronic properties. In Z. B. Maksic, editor, *Theoretical Models of Chemical Bonding (Book 3)*, pages 459–519. Springer, 1 edition, 1991.

[54] E. B. Wilson Jr. and J. B. Howard. The vibrationrotation energy levels of polyatomic molecules i. mathematical theory of semirigid asymmetrical top molecules. *J. Chem. Phys.*, 4:260, 1936.

[55] R. A. Kendall, T. H. Dunning Jr., and R. J. Harrison. Electron affinities of the first-row atoms revisited. Systematic basis sets and wave functions. *J. Chem. Phys.*, 96:6796–6806, 1992.

[56] C. W. Kern and R. L. Matcha. Nuclear corrections to electronic expectation values: zero-point vibrational effects in the water molecule. *J. Chem. Phys.*, 49:2081–2091, 1968.

[57] F. N. Keutsch, L. B. Braly, M. G. Brown, H. A. Harker, and P. B. Petersen. Water dimer hydrogen bond stretch, donor torsion overtone, and in-plane bend vibrations. *J. Chem. Phys.*, 119:8927–8937, 2003.

[58] K. S. Kim, B. J. Mhin, U.-S. Choi, and K. Lee. *Ab initio* studies of the water dimer using large basis sets: The structure and thermodynamic averages. *J. Chem. Phys.*, 97:6649–6662, 1992.

[59] H. P. Langtangen. *A Primer on Scientific Programming with Python*. Springer Publishing Company, Incorporated, 3rd edition, 2012.

[60] Andrew R. Leach. *Molecular Moldelling, Principles and Applications*. Pearson Education Limited, 2001.

[61] A. D. McNaught and A. Wilkinson. *Compendium of Chemical Terminology, 2nd ed. (the Gold Book)*. Blackwell Scientific Publications, Oxford, 1997.

[62] J. S. Muenter. Polarizability anisotropy of hydrogen fluoride. *J. Chem. Phys.*, 56:5409–5412, 1972.

[63] W. F. Murphy. The Rayleigh depolarization ratio and rotational Raman spectrum of water vapor and the polarizability components for the water molecule. *J. Chem. Phys.*, 67:5877–5882, 1977.

[64] D. Papoušek and M.R. Aliev. Molecular vibrational/rotational spectra. *Academia, Prague*, 1982.

[65] J. A. Pople, R. Krishnan, H. B. Schlegel, and J. S. Binkley. Derivative studies in hartree-fock and mller-plesset theories. *Int. J. Quantum Chem.*, 16:225–241, 1979.

[66] P. Pulay. *Ab initio* calculation of force constants and equilibrium geometries in polyatomic molecules. *Mol. Phys.*, 17:197–204, 1969.

[67] P. Pulay. Analytical derivatives, forces, force constants, molecular geometries, and related response properties in electronic structure theory. *WIREs Comput Mol Sci*, 4:169–181, 2014.

[68] P. Pulay and G. Fogarasi. Geometry optimization in redundant internal coordinates. *J. Chem. Phys.*, 96:2856, 1992.

[69] S. Reine, E. I. Tellgren, and T. Helgaker. *Phys. Chem. Chem. Phys.*, 9:4771, 2007.

[70] M. Ringholm, D. Jonsson, R. Bast, B. Gao, A. J. Thorvaldsen, U. Ekstrm, T. Helgaker, and K. Ruud. Analytic cubic and quartic force fields using density-functional theory. *J. Chem. Phys.*, 140:034103, 2014.

[71] K. Ruud, P.-O. Åstrand, T. Helgaker, and K. V. Mikkelsen. Full CI calculations of the magnetizability and rotational g factor of the hydrogen molecule. *J. Mol. Struct. (THEOCHEM)*, 388:231–235, 1996.

[72] K. Ruud, P.-O. Åstrand, and P. R. Taylor. An efficient approach for calculating vibrational wave functions and zero-point vibrational corrections to molecular properties of polyatomic molecules. *J. Chem. Phys.*, 112:2668–2683, 2000.

[73] E. Schrödinger. Quantisierung als eigenwertproblem. *Ann Phys*, 80:437–490, 1926.

[74] S. Simon, J. Bertran, and M. Sodupe. Effect of counterpoise correction on the geometries and vibrational frequencies of hydrogen bonded systems. *J. Phys. Chem. A*, 105:4359–4364, 2001.

[75] J. F. Stanton and J. Gauss. Ab initio calculations of force constants and equilibrium geometries in polatomic molecules. *Int. Rev. Phys. Chem.*, 19:61–95, 2000.

[76] P.J. Stephens, F.J. Devlin, C.F. Chabalowski, and M.J. Frisch. *J. Chem. Phys.*, 98:11623–11627, 1994.

[77] A. J. Thorvaldsen, K. Ruud, K. Kristensen, P. Jørgensen, and S. Coriani. A density matrix-based quasienergy formulation of the kohnsham density functional response theory using perturbation- and time-dependent basis sets. *J. Chem. Phys.*, 129:214108, 2008.

[78] M. Toyama, T. Oka, and Y. Morino. Effect of vibration and rotation on the intermolecular distance. *J. Mol. Spectrosc.*, 13:193–213, 1964.

[79] J. G. C. M. van Duijneveldt-van de Rijdt and F. B. van Duijneveldt. Convergence to the basis set limit in *ab initio* calculations at the correlated level on the water dimer. *J. Chem. Phys.*, 97:5019–5030, 1992.

[80] P.-O. Widmark, P.-Å. Malmqvist, and B. O. Roos. Density matrix averaged atomic natural orbital (ano) basis sets for correlated molecular wave functions. *Theor. Chim. Acta*, 77:291–306, 1990.

[81] P.-O. Widmark, B. J. Persson, and B. O. Roos. Density matrix averaged atomic natural orbital (ANO) basis sets for correlated molecular wave functions. II. Second row atoms. *Theor. Chim. Acta*, 79:419–432, 1991.

[82] D. E. Woon and T. H. Dunning Jr. Gaussian basis sets for use in correlated molecular molecular calculations. IV. Calculation of static electrical response properties. *J. Chem. Phys.*, 100:2975–2988, 1994.

[83] D. E. Woon and T. H. Dunning Jr. Gaussian basis sets for use in correlated molecular calculations. V. Core-valence basis sets for boron through neon. *J. Chem. Phys.*, 103:4572–4585, 1995.

[84] X. Xu and W. A. Goddard. Bonding properties of the water dimer: A comparative study of density functional theories. *J. Chem. Phys.*, 108:2305–2313, 2004.

[85] G.D Zeiss, W.J Meath, J.C.F MacDonald, and D.J Dawson. Dipole oscillator strength distributions, sums, and some related properties for Li, N, O, H_2, N_2, O_2, NH_3, H_2O, NO, and N_2O. *Can. J. Phys.*, 55:2080–2100, 1977.